CHARACTERIZATION AND UTILIZATION OF FLY ASH DERIVED FROM THE CO-COMBUSTION OF BIOMASS AND COAL AS A MINERAL ADMIXTURE FOR ORDINARY PORTLAND CEMENT

By

Andrea Johnson

This thesis is submitted in partial
fulfilment of the requirement for the degree of
Masters of Science
In
Environmental Engineering

Lakehead University
Thunder Bay, Ontario, Canada, 2009

Abstract

Co-firing coal with renewable/waste biomass for power generation can mitigate the atmospheric discharge of pollutants (*e.g.*, SO_2) and green-house gases. Wide-spread application of this technology is impeded, however, by current standards which prohibit fly ash derived from biomass as a partial substitute for portland cement in concrete.

In the first stage of this research, fly ashes from the combustion of coal (CFA) and the co-combustion of coal and biomass (CBFA) were characterized according to chemical and physical properties, as well as microstructure. The fly ashes were obtained from full scale combustion tests which took place at the Atikokan Ontario thermoelectric power station. The fly ashes were derived from the combustion of undiluted lignite coal (CFA) and 15:85 and 66:34 (on a thermal basis) wood pellet/lignite mixture, termed 15CBFA and 66CBFA, respectively. All fly ashes were found to be very similar in composition and meet requirements put forth by ASTM and CSA on the allowable amount of carbon for use as a partial cement substitute.

All the fly ashes had the same density within experimental uncertainty. Particle size distribution analyses, however, showed significant differences between CFA and 66CBFA on one hand and 15CBFA on the other. They were attributed to the 15CBFA formed during combustion when the fuel input into the boiler was at its maximum and soot blowers causing an upward flow of steam entrained larger particles (compared to CFA and 66CBFA which were collected when soot blowers were not in use). The microstructure of each fly ash was analysed by scanning electron microscopy and energy dispersive spectrometry. All of the fly ashes were primarily composed of spherical

particles which were either completely solid or porous. Although the composition of individual fly ash particles varied widely, each fly ash exhibited the same range of compositions. The majority of particles were aluminosilicates, with varied amounts of calcium and iron and to a lesser extent magnesium, sodium and trace elements. Some particles have concentrated amounts of iron, or calcium, but such particles were found in all fly ashes.

In the second phase of this research the effect of fly ash-amendment of mortars was investigated. In no instance did the type of fly ash make any difference. Increasing the fly ash content decreased the water requirement independently of the type of fly ash. Partial substitution of cement with fly ash (up to 40 wt%) had a moderate effect on the entrained air content of mortars (up to 2.5%), but this difference vanished upon addition of air entraining agent, again independently of fly ash type. Amending mortars with up to 40 wt% fly ash retarded the early strength development of mortars, but increased the later strength, with mortars containing CFA or 66CBFA consistently exhibiting higher compressive strengths than those containing 15CBFA. Mortars containing up to 40 wt% CFA, 15CBFA, or 66CBFA met required strength specifications by 28 days according to ASTM C618 (2003). Addition of 20 wt% CFA or 15CBFA was found to have little effect on resilience to rapid freeze-thaw of mortars after 140 cycles.

Some fly ash particles reacted to form calcium silica hydrate (CSH) gel apparently contributing to the strength of the mortars.

Acknowledgements

Several individuals are so deserving of my sincerest gratitude. First and foremost, I would like to thank my research supervisors, Dr. Lionel Catalan and Dr. Stephen Kinrade for their valuable input, time, and effort. Their unceasing and invaluable encouragement, guidance and advice during my Master's studies are extremely appreciated.

I would also like to recognize employees of the Atikokan Bioenergy Research Centre, including but not limited to Jane Todd, Ed Enge, Daryl Gaudry and Randy Angus for their help in collecting fly ash samples as well as process information.

Staff at the Lakehead University who also deserve my gratitude include Al Mackenzie, Keith Pingrintz, and Ain Raitsakas of the Lakehead University Instrumentation Laboratory for their training and help with the analyses. I am also grateful to Conrad Hagstrom and Garry Rathje for their help with scheduling experiments and using the equipment. Ann Hammond is also appreciated for her preparation of samples for analysis by SEM-EDS.

I would like to thank fellow researchers in the Industrial Waste Management and Utilization Laboratory for their help with using the laboratory equipment (in particular Dr. Nabajyoti Saikia, whose experience with cement and fly ash proved beneficial).

My family and in particular, my husband, Travis must be acknowledged for their unfailing support and encouragement.

Table of Contents

List of Tables

List of Figures

1.0 Introduction

Coal fly ash is a collection of airborne particulates generated as by-products of combustion in coal-fired thermal generating plants (Berry, 1976). According to the Association of Canadian Industries Recycling Coal Ash, 4,679,000 tonnes of coal fly ash are produced annually in Canada (CIRCA, 2008). A common strategy for minimizing the environmental impact of materials that have commonly been classified as wastes is to utilize them as resources. Presently, 31% of Canadian fly ash is recycled for use in various applications, primarily as a cement substitute (CIRCA, 2008). Europe boasts up to 88% recycling of fly ash (CIRCA, 2008), most of which is used in construction and mining (e.g., concrete addition, blended cement, road construction, infill stabilized base course, flowable fill, grouts for pavement subsealing, structural fills/embankments and soil improvement) (Meij and Van den Berg, 2001). Recycling can significantly decrease the volume of land-filled fly ash. In Canada, over 3.2 million tonnes of non-recycled fly ash are land-filled annually (CIRCA, 2008). The use of fly ash can also lower the cost of electricity due to revenue generated by fly ash sales (CIRCA, 2008). The most common application of fly ash is as a mineral admixture in cement mortars and concrete (ACAA, 2003; Meij and Van den Berg, 2001). As North America continues to develop, the need for building materials continues to grow. Concrete is a common construction material which consists of cement, aggregates, admixtures and water. Concrete solidifies and hardens after mixing due to chemical hydration of the cement.

Pulverized coal combustion in utility boilers was introduced over 70 years ago (Sarofim and Helble, 1994). Electricity can also be produced by the combustion of biomass, or by co-combustion of coal and biomass. Wood, peat, grain, municipal solid

waste, wheat straw, nut shells, meat and bone meal, bagasse and olive husks have been found useable in production of electricity (Wang *et al.*, 2008a; Steenari and Lindqvist, 1999; Lu G. *et al.*, 2008; Ipatti, 1998; Demirbas, 2005; Chao *et al.*, 2008; Chindaprasirt *et al.*, 2008; Schlorholtz, 2005; Senneca, 2008). With the growing concern over climate change and depletion of fossil fuel resources, there is pressure to transition to more renewable fuel resources (Wang *et al.*, 2008a; MacKinnon, 2008). The utilisation of renewable fuel sources for power generation is beneficial for many reasons. They typically release lower levels of sulfur and toxic metals, and zero net increase in the carbon dioxide level of the atmosphere (due to the natural carbon cycle) (Wang *et al.*, 2008c; Lu G. *et al.*, 2008; Steenari and Lindqvist, 1999). Renewable fuels are sustainable compared to finite fossil fuels (Wang *et al.*, 2008a; Lu G. *et al.*, 2008; Steenari and Lindqvist, 1999). Fly ash produced from biomass however, is not allowed for use as a portland cement substitute by current North American standards (ASTM C618, 2003). In 2005, Europe accepted fly ash from the co-combustion of coal and certain biomass: vegetable matter (such as wood chips, straw and olive shells); green wood and cultivated biomass; animal meal; municipal sewage sludge; paper sludge; petroleum cake and virtually ash free liquid and gaseous fuels (EN 450, 2005; Vom Berg and Feuerborn, 2003).

If fly ash derived from biomass was found suitable for use as a substitute for portland cement, then the benefits would be numerous. In addition to the aforementioned environmental benefits of renewable fuel use, fly ash sales would generate revenue for coal fired power plants and the concern of lost revenue due to land-filling fly ash from biomass would disappear (CIRCA, 2008). Furthermore, the energy and cost of raw

material production would decrease for construction materials which can incorporate fly ash (Wang *et al.*, 2008a; McKinnon, 2008).

In the following section, fly ash generation and the chemical and physical characteristics of fly ash will be discussed. Subsequently, an overview of fly ash production in the USA and in the European Union will be presented, followed by the general applications of fly ash. Particular emphasis will be placed on reviewing the particular application of fly ash as a mineral admixture in cement mortars/concrete, including the chemistry involved and the properties of cement mortars/concrete incorporating fly ash. Finally, the limitations of the current knowledge will be discussed and will form the basis of the research objectives of this study.

1.1 Fly Ash Generation

The process by which fly ash is generated is complex; mineral matter in coal undergoes a number of transformations and interactions during combustion (Wigley and Williamson, 1998; Sarofim and Helble, 1994; Wilemski and Srinivasachar, 1994). Organically bound minerals, dispersed inorganics, and included minerals (those imbedded in the carbaceous coal particles) can form fly ash by progressing through several physical and chemical processes (Wigley and Williamson, 1998; Sarofim and Helbe, 1994; Wilemski and Srinivasachar, 1994).

During combustion, fractions of char particles and particle fragments can either vapourize or undergo char burnout (Sarofim and Helble, 1994). Those experiencing char burnout will directly result in fly ash particles, while vapourized fractions will condense

to form fly ash. Williamson and Wigley (1998) described in detail the physical and chemical processes responsible for fly ash formation:

Coalescence

When a fuel particle contains more than one occurrence of mineral matter, the mineral matter may be expected to show a varying degree of coalescence during combustion. The coalescence causes an increase in size during the transformation from mineral to ash particle. Coalescence is therefore responsible for modifications in mineral chemical distribution, as it will produce ash particles with intermediate chemical compositions.

Volatile Loss

Some minerals such as calcite, pyrite, ankerite, and gypsum expel volatile components upon heating, which affects both chemical composition and physical characteristics of ash particles (with increased volatile loss resulting in decreased size and mass).

Fusion

Fusion is responsible for transforming irregularly shaped mineral matter to spherical ash particles. Fused material may also separate from the main mass of mineral matter and thus cause formation of smaller ash particles.

Vaporization and Condensation

Limited vaporization and condensation of potassium, sodium, and possibly calcium occurs. Slightly higher potassium and sodium contents in fly ash compared to coal have been attributed to the capture of volatilized alkalis by ash particles. The slightly lower calcium content has been attributed to the loss of some carbonate-bound mineral matter to the gaseous phase.

1.2 Fly Ash Characterization

Fly ash is classified according to ASTM designation C 618 (2003) in the United States, CSA-A3001 (2003) in Canada, and EN 450 (2005) in Europe. These designations classify fly ash according to both physical and chemical properties.

1.2.1 Physical Properties

Fly ash is a heterogeneous mixture of mostly spherical particles formed by rapid cooling of combustion products in the post-combustion zone of the boiler (Berry, 1976; Bouzoubaa and Foo, 2004). Particle diameter typically ranges from 1 to 150 μm (Berry, 1976), and is generally affected by equipment configuration and fuel loading rates (Clendenning and Durie, 1962). When loads are relatively small (i.e., when the amount of fuel fed to the process is smaller), the coal may experience finer grinding due to increased residence time in the pulverizers (Clendenning and Durie, 1962), although this is not always the case (Boegh and Gaudry, 2008). Consideration must also be paid to the fact that during high loads (i.e., approaching 100%), soot blowers are used to introduce steam to blow off layers of ash as they collect on the boiler tubes (Johnson *et al.*, 1994; Gaudry,

2008). The upward force of the steam can entrain larger particles of fly ash. The particle size of fly ash can also be affected by the boiler temperature, which is also a function of loading. At higher loads, the temperature is higher, as more fuel is being combusted. Conversely, lower loads produce lower boiler temperatures and lower exit gas temperatures. Lower exit temperatures result in rapid cooling of fly ash, thus producing smaller fly ash particles (Gaudry, 2008).

Coal fly ash has a specific gravity typically ranging from 2.65 to 2.80 g/mL (Berry, 1976). Fly ashes derived from co-combustion of biomass and coal have been found to have similar physical properties, such as particle size distribution, specific gravity, and shape of particles (Wang *et al.,* 2008a). The particle size distribution of fly ash has been connected to their pozzolanic activity (which will be defined in another section of this literature review), with smaller particles having increased reactive surface areas (Wang *et al.,* 2008a; Berry, 1976; Berry and Malhotra, 1978).

The colour of fly ash can range from tan to dark grey, depending on its chemical and mineral composition (Berry, 1976; ACAA, 2003). Tan and lighter coloured fly ash is typically associated with high lime content, where brownish coloured fly ash has higher iron content (ACAA, 2003). On occasion, fly ash can have a dark grey to black colour, which is associated with elevated unburned carbon content (ACAA, 2003).

Scanning electron microscope (SEM) images of fly ash show mainly spherical particles, varying greatly in size and composition (Wang *et al.,* 2008a; Del Monte and Sabbioni, 1984; Goni, 2007; Schorholtz, 2005).

Fly ash particles can be categorized into a few major groups: glassy aluminosilicates, cenospheres, spherical iron-rich particles, and spongy carbaceous

materials. Smaller portions of fly ash can be grouped into quartz particles with round edges, and transparent spherical particles. The relative abundance of these fractions will greatly depend on the feed coal, as well as the process configuration (Del Monte and Sabbioni, 1984; Clendenning and Durie, 1962; Berry, 1976; Berry and Malhotra, 1978). Generally it can be expected that glassy particles, cenospheres and iron-rich particles will be present in all fly ashes (Del Monte and Sabbioni, 1984; Clendenning and Durie, 1962; Berry, 1976; Berry and Malhotra, 1978; Vassilev *et al.*, 2005). Fly ash particles have been separated by size, magnetic susceptibility, solubility, and density (Ngu *et al.*, 2007; Watt and Thorne 1965; Berry 1976; Vassilev *et al.*, 2005; Del Monte and Sabbioni, 1984).

Glassy Aluminosilicatic Particles

This is generally the largest portion of fly ash and is formed by melting and rapid solidification of clay minerals such as kaolinite and illite (Del Monte and Sabbioni, 1984; Berry, 1976). Cereda *et al.* (1995) suggested that the aluminosilicatic glassy portion can comprise up to 70% of fly ash. This fraction contains Si and Al as the principal elements and minor elements such as Fe, Na, Mg, S, K, Ca, Ti, V and Mn (Del Monte and Sabbioni, 1984; Henry *et al.*, 2004).

Cenospheres

Another large portion of the fly ash is comprised of hollow spheres which result from the entrapment of gaseous product during solidification (Berry, 1976; Ngu *et al.*, 2007). These cenospheres have specific gravity less than one at standard temperature and

pressure, and thus will float on water (Ngu *et al.*, 2007). Cenospheres have been qualitatively described as being spongy, vesicular, and at times showing a surface on which agglomerates have formed (Del Monte and Sabbioni, 1984; Vassilev *et al.*, 2005). Generally, this fraction of fly ash has a higher content of organic matter (Vassilev *et al.*, 2005). Ash cenospheres can be used to produce various lightweight construction products including low-density cements and polymer composites (Lilkov *et al.*, 1999; Cardoso *et al.*, 2002; Ngu *et al.*, 2007). The properties and performance of these lightweight materials depend on the ash cenospheres properties, such as particle size distribution, wall thickness, and shape (Blanco *et al.*, 2000; Cardoso *et al.*, 2002; Ngu *et al.*, 2007). Ash cenospheres vary greatly in composition, but generally contain 55-65 wt% SiO_2, 27-33 wt% Al_2O_3, and small amounts of Fe (Wilson and Burns, 1982; Ngu *et al.*, 2007).

Spherical Iron-rich Particles

Another significant fraction of fly ash is spherical iron-rich particles, which are mainly composed of iron oxides and feature superficial grains, or a dendritic surface (Del Monte and Sabbioni, 1984). Iron bearing minerals in fly ash are generated mainly from the decomposition and oxidation of pyrite, siderite, and ankerite from the coals (Vassilev *et al.*, 2005). Their main phase constituents are magnetite>glassy alumino-silicates >hematite>quartz>calcite>melite>char>mullite>plagioclaise (Vassilev *et al.*, 2005). Even as far back as the 1960s, it was known that the iron-rich fraction of fly ash was composed of magnetite and hematite (Watt and Thorne, 1965).

Spongy Carbon-rich Particles

Spongy carbon-rich particles are typically present in fly ash in smaller amounts (Del Monte and Sabbioni, 1984; Vassilev *et al.,* 2005; Wilson and Burns, 1982). The amount of carbaceous material in fly ash depends on the type of coal used, with lignite and subbituminous coals typically yielding less than 1% carbon and bituminous coals less than 10% (Berry, 1976; Wilson and Burns, 1982). These particles are identifiable by their extremely porous nature. They can be spherical or irregularly shaped with numerous cavities which may be joined together (Del Monte and Sabbioni, 1984). Some studies show that sulfur is associated with the carbon-rich particles (Del Monte and Sabbioni, 1984; Berry, 1976).

Other Particles

There are a few other fractions of fly ash reported in the literature, including quartz particles with round edges (indicative of partial melting during combustion), mullite particles, particles composed mainly of rutile (titanium oxide), and transparent spherical particles which are composed mainly of calcium oxide (Del Monte and Sabbioni, 1984; Wilson and Burns, 1982).

Little image analysis of fly ash derived from biomass has been done to date (Wang *et al.*, 2008a). Images taken by Wang *et al.* (2008a) showed wood fly ash particles having irregular shapes compared to the mostly spherical shapes in the fly ashes from co-combustion.

1.2.2 Chemical Properties

Variations in chemical composition of fly ashes are largely dependent on the variation of mineral occurrences in the fuel (Wigley and Williamson, 1994). Fly ash resulting from coals rich in iron (i.e. anthracite, bituminous) have lower iron content compared to the parent coal (due to enrichment of iron in the ash which becomes deposited on boiler tubes/walls). Current standards (ASTM C618, 2003; CSA-A3001, 2003) classify fly ash mostly on the basis of the types and relative abundance of coal from which the ash is derived. The four major subdivisions of coal in decreasing rank are anthracitic, bituminious, sub-bituminious and lignitic. The concentrations of CaO, MgO, and Na_2O generally increase with decreasing rank (Berry, 1976).

The chemical composition of fly ash largely reflects both the general composition and the large variability of coal ash (Berry, 1976). Generally, fly ash is composed of minerals and glasses formed from SiO_2, Al_2O_3, Fe_2O_3, CaO and MgO (Berry, 1976). Helmuth (1987) suggested that these elements are found in fly ash because of their lower volatility and the short time the particles actually remain in the furnace during combustion.

The metal content of fly ash may be determined through acid digestion and inductively coupled plasma (ICP) analysis (ASTM C114, 2003). X-ray fluorescence (XRF) may be used to determine the major oxides present in the fly ash, while X-ray diffraction (XRD) may be used to identify ash mineralogy. ASTM C618 (2003), classifies fly ash as type C or type F based on the combined mass fraction of silicon dioxide, aluminium oxide, and iron oxide. Class C must contain a minimum 50 wt% of these oxides and class F must contain a minimum of 70 wt%. Canadian standard CSA-

A3001 (2003) classifies fly ash based on its calcium content: Class F, CaO < 8 wt%; Class CI, CaO = 8-20 wt%; Class CH, CaO > 20 wt%. Both CI and CH fly ashes are similar to Class C fly ash in the ASTM standards, and therefore will be referred to as "Class C" fly ashes in this literature review.

The major use of fly ash is as a pozzolan, which is defined as a siliceous or aluminosiliceous material that in itself possesses little or no cementious value, but when finely divided and in the presence of moisture will chemically react with calcium hydroxide at ordinary temperature to form compounds possessing cementitous properties (ASTM C595, 2003; Berry, 1976; Manz, 1999). Since it is the silica and aluminum phases which will provide this pozzolanic activity, the amounts of these compounds in fly ash are important. Class F fly ash is a "true pozzolan," meaning that it possesses little or no independent cementious properties (Manz, 1999; ASTM C618, 2003). Because Class C fly ash has a higher content of CaO compared to Class F fly ash, it can exhibit cementitious properties as well as pozzolanic ones (ASTM C618, 2003). This means that Class C fly ash is not a true pozzolan, since it will undergo hydration reactions without the addition of calcium hydroxide (Manz, 1999).

Sulfur trioxide content is limited to a maximum of 5 wt% for both Class C and Class F fly ashes (ASTM C618, 2003; CSA-A3001, 2003), because it promotes formation of hydration products that undergo expansion and thereby degrade strength (ACAA, 2003).

Another criterion is the loss on ignition (LOI), which is an indication of the carbon content. The amount of residual carbon particles present in fly ash is affected by the rate of combustion, air to fuel ratio and degree of pulverization of the coal (Berry,

1976). Also, relatively high LOI can result when the equipment is operating at low loads and during start-up (Clendenning and Durie, 1962). Both Class F and Class C fly ash must have an LOI lower than 6 wt% in North America and Europe, standards allow as much as 9 wt% (ASTM C618, 2003; CSA-A3001, 2003; EN450-2, 2005). It has been suggested that the major limitation of the reuse of fly ash derived from co-combustion is the typically high residual carbon content (Wang *et al.,* 2008a). These criteria become important when using the fly ash to blend with cement. The carbon content in fly ash is an important property, because it affects the air entrainment of cement mortar and concrete. The unburned carbon can adsorb air entraining agents (i.e., additives used to increase the air content of cement mortar and concrete) and also increase water requirement (i.e., the amount of water required for a specified consistency of mortar or concrete) (ACAA, 2003). Elevated levels of carbon present in ash generally decrease the cementitious properties of mortars (Chusilp *et al.,* 2009, Larson, 1964; ACIC, 1962; Bloem, 1954; Campbell, 1961; Grieb and Woolf, 1961; Friis, 1958; ASTM Committee, 1962). Air content has been found to be an important parameter in durability (see section 1.4.1). It has also been suggested that the adsorption rate and capacity of the carbon is of more importance than the LOI in predicting the stability of entrained air in concrete (Manz, 1999; ACAA, 2003).

European standards have evolved to include fly ashes from the co-combustion of biomass and coal (EN 450, 2005; Vom Berg and Feuerborn, 2003). These fly ashes must also meet strict standards on carbon content (< 5 wt%), total alkali (< 5 wt%) and chloride (< 0.1 wt%) (Vom Berg and Feuerborn, 2003).

Fly ashes from pure biomass and biomass-coal blended combustion have been analysed for metal oxide composition and loss on ignition in several studies (Wang *et al.*, 2008a, Ipatti, 1998; Demirbas, 2005). Some examples are provided in Table 1-1.

Table 1-1: Examples of fly ash samples from biomass and biomass-coal co-combustion.

Abbreviation	Combustion Materials	Reference
SW	20% switch grass 80% Galatia coal	Wang *et al.*, 2008a
SAW	20% sawdust 80% Powder River Basin coal	Wang *et al.*, 2008a
P	Peat Fly Ash	Ipatti, 1998
HNS	Hazel Nut Shell Fly Ash	Demirbas, 2005
OH	Olive Husk Fly Ash	Demirbas, 2005
SS	Sunflower Shell Fly Ash	Demirbas, 2005
BW	Beech Wood Fly Ash	Demirbas, 2005

The elemental composition and LOI of the fly ashes specified in Table 1 have been compiled in Table 2 for ease of comparison. Differences in fuel source clearly lead to a wide range in fly ash chemical composition. For example, the K_2O content varies from as low as 1.7% to as high as 33.2%. Similar differences are seen for other oxides. The combined mass fraction $SiO_2 + Al_2O_3 + Fe_2O_3$ is also calculated and noted in Table 1-2 for each fly ash to analyse compliance with standard Classes (ASTMC618, 2003; CSA-A3001, 2003; Meij and Van den Berg, 2001). It also varies widely.

Table 1-2: Elemental analysis and LOI of fly ash samples from biomass and biomass-coal co-combustion (Table 1-1).

(Weight %)	SW	SAW	P	HNS	OH	SS	BW
SiO_2	52.16	35.23	62.0	23.4	21.1	20.6	38.4
Al_2O_3	23.55	20.87	12.5	4.4	10.3	4.1	5.9
Fe_2O_3	7.57	6.22	6.4	2.0	5.2	1.7	7.3
CaO	2.37	21.86	8.0	19.6	17.5	19.9	23.6
MgO	1.31	5.12	1.8	8.6	4.8	5.2	1.4
Na_2O	0.7	1.72	2.2	3.0	30.0	3.2	0.8
K_2O	4.01	1.89	1.7	28.8	4.5	33.2	13.8
Cr_2O_3	0.02	0.01					
TiO_2	1.45	1.42		0.1	0.2	0.1	-
MnO	0.04	0.07					
P_2O_5	1.04	1.73		2.5	2.0	4.3	1.5
SO_3	2.25	3.87		0.8	0.5	1.0	2.2
$SiO_2 + Al_2O_3 + Fe_2O_3$	83.28	62.32	80.9	29.8	36.6	26.4	51.6
LOI	3.85	1.29	0.46	6.7	3.7	6.5	4.8
ASTM C618 Class	F	C	F	nc[a]	nc	nc	C

[a] nc = non-compliance with ASTM C618

Fly ashes SW, SAW, P and BW all comply with ASTM C618 (2003) standards for $SiO_2 + Al_2O_3 + Fe_2O_3$ and LOI, while the other fly ash samples do not. This poses potential issues regarding the use of biomass fly ash as a cement substitute. Fly ash from blended coal-biomass burns fit well into the classification as outlined by ASTM designation C 618 (2003). However, pure biomass fly ashes often fail to fit into the classification (which is in agreement with Table 1-2) (ASTMC618, 2003; Meij and Van den Berg, 2001; CSA-A3001, 2003).

1.3 Fly Ash Applications Other than as Cement Admixture

In order to compare to the world scene, data for fly ash production and recycling is for Canada (, the USA and the European Union is presented in Table 1-3. In 2001, the USA produced 62 million metric tonnes of fly ash, of which 32% was recycled for various applications (ACAA, 2003). In 1999, the European Union reported 38 million tonnes of fly ash production, of which close to 50% was recycled (Meij and Van den Berg, 2001).

Table 1-3: Applications of fly ash in Canada, the USA and European Union

Application	Canada (%)	USA (%)	European Union (%)
Cement/Concrete	85.4	60.9	68.1
Flowable Fill	[a]	3.7	7.6
Structural Fill	[a]	14.6	
Road Base/Sub-base	1.3	4.7	21.5
Soil Modification	[a]	3.4	[a]
Mineral Filler	[a]	0.5	[a]
Mining Applications	6.8	3.7	[a]
Waste Stabilization/Solidification	[a]	6.3	[a]
Other	6.5	2.2	2.7

[a] Figure not provided.

Stabilized Base Course

The pozzolanic nature of fly ash enables it to be used in combination with aggregate, cement or lime as a stabilized base course (ACAA, 1991). 2003). Typical proportions of fly ash are 2-8 percent (ACAA, 2003). Generally only Class F fly ash is used, and the maximum allowable sulfur content is 5% SO_3 in order to avoid expansion (AASHTO, 1999, ACAA, 2003). The stabilizing effect of the fly ash provides superior strength and durability, allows the use of low quality aggregates, and reduces the project costs

(ACAA, 1991). Several weeks of warm weather are required for strength development that is adequate to resist freeze-thaw cycling (AASHTO, 1999).

Flowable Fill

Flowable fill is a self-compacting low strength material with a flowable consistency that is used as an economical fill or backfill material (NRMCA, 2000). It usually contains water, fly ash and portland cement, plus sometimes coarse and/or fine aggregates (ACI, 1999). Virtually any fly ash can be used and it does not have to meet ASTM C618 (2003) requirements (ACAA, 2003). The properties of fly ash which lend to its usefulness in flowable fill are the size distribution and spherical shape of the particles (ACAA, 2003). Fly ash can be used in proportions of up to 95% (NRMCA, 2000). The most important physical characteristics of flowable fill are strength development, flowability, hardening, and bleeding (ACAA, 2003). Flowable fill must have an ultimate compressive strength less than 1.4 MPa (200 psi) to allow excavation by mechanical equipment (NRMCA, 2000). For manual excavation, the strength is limited to 0.3 MPa (50 psi) (NRMCA, 2000). The flow is important in order that it fits into place and consolidates due to its fluidity without the assistance of vibration (NRMCA, 2000).

Asphalt Pavements

Fly ash is used as cost-effective mineral filler in hot mix asphalt paving applications (AASHTO, 1986). When fly ash is locally available, it is hard for other mineral fillers to compete on the basis of cost (ACAA, 2003). Mineral fillers increase the stiffness of the asphalt mortar matrix, and help increase the durability of the asphalt (ACAA, 2003). Fly

ash typically meets mineral filler specification requirements for graduation, organic impurities and plasticity, with allowable LOI of up to 10% (Minnick, 1994).

Structural Fills and Embankments

The specifications for fly ash structural fills and embankments are similar to those for engineered soil fills (ACAA, 2003). Particle size distribution of fly ash will affect properties of the embankment: moisture-density relationships; shear strength; compressibility; permeability; capillarity; and frost susceptibility (USDOT, 1988). Also, the chemical characteristics of the fly ash affect the physical behaviour (i.e., strength development), as well as the quality of the leachates (ACAA, 2003). Due to frost issues, fly ash is not recommended for use as an embankment below the groundwater table, or when the embankment design cannot provide adequate drainage (ACAA, 2003).

Grouts for Pavement Sub-sealing

Voids beneath pavement slab sections can be sealed with fly ash grouts. Fly ash is used in grout due to its pozzolanic properties as well as its low water requirements for flow. Fly ash grouts contain up to 3 parts fly ash to one part cement (ACPA, 1994). They are required to flow into very small voids and still have adequate strength to support the slab (ACAA, 2003). The unconfined compressive strength requirements for a grout mixture are typically in excess of 8.3 MPa (1200 psi) at 28 days (ACPA, 1994). Using fly ash grout differs from flowable fill, as the amount of applied substance is much smaller (ACAA, 2003). A good stabilization material should remain incompressible, insoluble,

and resistant to erosion (ACPA, 1994). Fly ash grout can not be applied when the ambient temperature is below 2 °C, or when the subgrade is frozen (ACAA, 2003).

Mine Backfill

Backfilling in Canadian mines has been practised for close to 100 years (Nantel, 1998). Much of the success of modern underground mining arises from the ability to fill cavities created by mining as to establish and retain safe working conditions in an economical manner (Thomas *et al.,* 1979). Mine tailings or waste rock can be mixed with binders such as cement, slag or fly ash for use as backfill or in some cases fly ash is the only material used for backfill (Burton *et al.,* 2009). Pozzolanic properties of fly ash make it applicable for use in backfills and it does not have to meet ASTM regulations as stringent as those for use in concrete. Fly ash slurry (a mixture of cementitious fly ash mixed with water) can be highly cost effective; backfilling underground mine voids with flowable cement fill would be 10 to 20 times more expensive than with fly ash (Burton *et al.,* 2009).

Treatment of Acid Mine Drainage and Acidic Wastes

Fly ash has recently been found to be a very efficient scrubber for acidic wastes produced by the phosphate industry and acidic sludge produced from the regeneration of used motor oil (Cohen and Pelly, 2008). Furthermore, the fixation of trace elements and organic components by the fly ash particles is highly efficient, and the final product has proven to be useful as an aggregate in the manufacture of bricks that meet strength and leaching requirements (Cohen and Pelly, 2008).

Coal fly was successfully used to treat and remove toxic elements from acid mine drainage (AMD) (Vadapalli *et al.,* 2008). Zeolites were prepared from the product and in turn used to treat AMD (Vadapalli *et al.,* 2008). Ground work has also been completed for use of coal fly ash as backfilling material for an abandoned mine containing acid mine drainage (Dube, 2008).

Fire Protecting Insulation

Passive fire protection is achieved through the use of pastes containing up to 80% fly ash (dry weight basis) with the remainder composed of binder and additives (Vilches *et al.,* 2005). Some biomass fly ashes have superior insulating capacity when compared to conventional coal fly ash (Vilches *et al.,* 2005).

Waste Stabilization/Solidification

Stabilization/Solidification (S/S) technologies are widely used for treatment of hazardous inorganic waste and contaminated soils before final disposal (Conner, 1990; Conner and Hoeffner, 1998; Barth *et al.,* 1990; Pereira *et al.,* 2001). Fly ash is a very common binder in waste stabilization formulations due to its pozzolanic nature, as well as its capabilities as a bulking agent (Periera *et al.,* 2001). Fly ash is commonly mixed with portland cement and water for use as the stabilizing material (Periera *et al.,* 2001; Conner and Hoeffner, 1998). The ettringite formed by the hydration reactions of fly ash was found to be particularly applicable in the S/S of wastes that were high in boron, selenium (Hasset and Pflughoeft-Hasset, 1997; Pereira *et al.,* 2001), lead and zinc (Chang *et al.,* 1999; Pereira *et al.,* 2001).

In some cases, it is fly ash that is being stabilized/solidified. Incineration is a common means of disposing of municipal solid waste (MSW). However, it results in ash products (both fly ash and bottom ash) which contain easily leachable metals, soluble salts and organic compounds (Shi and Kan, 2008; Alba *et al.,* 1997; Aubert *et al.,* 2004). Shi and Kan (2008) suggested that the use of MSW fly ash as a replacement of portland cement in concrete and cement mortars could provide S/S of the hazardous compounds, as well as provide the benefits of cement substitution by fly ash (Shi and Kan, 2008).

Polymer Composites/Geopolymers

Fly ash has recently been used as a component of geopolymers, which are hydraulic cements produced from aluminosilicate minerals or industrial waste (Duxon *et al.,* 2007). The reactive fly ash glasses help generate a binder that is comparable to hydrated portland cement in appearance and properties, but with dramatically reduced CO_2 footprint (Duxon *et al.,* 2007).

Fly ash used in polyurethane composites improves their strength, modulus and toughness (Lu Z., 2008).

A method for manufacturing bricks from fly ash has recently been developed (Green Brick Company, 2008). The bricks are composed of fly ash, water and an air entraining agent, and are prepared by compressing at 4000 psi followed by curing for 24 hours in a 66 ^{o}C steam bath (National Science Foundation, 2007).

Soil Stabilization

The engineering performance of some soils can be improved through soil stabilization (ACAA, 2003). The properties most often altered include density, water content, plasticity, and strength (ACAA, 2003). Fly ash has been proven in geotechnical applications to enhance strength properties (due to its pozzolanic and sometimes cementitous nature), control shrink and swell properties, and reduce moisture in soil to permit compaction (ACAA, 1999).

The use of fly ash in soil stabilization/modification may be limited due to local environmental regulations (ACAA, 2003). Commonly, a leaching test is completed on the fly ash prior to use (ASCE, 1999).

Agricultural Amendment

Benefits of coal fly ash use in agriculture are numerous. Due to the alkaline nature of fly ash, it can be considered for pH adjustment. Fly ash also contains several macronutrients (such as P, K, Ca, Mg, and S) and micronutrients (such as Zn, Cu, Co, B and Mo) required for plant growth (Adriano *et al.,* 1980; McCarty *et al.,* 1994; Rautaray *et al.,* 2003). It also releases Si, which is considered to be a quasi-essential element (Epstein, 1999, Lee *et. al.,* 2006). Attention needs to be paid to possible uptake of heavy metals present in the fly ash (Adriano *et al.,* 1980; Rautaray *et al.,* 2003). A greenhouse study conducted to ameliorate acidic coal mine soils showed that lime and fly ash significantly increased their pH (Taylor and Schuman, 1998). This effect is due to the basic nature of fly ash. Fly ash additions were also found to increase the yield of crops such as corn,

sorghum sudangrass, wheat, mustard, and tomatoes (Sajwan, 1995; Kalra *et al.,* 1998; Kukier and Summer, 1994; Ahmad and Alam, 1997).

Fly ash can help increase the water holding capacity of soils (Menzies and Aitken, 1996). Hydraulic conductivity was reduced and moisture retention improved by ash-amendment of soil used to grow wheat, mustard, or rice (Kalra et al., 1998).

Raw Material for Cement Manufacture

Portland cement clinker is a granular product produced by grinding raw materials such as limestone, shale, clay and sand in predetermined proportions, and heating the mixture of materials at very high temperatures (> 1500 °C) in rotating kilns. This process is very energy intensive. Typically, the energy costs involved with cement production account for 25 to 35% of the total direct costs (CIPEC, 2001). Although efforts have been made to increase energy efficiency in the cement industry, the energy demands remain high. According to the Cement Association of Canada, in 2006, the energy cost of producing one tonne of cement was 4.46 GJ (CAC, 2008), thus rendering cement the third most energy intensive material to produce after steel and aluminium (Bouzoubaa and Foo, 2004).

Fly ash can be used as a raw material to manufacture cement for several reasons. First, due to its richness in silica, aluminum, calcium and iron, fly ash can replace raw materials in cement feed, such as shale and clay, which are otherwise mined or purchased (Gajda *et al.,* 2006). Second, the carbon content in certain fly ashes can provide a fuel supplement for the energy-intensive cement manufacturing process (Gajda *et al.,* 2006). An approximate fuel savings of 4% and a nearly 10% increase in cement production was

realised when several hundred tons of dry fly ash, with up to 20% unburned carbon, was used as a raw mix component in cement plants in the US Midwest. Cements produced from the demonstrations showed properties comparable to those of the normally produced cements (Gajda *et al.*, 2006).

Fly ash from municipal solid waste incineration was also found to be a suitable raw material for cement manufacture in Taiwan, as long as the concentrations of salts (chloride in particular) are limited (Pan *et al.*, 2008).

1.4 Fly Ash as Mineral Admixture for Cement Mortars and Concrete

Fly ash may be used as a partial replacement of cement in concrete as long as it meets specific requirements. Fly ash substitution for structural concrete applications typically ranges from 15 to 35 wt%, and amounts up to 70 wt% have been used for mass concrete in dams, walls and roller-compacted concrete pavements (Manz, 1999). These requirements are outlined in ASTM C618 (2003).

ASTM C618 (2003) is entitled "Standard Specification for Coal Fly-ash and Raw or Calcined Natural Pozzolan for Use in Concrete." It should be noted that although the designation deals with specifications for fly ash use in *concrete*, many of its requirements are for cement *mortars*. Concrete refers to a mixture of cement, water, coarse aggregate and fine aggregate whereas mortar refers to a mixture of cement, water and fine aggregate (ASTM C109, 2003). One of the major limitations of the current ASTM designation is that it only allows the use of 100% coal fly ash and not fly ash from biomass, despite the documented suitability of various biomass-derived fly ashes as cement admixtures (Wang *et al.*, 2008a; Steenari and Lindqvist 1999; Lu G. *et al.*, 2008; Ipatti, 1998; Demirbas

2005, Chao *et al.*, 2008; Chindaprasirt *et al.*, 2008; Schlorholtz, 2005). Land-filling of all fly ash from blended burns may cause a reconsideration of the true benefit of biomass-fuels. Therefore, research must be done into the suitability of biomass-coal fly ash for traditional fly ash use.

1.4.1 Cement Chemistry and Fly Ash

Cement is a common binding agent used mainly in making concrete (CIPEC 2001). Cement is a finely ground, usually grey coloured, mineral powder, that when mixed with water acts as a glue to bind together the sand, gravel and crushed stone to form concrete (Lehigh Cement, 2008). Although there are several types of cement, portland cement is the most common for general use (Canadian Encyclopedia, 2008). Portland cement was patented by Joseph Aspdin in 1824 (Canadian Encyclopedia, 2008).

A cement chemistry shorthand notation is commonly used for simplification (Taylor, 1997). This notation is shown in the following table for the compounds discussed in this thesis:

Table 1-4: Cement chemistry abbreviations

Shorthand notation	C	S	A	F	H	$\bar{S}$
Actual Meaning	CaO	SiO_2	Al_2O_3	Fe_2O_3	H_2O	SO_3

Portland cement consists of five major components and a few minor components. The composition of a typical portland cement is listed by weight percentages in the following table (Taylor, 1997).

Table 1-5: Portland cement composition (Kosmatka *et al.*, 2002)

Cement Compound	Weight Percentage (%)	Chemical Formula	Shorthand Notation
Tricalcium silicate	40 – 63	Ca_3SiO_5 or $3CaO{\cdot}SiO_2$	C_3S
Dicalcium silicate	9 – 31	Ca_2SiO_4 or $2CaO{\cdot}SiO_2$	C_2S
Tricalcium aluminate	6 – 14	$Ca_3Al_2O_6$ or $3CaO{\cdot}Al_2O_3$	C_3A
Tetracalcium aluminoferrite	5 – 13	$Ca_4Al_2Fe_2O_{10}$ or $4CaO{\cdot}Al_2O_3{\cdot}Fe_2O_3$	C_4AF
Gypsum	3 – 5	$CaSO_4{\cdot}2H_2O$	$C\bar{S}H_2$

With the addition of water to the cement, each compound participates in hydration reactions. The hydration reactions for major components are as follows (Taylor, 1997):

C_3S + water → CSH (calcium silicate hydrate) + CH (calcium hydroxide)

C_2S + water → CSH + CH

$C_3A + CaSO_4{\cdot}2H_2O$ + water → $C_6A\bar{S}_3H_{32}$ (ettringite, AFt)

$C_3A + C_6A\bar{S}_3H_{32}$ + water → $C_4A\bar{S}_3H_{12}$ (monosulfate, AFm) [with gypsum]

C_3A + water → $C_4AH_{13} + C_2AH_8$ → $2C_3AH_6$ (hydrogarnet) + water [without gypsum]

When water comes into contact with C_3S, a five-stage hydration reaction takes place:

1. An immediate reaction, with calcium ions passing into solution from the surface of the C_3S grains. This is a period in which rapid heat evolution occurs, as well as a rapid rise in pH. The pH rises up to 12, which makes a very alkaline solution.
2. A "dormant" period of relative inactivity in which a slow rise in calcium ion concentration continues to take place until the concentrations of calcium and hydroxide reach a critical value in solution.
3. An acceleration period in which solid CH crystallizes from solution and CSH deposits into available water filled space.
4. A deceleration period which is the consequence of hydration products being formed, thus decreasing the porosity of the matrix and the transportation of ionic species on the liquid-solid interface.
5. Very slow reaction until completeness.

The fact that fly ash is a pozzolan enables it to be incorporated into the reaction scheme. The hydration product CH reacts with the aluminosilicate phases in fly ash according to:

$$CH + S + H \rightarrow CSH$$

The stoichiometric coefficients of this reaction are not fixed (Berry, 1976; Wang *et al.*, 2008a; Bouzoubaa and Foo, 2004). The complicated reaction scheme of both the cement and the fly ash leads to a variety of products collectively termed CSH gels (Wang *et al.*, 2008c). CSH gels account for the main strength gain of concrete. Since the fly ash

particles produce CSH gels, they contribute to the strength of the concrete. Unlike the CSH gel of hydrated portland cement, the CSH gels in mortars containing coal fly ash contain elements such as Fe, Na, K, S and Mg, and also show substitution of Si by Al and Fe (Goni, and Gurrero, 2007).

In addition to the formation of the CSH gels, calcium sulfoaluminates are also produced in early curing ages (Minnick, 1967, Shikami, 1956; Saji, 1959).

1.4.2 Properties Affected by Fly Ash Addition

Workability

When fly ash is substituted for portland cement in cement mixtures, a mortar is created that has different properties from those of a pure cement mortar (ASTMC618, CSA-A3001). The properties of the cement mortar will be directly dependent on the characteristics of the fly ash. The mortar exhibits various physical properties which can be grouped into a broader category termed "workability." The workability of a concrete mortar can vary drastically with fly ash addition (ASTMC618, 2003; CSA-A3001, 2003; Berry, 1976; Berry and Malhotra, 1978).

The water requirement is a means to measure workability (Berry and Malhotra, 1978; ASTM C311, 2003). Generally, increasing the percent substitution of portland cement with fly ash decreases the water required to achieve a given flow relative to a control mortar with no fly ash addition. Pasko and Larson (1962) and Larson (1964) found that a 30% replacement of portland cement by a coal fly ash resulted in a 7.2% reduction in water requirement. Samarin *et al.,* (1983) found that the reduced water requirement due to fly ash addition resulted in less excess water in the pore space and an

increase of strength. Partial replacement of portland cement by fly ash in concrete reduces water requirement to obtain a given consistency, or increases the workability and slump for a given water content compared to that of concrete without fly ash (Bouzoubaa and Foo, 2004). Fly ash particles have a spherical shape and smooth surface as opposed to cement particles, which exhibit more angular shapes. This may partially explain the increased workability and decreased water requirement (Berry and Malhotra, 1978). Another explanation could be that fly ash is less reactive towards hydration reactions than cement, leaving more water that can to contribute to flow. Greater workability can result in concrete elements having sharp and distinctive corners and edges, as well as a better appearance (Samarin et al., 1983).

Biomass-coal blended fly ashes have been found to have similar effects on workability. Fly ashes derived from biomass such as peat and switch grass were also found to improve the workability and cohesion of concrete (Ipatti, 1998; Schlorholtz, 2005; Wang *et al.,* 2008b).

Entrained Air

Several properties of concrete are improved when air is entrained. The inclusion of air as small (less than 250 μm) bubbles makes the concrete more resistant toward damage from freezing and thawing and improves its workability and cohesion (Paille're, 1995; Bruere, 1971), with negligible increase in the production costs (Rixom, 1998; Dodson, 1990). On the other hand, too high air content reduces the strength of the concrete (Bruere, 1971; Nasvik and Pistilli, 2004). Air entraining agents (AEAs) are commonly used to control the amount of air entrained in concrete. These AEAs are typically aqueous mixtures of

ionic or non-ionic surfactants derived from either natural sources (wood resins, tall oil) or chemical synthesis (Hewlett, 1997; Gao *et al.*, 1997). Surfactants adsorb strongly at the air–water/cement interface, with their non-polar end toward the interior of the air bubble and their polar end in the aqueous phase or adsorbed on the surface of the cement particle (Hewlett, 1997; Bruere, 1971). This effect stabilizes the air bubbles, which would otherwise coalescence into larger bubbles leaving the concrete mixture (Ramachandran, 1984).

Fly ashes derived from coal as well as from biomass have been shown to decrease the air entrained in a concrete sample, or to increase the amount of air entraining agent required to maintain appropriate air content (ACIC, 1962; Bloem, 1954; Campbell, 1961; Grieb and Woolf, 1961; Friis 1958; ASTM Committee IIIH, 1962; Bouzoubaa and Foo, 2004). The carbon content of the fly ash has a large affect on the amount of air entraining agent required (Berry and Malhotra, 1978). Active carbon present in fly ash adsorbs AEA. A large part of the carbon surface is non-polar compared with the polar surface of the inorganic particles (Pedersen *et al.*, 2008). This provides active adsorption sites for the hydrophobic part of the surfactants. Thus, the carbon competes with the air/water interface (Pedersen *et al.*, 2008).

Mortars amended with fly ashes derived from combustion of coal, wood or switch grass plus coal required increased amounts of AEA in order to meet a target entrained air of 4 to 6 vol% (Wang *et al.*, 2008b). Mortars containing fly ash derived from biomass were found to vary greatly in required AEA, with some requiring less AEA than mortars containing coal fly ash. This contrasts with the expectation that the air entraining demand of fly ash in concrete is primarily affected by adsorption of the air entraining agents on

carbon (Larson, 1964; ACIC, 1962; Bloem, 1954; Campbell, 1961; Grieb and Woolf, 1961; Friis, 1958; ASTM Committee IIIH, 1962). Wang *et al.* (2008b) concluded that a fly ash derived from wood had a very high LOI compared to other fly ashes, but it did not require more air entraining agent.

There is some disagreement between researchers regarding the significance of increased AEA requirements with ash-amendment. Although popular opinion is that this is an issue of great importance (Larson, 1964; ACIC, 1962; Bloem, 1954; Campbell, 1961; Grieb and Woolf, 1961; Friis, 1958; ASTM Committee IIIH, 1962), some authors suggest that the economical effect of increased AEA requirement is negligible because very little agent is required to raise the air content substantially (Wang *et al.,* 2008b).

Setting Time

The setting time of cement mortar/concrete is an indication of how long the material takes to reach certain hardness (ASTM C403, C191, C266, 2003). For concrete it is measured by ASTM method C403 (2003), where the penetration pressure of a standard needle is monitored as a function of time. For cement mortar or paste it is assessed using a Vicat or Gillmore apparatus (ASTM C191, C266, 2003) whereby depth of penetration of a needle is monitored with time.

Some studies have shown that the addition of fly ash has only a marginal effect on the setting time of mortars (Samarin *et al.,* 1982). In studies comparing the setting time of fly ash derived from biomass or coal-biomass blends, it was found that fly ash addition prolonged the setting time slightly, but that there was no major difference between types

of fly ash (Wang *et al.*, 2008b). Fly ashes derived from wood and switch grass showed more rapid setting times than a Class C coal fly ash (Wang *et al.*, 2008b).

Compressive Strength Development

Strength development is assessed to determine the appropriate uses of concrete mortars (CIPEC, 2001). Strength and strength development are affected by the properties of the fly ash (e.g., chemical composition, particle size), the cement used, the mix proportioning, and the curing conditions (Burden, 2003; Samarin *et al.*, 1983; Berry and Malhotra, 1978). Standards for fly ash use as an admixture for concrete stipulate the compressive strength requirements of cement mortars (ASTM C618, 2003; CSA-A3001, 2003). Compressive strength is a measurement of strength to failure of cubes or cylinders of cement mortar (ASTMC109, 2003; CSA-A3001, 2003). ASTM C618 (2003) and CSA-A3001 (2003) both stipulate that the compressive strength development of mortars containing fly ash must be at least 75% that of ash-free mortar after either 7 or 28 days of curing (ASTMC618, 2003; CSA-A3001, 2003).

Although concrete and cement mortars containing fly ash generally gain strength at a slower initial rate compared to those containing no fly ash, the long term strength is usually higher (Manz, 1999; Washa and Withey, 1953; Lamond, 1983; Samarin *et al.*, 1983; Costa and Massazza, 1983; Abdun-Nur, 1961; Pasko and Larson, 1962). This is mainly attributable to the pozzolanic nature of fly ash. (Samarin *et al.*, 1983, Berry and Malhotra, 1978; Ipatti, 1998; Wang *et al.*, 2007; Bouzaba and Foo, 2004). It reacts with CH, which does not contribute to strength, and forms CHS gels which do. Fly ashes with small particle size have increased reactive surface areas, and thus can contribute to higher

strength development due to pozzolanic reactions (Wang *et al.*, 2007; Berry, 1976; Berry and Malhotra, 1978). Further strength enhancement results from the reduced water requirement (Samarin *et al.*, 1983; Burden, 2003).

The effects of biomass-derived fly ash have also been studied (Schlorholtz, 2005; Wang *et al.*, 2007, Ipatti 1998). Fly ash from the co-combustion of switch grass with coal (Wang *et al.*, 2008a) and from the combustion of pure peat (Ipatti 1998) were found to meet strength requirements (as per ASTMC618 (2003) and CSA-A3001 (2003)) at cement substitutions of up to 59 and 33 wt%, respectively.

Durability to Freeze-Thaw

Cycles of freezing and thawing due to seasonal temperature changes are very destructive to concretes that have not been specifically treated to withstand such harsh conditions (Berry and Malhotra, 1978). The major factor contributing to freeze-thaw durability is the amount of air entrained, with higher air content correlating with higher durability. Generally, fly ash has been found to have little effect on the durability to freezing and thawing as long as a suitable amount of air (4-6 vol%) is entrained, which, as already discussed, usually necessitates further AEA addition (Wang *et al.*, 2008c; Larson, 1964; Washa and Withey, 1953; Lamond, 1983; Samarin *et al.*, 1983; Costa and Massazza, 1983; Abdun-Nur, 1961; Pasko and Larson, 1962).

Only a limited number of studies are available on the freeze-thaw durability of mortars/concrete made with fly ash derived from biomass. Wang *et al.* (2008c) reported weight loss after 300 freeze-thaw cycles on concrete samples with 25 wt% fly ash substituted for cement.

Resistance to Chemical Attack

The addition of fly ash to concrete has been shown to influence its durability to chemical attack (Berry and Malhotra, 1978). Leaching of calcium hydroxide, acidic dissolution of cementitious hydrates, the action of atmospheric and dissolved carbon dioxide and the reactivity of cement components to ions in solution cause deterioration of concrete exposed to chemical action (Berry and Malhotra, 1978). Sulfate and chloride ions in soil, aggregates, ground and sea water also cause the deterioration of cement structures. The addition of alternative materials such as fly ash, ground blast furnace slag and silica fume is known to enhance concrete durability due to refinement of the pore structure, lower pore solution pH, and pozzolanic reaction of fly ash (Lorenzo *et al.*, 2003). Calcium hydroxide is removed by the pozzolanic action of fly ash, which leads to long-term gains in strength and resistance to aggressive environments (Lea, 1973; Berry and Malhotra, 1978). Recently, the addition of fly ash derived from co-firing of biomass and coal was also found to improve the durability of concrete in a chloride environment (Wang *et al.* 2008c).

1.5 Atikokan Bio-energy Research Centre – Project Background

Government of Ontario has committed to phasing out coal powered electricity by 2014 (IESO, 2008). The government has been working with Ontario Power Generation, which produces approximately 70% of Ontario's power (Todd, 2009). Discontinuing coal powered electricity is a very ambitious goal, as in 2008 over 20% of Ontario Power Generation's power was derived from fossil fuels (with the majority being coal fuelled) (Todd, 2009). In order to meet this goal, Ontario Power Generation has implemented a biomass strategy, of which the main goal is to continue testing until all of Ontario's fossil plants have a biomass option (Todd, 2009). Among many challenges is fly ash reuse (Todd, 2009).

Major objectives of this testing program include understanding fuel availability, handling and storage investment, understanding necessary combustion modifications, as well as an extensive economic evaluation. OPG has also made several commitments, such as refusing the use of food crops for power generation, ensuring the sustainable harvest of wood fuel, and obtaining biomass with minimal impact on consumers and existing resource users.

One phase of this testing program is the co-firing of coal with biomass, in order to achieve benefits such as: renewable energy; meeting energy demands in real time; reductions in greenhouse gas, sulphurous, nitrogenous and mercury emissions; making use of existing plants (which lowers capital cost). Major challenges which require further investigation include: fuel cost (biomass is more expensive than coal); biomass requires covered shipping and storage; potential boiler issues (such as slagging, fouling, and capacity; ash re-use considerations.

The Atikokan Generating Station (AGS), which is a coal-fired power generating station with a 211 MW capacity in Atikokan, Ontario was chosen to host the Atikokan Bio-energy Research Centre. AGS typically fires lignite coal and has a boiler design favourable for 100% biomass fuel combustion (due to boiler tubes being further spaced apart). AGS also has a rail spur for delivery of fuel. To date, burns of up to 100% wood pellets have been successful.

1.6 Opportunities for Further Studies

Although much work has been completed on the characterization and utilization of coal fly ash for partial substitution of portland cement in concrete, even dating back to the 1930s (Davis et al., 1937), little work has focused on the use of fly ash derived from biomass for the same purpose. Studies involving biomass derived fly ash suffer from a number of limitations that are discussed below.

In some studies, the fly ash was not obtained from the co-combustion of biomass and coal, but rather was a blend of fly ashes derived from the separate combustions of pure biomass and pure coal (e.g, Wang *et al.,* 2008a,b,c). The compositions of the individual fly ashes used for blending may have been very different from that which would have resulted from combusting biomass and coal together.

The fly ash in some studies was not from a full scale thermoelectric power generating station. Although in some research cases, it is reasonable to use smaller scale equipment, fly ash has been found to vary vastly in physical characteristics depending on the equipment configuration (Clendenning and Durie, 1962; Berry, 1976). Therefore it is necessary to study the effects of co-combusting coal and biomass on fly ash from a full scale thermoelectric power station.

The reported elemental composition of biomass derived fly ash includes major oxides (SiO_2, Al_2O_3, Fe_2O_3, CaO, MgO, K_2O, Na_2O) and the LOI (Karayigit and Gayer, 2001; Wang *et al,.* 2008; Steenari and Lindqvist, 1999; Demirbas, 2005; Ipatti, 1998; Schlorholtz, 2005; Chindaprasirt *et al.,* 2008). However, in many cases, metal constituents have not been reported. Amounts of metals present in biomass-derived fly ash will most likely be significantly different from those found in coal fly ash due to the

nature of the combustion fuel. Although the composition of coal varies depending on its origin, it typically includes mercury, which can be harmful to the environment. Analysis of the metals present in fly ash derived from biomass and comparison with coal fly ash may provide a more complete assessment of potential environmental benefits or concerns associated with using biomass as a fuel.

Since the reactivity of fly ash has been associated with particle size (Clendenning and Durie 1962; Wang *et al.* 2008c), it would be useful to analyse the particle size distribution of biomass-derived fly ash. However, few studies on the characterization of biomass derived fly ash report on physical characteristics such as particle size or density.

A major limitation to current reports which characterize the microstructure of biomass-derived and coal fly ash is the lack of quantitative data. Therefore, it would be beneficial to perform a full quantitative calibration with appropriate standards for energy dispersive spectrometry, and then complete analysis on a multitude of fly ash particles.

ASTM C109 (2003) is the testing standard for compressive strength analysis to regulate the use of fly ash as a substitute for portland cement and involves a 20 wt% substitution of portland cement by fly ash. Nevertheless, the pressure to mitigate industrial waste, as well as the economical benefits for portland cement substitution by fly ash are compelling reasons to increase the amount of fly ash beyond 20 wt%. Another limitation of ASTM C109 (2003) is that compressive strength is only measured after 7 and 28 days of curing. Because fly ash generally retards the development of strength, especially at high percent substitutions, the compressive strength should be analysed beyond the 28 days prescribed in ASTM C109 (2003). Many studies have included compressive strength values beyond 28 days (including over 180 days) (Wang *et al.*,

2008b; Ipatti 1998; Schorhotlz, 2005). Therefore, by extending the curing time to more than 180 days, the long term effects of the fly ash can be examined.

Freeze-thaw analysis is rarer than that of compressive strength, and the required tests can last for a substantially longer time (up to 300 cycles of 5 hours per cycle) (ASTM C666, 2003). Although some data is reported on the effect of biomass-derived fly ash-amendment (e.g., Wang *et al.*,2008c), it is generally scarce and limited. Hence, the resilience of mortars containing fly ash to freeze-thaw cycles is worthy of further study.

2.0 Research Objectives

The objectives of this thesis research were:

1. Characterize the chemical and physical properties of fly ash from the combustion of coal (CFA) and the co-combustion of coal and biomass (CBFA) and compare them on the basis of:
    a. Composition (bulk samples and individual particles)
    b. Mineralogy
    c. Density
    d. Particle size distribution
2. Analyse and compare the microstructures of particles of CFA and CBFA
3. Assess the potential of the above fly ashes as partial substitutes for portland cement in cement mortars by examining:
    a. Water requirements for mortars containing varying proportions of fly ash.
    b. Air content of fresh cement mortars containing varying proportions of fly ash and varying amounts of AEA.
    c. Compressive strength development of mortars containing varying proportions of fly ash.
    d. Durability to freeze-thaw of mortar cubes containing varying proportions of fly ash.
4. Examine the microstructure of mortars containing varying proportions of fly ash, in order to investigate the reactivity of individual fly ash particles and the effect of fly ash on the hydration of cement mortars.

3.0 Materials and Methods

3.1 Materials

3.1.1 Fly Ashes

The fly ashes used in this research included a conventional coal fly ash (CFA) and fly ashes generated from the co-combustion of coal and biomass (CBFA). All fly ashes came from the AGS. The coal used at the AGS was lignite coal from Saskatchewan, and the biomass was pelletized wood chips, primarily from Western Canadian forests which were destroyed by pine beetle infestation.

Combustion Fuels

The wood pellets ranged in size from a fraction of a centimetre to a few centimetres, as seen in Figure 3-1. The pellets were added to the process through the coal hoppers, which was the same manner as coal. Figure 3-2 displays a large bag of pellets being lifted over a triangular metal piece used to break the bag open, releasing the pellets. The pellets were then carried by conveyer and directed to a pulverizer which was used exclusively to crush the pellets to a consistency fine enough to allow them to be blown into the boiler with coal.

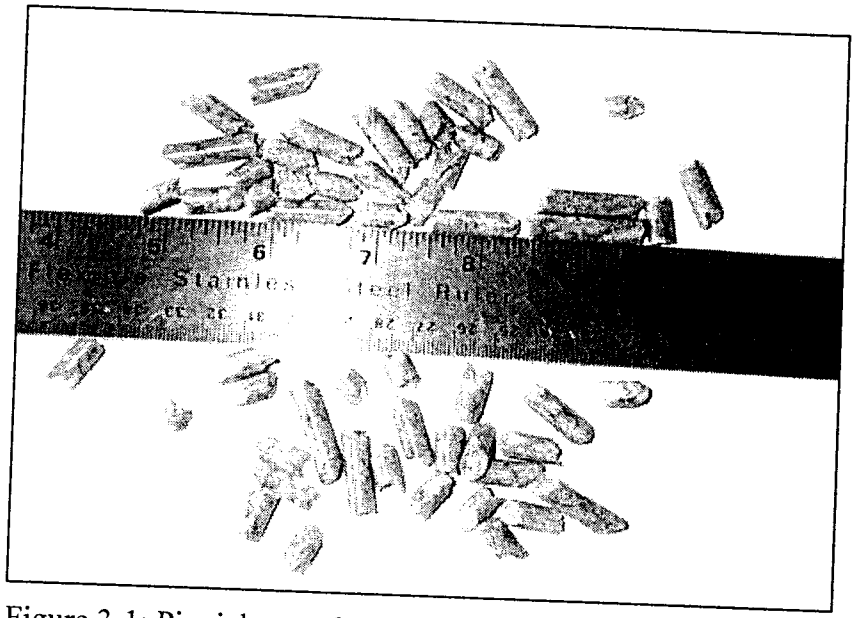

Figure 3-1: Pinnicle wood pellets, used at AGS.

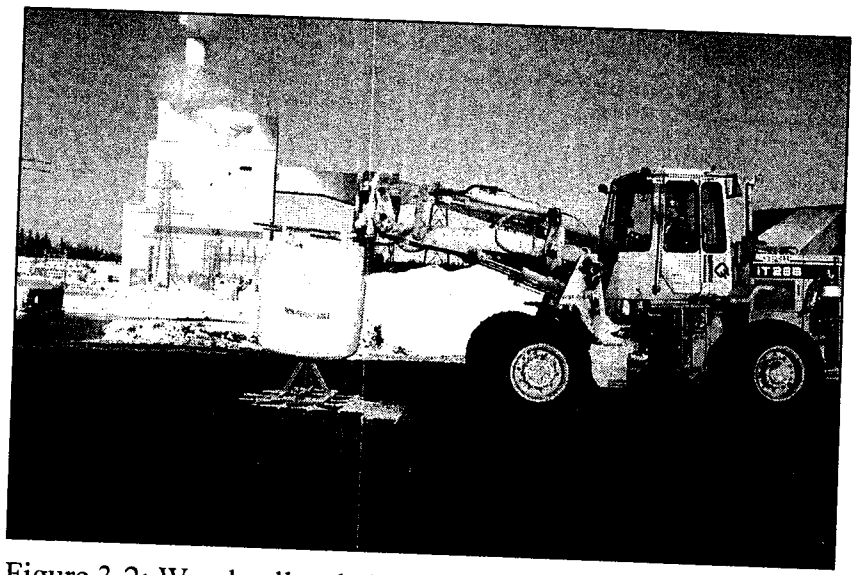

Figure 3-2: Wood pellets being added to the coal hopper at AGS.

Analyses of the lignite coal and wood pellets were provided by OPG. Table 3-1 provides proximate analysis results for the fuels as-fired. Even in examining the most basic of fuel properties, it can be seen that the lignite coal and wood pellets are very different. The wood pellets are much more abundant in volatile matter and much less abundant in fixed carbon compared to the lignite coal. The calorific value of the wood pellets is higher than that of the coal, which would indicate that wood pellets will be able to provide adequate heating value for power generation. The main disparity between the two fuels, which will become most important for this research, is the fact that the ash content of wood pellets is at least 20 times lower than that of lignite coal.

Table 3-1: Proximate analysis of lignite coal and wood pellets (OPG)

Parameter	**Lignite Coal**	**Wood Pellets**
Volatile Matter	25%	81.65%
Fixed Carbon	31%	12.50%
Ash	10%	< 0.50%
Moisture	34%	5.83%
Calorific Value	15,800 kJ/kg	18,674 kJ/kg

Table 3-2 displays ultimate analysis results for lignite coal and wood pellets on a dry basis. Again the different fuels possess significantly different values for many of the parameters in ultimate analysis. Lignite coal has higher carbon, nitrogen and sulfur contents (and as aforementioned a much higher ash content), but lower contents of hydrogen and oxygen compared to wood pellets. The disparity in these parameters may affect combustion conditions, which can have significant effects on fly ash properties.

Table 3-2: Ultimate analysis of lignite coal and wood pellets (OPG)

Parameter (%)	Lignite Coal	Wood Pellets
Carbon	63.10	51.96
Hydrogen	4.12	6.14
Nitrogen	1.02	0.22
Sulfur	0.55	0.01
Oxygen	18.00	41.65
Ash	13.16	0.02
Total	100.00	100.00

Table 3-3 provides the inorganic elemental compositions of lignite coal and wood pellets on a dry basis. The wood pellets have relatively low amounts of inorganic material, which would be expected due to the extremely high volatile matter and low ash content of the wood pellets. Lignite coal contains a greater amount of every constituent than wood pellets, with the exception of manganese.

The major inorganic constituents of lignite coal are Si>Al≈Ca>Na>Fe>Mg≈Ba>Ti≈Sr, compared to wood pellets, for which the major inorganic constituents are Ca>K>Mg≈Si>Mn>Al≈Fe.

X-ray diffraction analysis of wood pellets and coal was completed at Lakehead University. XRD results revealed quartz (SiO_2) and kaolinite ($Al_2Si_2O_5(OH)_4$) present in lignite coal and cellulose ($(C_6H_{10}O_5)_n$) present in wood pellets.

Table 3-3: Elemental analysis of lignite coal and wood pellets (OPG)

Weight (mg/kg)	Lignite Coal	Wood Pellets
Aluminum	13651.00	43.00
Barium	1880.00	4.97
Boron	176.00	1.54
Calcium	12953.00	694.45
Iron	4920.00	29.90
Magnesium	2239.00	177.86
Phosphorus	304.00	16.074
Potassium	535.00	401.13
Silicon	25452.00	162.35
Sodium	7461.00	10.30
Strontium	631.00	3.78
Titanium	699.00	2.14
Antimony	0.40	<0.10
Arsenic	2.80	<0.10
Beryllium	0.70	<0.10
Bismuth	0.30	<0.10
Cadmium	0.10	<0.100
Chromium	10.40	3.40
Cobalt	1.40	<0.10
Copper	7.40	0.84
Lead	7.40	<0.10
Lithium	9.90	0.18
Manganese	19.00	87.47
Mercury	0.09	<0.10
Molybdenum	2.50	<0.10
Nickel	9.70	1.25
Rubidium	2.60	0.61
Selenium	1.10	<0.10
Silver	0.20	<0.10
Tellurium	0.30	<1.0
Thallium	0.10	<0.10
Thorium	3.40	<0.10
Tin	1.20	<0.10
Uranium	1.90	<0.10
Vanadium	11.00	<0.10
Zinc	10.00	9.12
Zirconium	35.00	<0.10

Fly Ash Collection

The fly ashes were taken from collection hoppers located below the electrostatic precipitators. Figure 3-3 displays photographs taken at AGS of the ash hoppers. The image to the right is a close up view of the sample port where the fly ashes were collected into five gallon buckets. In order to ensure representative samples of fly ash, the hoppers were emptied prior to each co-combustion test and allowed to have the fly ash run through them for one to two hours during the co-combustion prior to fly ash collection. The pilot scale co-combustion test burns occurred at various dates through 2008. The coal fly ash was collected prior to any biomass firing at the AGS.

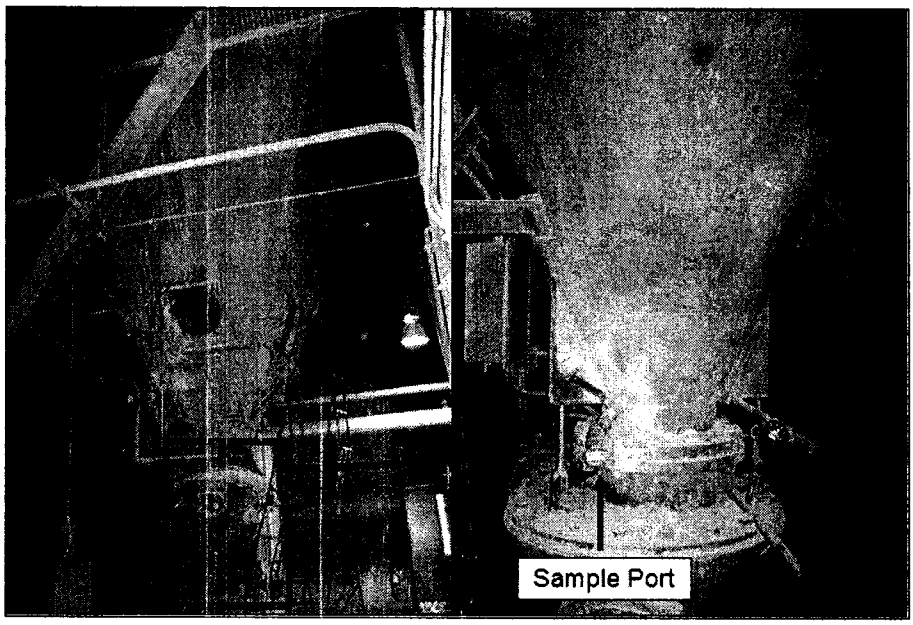

Figure 3-3: AGS fly ash collection hoppers located below electrostatic precipitators

AGS did several successful tests of co-combustions of lignite coal and wood pellets. For each co-combustion test, the amounts of energy contributed by the combustion of the wood pellets and that of coal were determined from their heating

values. A description of the fly ash samples, including date of collection, combustion materials, and loading of the boiler is provided in Table 3-4. The acronym CFA is used to refer to coal fly ash, which was obtained by combusting undiluted lignite coal. The acronym CBFA is used to refer to coal-biomass fly ash. The 2 digits before the acronym indicate how much energy was contributed by the wood pellets (i.e. 15CBFA refers to 15% energy from wood pellets and 85% from lignite coal). The approximate weight percent of the fuel components are provided in the second column of Table 3-4.

Table 3-4: Fly ash samples collected at AGS

Identification	Combustion Fuel (wt %)	Collection Date	Percent of Full Load (%)
CFA	100% Lignite Coal	Oct. 23/07	~50
15CBFA	13% Wood Pellets 87% Lignite Coal	Jan. 19/08	100
66CBFA	62% Wood Pellets 38% Lignite Coal	Jul. 8/08	~50
BFA	100% Wood Pellets	Jul. 10/08	-

3.1.2 Other Materials

Cement

The cement used in the manufacture of cement mortars was ordinary portland cement (OPC) Type I, which is specified by ASTM C150 (2003). The manufacturer of the cement was Lafarge, Montreal, PQ.

Sand

ASTM C109 (2003) requires the use of graded sand conforming to specifications outlined in ASTM C778 (2003). Sand was provided by Hoskin Scientific, Burlington ON. X-ray diffraction of the sand confirmed that the sole mineral phase was SiO_2, conforming to ASTM standards. The grading of the sand was also checked by sieve analysis and was found to meet requirements (ASTM C778, 2003). Table 3-5 shows the actual grading of the sand compared to ASTM requirements.

Table 3-5: Gradation of standard sand

Sieve #	**% Passing**	**ASTM Requirement % Passing**
850	100.0	100
600	99.6	96 to100
425	71.6	65 to 75
300	23.3	20 to 30
150	0.1	0 to 4

Mixing Water

Nanopure water (18.2 Ω, Barnstead D11911 Nanopure Diamond) was used for preparing all the mortar samples.

3.2 Methods

3.2.1 Fly Ash Characterization

The elemental composition of the fly ashes was analyzed by x-ray fluorescence (XRF) (major elements by borate fusion whole rock analysis and chloride by internal standard), LECO (sulfur), inductively-coupled plasma-atomic emission spectroscopy (ICP-AES) following acid digestion (trace metals), and cold vapour atomic absorption spectroscopy (AAS) (mercury). The carbon content was measured gravimetrically as loss on ignition (LOI). The aforementioned analyses were carried out at SGS Laboratories in Lakefield, Ontario. Mineralogical composition was determined by XRD. Particle size distributions (in triplicate) by laser particle size analyzer with deionized water (Malvern Mastersizer 2000). Although analysing particle size by wet method risks the dissolution of some particles, the solubility of predominant phases (aluminosilicates and calcium aluminosilicates) is extremely small. Fly ash specific gravity (SG) was determined by filling a 250 mL volumetric flask with kerosene and then removing 25 mL by pipette. A spatula was then used to introduce fly ash into the flask until the 25 mL volume had been replaced. The mass of fly ash was recorded and subsequently divided by the 25 mL volume in order to determine SG.

Images of each fly ash were taken with a scanning electron microscope (SEM) (JEOL JSM-5900LV), Stubs with adhesive were used to view powdered samples of each fly ash and viewed in secondary electron (SE) mode in order to examine the surface morphology of the fly ash particles. Polished slices were prepared by cutting and polishing using an oil based medium (kerosene) to maintain the integrity of water sensitive phases in the fly ash. The polished sections were vacuum-epoxy resin and

viewed in back-scattered electron (BSE) mode to enhance contrast between mineral phases. EDS analysis of polished slices of fly ash particles allowed to quantify more accurately the mineral phases present. All samples were carbon coated prior to SEM viewing. Quantitative elemental analysis of the fly ash sections was carried out by X-ray energy dispersive spectrometry (EDS) with an Oxford Link ISIS system, using calibration standards: garnet for Al, Fe, Mg and Si; orthoclase for K and Na; wollastonite for Ca; and barium sulfate for Ba and S. An accelerating voltage of 20kV, beam current of 0.475 mA, working distance of 10mm, and a vacuum pressure of $5x10^{-5}$ torr were consistently used for viewing of all samples.

3.2.2 Mortar Preparation and Testing

Mortars were prepared according to ASTM C109 (2003) using a Hobart five quart mixer. Fly ash was substituted for up to 40 wt% of the cement, as shown in Table 3-6. The specified amount of nanopure water was placed into the mixing bowl, followed by the cementitous material (fly ash + OPC). This was then mixed for 30 seconds on the lowest speed setting. The graded sand was then added gradually over a period of 30 seconds. The speed of mixing was changed to a medium, and mixing continued for 30 more seconds. During the next 90 seconds, the mortar remained in the bowl without being mixed, with the first 15 seconds being used to scrape down the sides and bottom of the bowl with a kitchen spatula. After the 90 seconds had elapsed, the mortar was mixed at medium speed for a full 60 seconds.

Next, the consistency of the cement mortar was determined according to ASTM C1437 (2003). This method involved the use a flow table to measure the percent increase

in diameter. A flow table is a device which employs a crank to lift and then drop a flat circular surface (the table). After preparation, the mortar was placed in a mold which is the frustum of a cone, with the base diameter measuring 10 cm. The mortar was placed to fill the flow table mold half way, and then was tamped 20 times in a radial manner in order to ensure that no cavities existed within the mold. The remainder of the mold was then filled with mortar and tamped in the same fashion. A straight edge was used to cut off the excess mortar overflowing the top of the mold. Immediately after the mold was filled, the table was wiped clean of any material which would impede the flow of the mortar during the testing. The mold was then removed and the crank was used to drop the table 25 times in a 15 second period. The dropping of the table forced the once 10 cm wide circle of cement mortar to enlarge. The percent change in diameter is calculated and used to indicate the consistency of the cement mortar.

The water content of the mortars containing fly ash was adjusted to achieve a consistency (diameter increase in the flow table testing) of ± 5% that of ash-free mortar (ASTM C109, 2003). The water requirement was found to be independent of the type of fly ash used. Consistency was determined according to ASTM C1437 (2003).

Table 3-6: Mix proportioning of mortar samples

Sample	OPC (g)	Fly ash (g)	Sand (g)	Water (mL)
0% Fly ash	500	0	1375	242
10% Fly ash	450	50	1375	232
20% Fly ash	400	100	1375	228
30% Fly ash	350	150	1375	212
40% Fly ash	300	200	1375	200

Air Content

For analysis of air entraining agent requirements, the air entraining agent (AEA) employed was AIREXTRA (Eucon Canada, Toronto), an aqueous solution of sulfonated fatty acids which conforms to ASTM C260 (Euclid, 2008). It was added to the mixing water at concentrations of 0, 0.2, 0.6 or 1.2 mL AEA/kg of cementitous material (fly ash + OPC). The dosing design covers the manufacturer's suggested dosing range of 0.3 to 1.0 mL AEA/kg of cementitous material (Euclid 2008). The air content of fresh mortar samples was determined in quadruplicate, according to ASTM C185 (2003). This method involved the use of a mold, which can hold 400 mL of mortar. Immediately upon mixing the mortar (as described above), 400 mL of mortar was placed in the 400 mL mold in three equal layers. Each layer was tamped 20 times. The final layer of mortar overfills the mold and was removed by cutting the surface of the mortar with a straight edge after tamping. The mass of the mold was subtracted in order to determine the actual mass of 400 mL of mortar (W_a).

The air content of the mortar was then determined by employing the following formula:

$$AC = 100\left[1 - \frac{W_a}{W_c}\right] \qquad [3\text{-}1]$$

Where AC = air content (%)

W_a = actual mass per unit volume as determined by test method

W_c = theoretical mass per unit volume, calculated on an air-free basis:

$$W_c = \frac{m_C + m_{FA} + m_S + m_W}{\frac{m_C}{SG_C} + \frac{m_{FA}}{SG_{FA}} \frac{m_{sand}}{SG_S} + \frac{m_W}{1}} \qquad [3\text{-}2]$$

Where m_C = mass of cement (g)

m_{FA} = mass of fly ash (g)

m_S = mass of graded sand (g)

m_W = mass of water (g)

SG_C = specific gravity of cement = 3.15 (ASMT C185, 2003)

SG_{FA} = specific gravity of fly ash (as previously determined)

SG_S = specific gravity of sand = 2.65 (ASTM C185, 2003)

Compressive Strength Development

For compressive strength analysis, the mortar (which had not been subjected to air content analysis) was immediately cast into two-inch cubes (American Cube Molds, Twinsburg, Ohio), which were cured for 24 hours in 100% humidity at 23 ± 2 °C. The molds used a metal mold frame into which three 2-inch cube polypropylene water tight liners were inserted. As required by ASTM C109 (2003), the cubes were removed from their molds at 24 hours. The liners were cut off and disposed of. Next, the mortar cubes

were submerged in saturated lime water until testing, in accordance with ASTM C109 (2003). After 1, 3, 7, 28 or 90 days of curing, the cubes were capped with polyurethane pads and retainers (American Cube Molds, Twinsburg, Ohio (ACM, 1994)), and their compressive strength was measured in quadruplicate using a Tinius Olsen analyser. Compressive strength analysis at 90 days is not prescribed by ASTM C109, but was necessary in order to examine the pozzolanic effects of the fly ash in the mortars. In compliance with ASTM C109, at the specified time of testing, the mortar cubes were wiped to a surface-dry condition, and loose grains and incrustations were removed from the faces which came into contact with the capping system. During testing, the capped cube was placed on a spherically seated block which was free to tilt. The load was then applied with a relative rate of movement within the range of 900 to 1800 N/s. This rate of movement was achieved during the first half of the anticipated maximum load, and no adjustments were made thereafter.

The compressive strength was then determined by:

$$CS = \frac{P}{A} \qquad [3\text{-}3]$$

Where CS = compressive strength of specimen (MPa)

P = total maximum load (MN)

A = area of specimen = 0.00258 m^2

Resistance to Freeze-Thaw Cycles

Mortar cubes were cured in saturated lime water for 14 days prior to subjection to freeze-thaw cycles, as prescribed in ASTM C666 (2003). For the purpose of this research, smaller sample sizes were used than those detailed in ASTM C666 (2003), since fly ash was not available in such large quantities. For each cycle, the cubes were placed in a freezer until their core temperature had decreased from 4°C to -18°C and then removed until it returned to 4°C. As ASTM (2003) specifies, cycles lasted between 2 and 5 hours, with no less than 20% of the time taken for thawing. When the cycles had to be stopped for a period of time, the cubes were kept in a frozen state, with the centre of the cubes never reaching lower than -20°C. During thawing of the cubes the temperature is not to exceed 6°C. Temperature was monitored using a reference mortar cube with a thermocouple imbedded at its centre by candle wax. All mortar cubes were subjected to the cycles simultaneously. Changes in dimension, mass, and compressive strength were measured every 35 cycles, as ASTM C666 (2003) prescribes number of cycles not to exceed 36 cycles without testing. The dimension of the cube was determined by taking two measurements of each cube using a calliper. The reported length of a cube side is an average of two measurements of four cubes for each mortar type at the specified time.

Microstructure and Micromineralogy of Mortar Samples

In order to examine micromineralogy, polished sections were prepared from the centre of 28-day old mortar samples containing fly ash. Preparing a polished specimen of cement mortar for examination under the SEM is facilitated if the porous space is first filled with a hard material such as epoxy resin, which stabilizes the microstructure and prevents damage during polishing. Filling the pores with epoxy is achieved using vacuum impregnation, in which the dried specimen is immersed in epoxy solution while under a vacuum and then is brought to atmospheric pressure while still immersed. The sections were lapped and polished using oil-based media so as not to alter the water-soluble minerals. After carbon-coating, the sections were imaged by SEM and quantitative EDS in the same manner as the polished samples outlined in 3.2.1.

4.0 Characterization of Fly Ash

4.1 Composition and Mineralogy

Table 4-1 shows the composition and LOI of the fly ashes. Co-firing biomass with coal did not markedly change the fly ash composition, owing to the low ash content of wood pellets (0.02 to 0.5 wt%) compared with lignite (10.0 wt%) (Section 3.1.1). All fly ashes contained 43-45 wt% SiO_2, 21-21.5% Al_2O_3, 13.6-14.5% CaO and 3.9-4.2% Fe_2O_3, putting them at the boundary between class C and class F composition (ASTM C618, 2003). The carbon content, reported as LOI, ranged from 0.40 to 0.91 wt%, which is much lower than the 6 wt% limit prescribed by ASTM C618 (2003). Fly ash compositions closely resembled that of fresh coal fly ash collected from the same boiler at AGS at an earlier date (prior to biomass testing) and reported by Yeheyis *et al.* (2008).

Table 4-1: Major elements of fly ash samples

Weight (%)	CFA	15CBFA	66CBFA
Total	96.34	97.11	97.10
SiO_2	43	45.2	43.6
Al_2O_3	21	21.5	21.0
Fe_2O_3	4.2	4.0	3.90
MgO	2.6	2.5	2.91
CaO	14.5	13.6	14.5
Na_2O	7.5	7.3	7.46
K_2O	0.6	0.7	1.17
TiO_2	0.9	1.0	0.89
P_2O_5	0.6	0.6	0.67
MnO	0.02	0.02	0.12
Cr_2O_3	0.0	0.0	0.0
V_2O_5	0.02	0.03	0.02
S	0.62	0.26	0.51
$SiO_2 + Al_2O_3 + Fe_2O_3$	68.2	70.7	68.5
LOI	0.78	0.40	0.91

Table 4-2 shows the concentrations of minor elements in fly ash samples. No significant difference in the concentrations of minor elements was observed between CFA and CBFAs, (again due to the extremely low ash content of wood pellets compared to lignite coal). All fly ashes contain significant amounts of toxic metals such as Cu, Co, Pb, Mo, Ni and Zn, which may leach by contact with water. However, the concentrations of all minor and trace elements are within the ranges reported for other fly ashes (Scheetz, 2009). When fly ash is blended with cement, toxic metals are stabilized by hydration products and their leachability is thus significantly reduced (Gougar *et al.*, 1996).

Table 4-2: Metals and chloride content of fly ash samples

(g/t)	CFA	15CBFA	66CBFA
Ag	<2	<2	<2
As	<30	<30	36
Ba	3800	3900	6700
Be	3.7	4.2	4.7
Bi	<20	<20	<20
Cd	<2	<2	<2
Co	17	16	<25
Cu	37	41	49
Hg	<0.3	<0.3	<0.3
Li	20	16	57
Mo	13	10	<15
Ni	28	27	31
Pb	39	48	55
Sb	<10	<10	<10
Se	<30	<30	<30
Sn	<20	<20	<20
Sr	3500	3300	3600
Tl	<30	<30	<30
U	<20	<20	<20
Y	41	45	47
Zn	37	53	150
Cl	30	20	63

Analysis by XRD (Figure 4-1) determined that all fly ashes exhibit a strong "halo" or "hump" in the 18-38° 2θ region due to the predominant amorphous phase. The principal crystalline component is quartz (SiO_2), plus there is some periclase (MgO), and possible traces of anhydrite (CaSO4), anorthite ($(Ca,Na)(Al,Si)_2Si_2O_8$), belite (Ca_2SiO_4), calcite ($CaCO_3$), feldspar ($K_{0.5}Na_{0.5}AlSi_3O_8$), gehlenite ($Ca_2Al_2SiO_7$), hematite (Fe_2O_3), lime (CaO), and mullite ($Al_{4.54}Si_{1.46}O_{9.73}$).

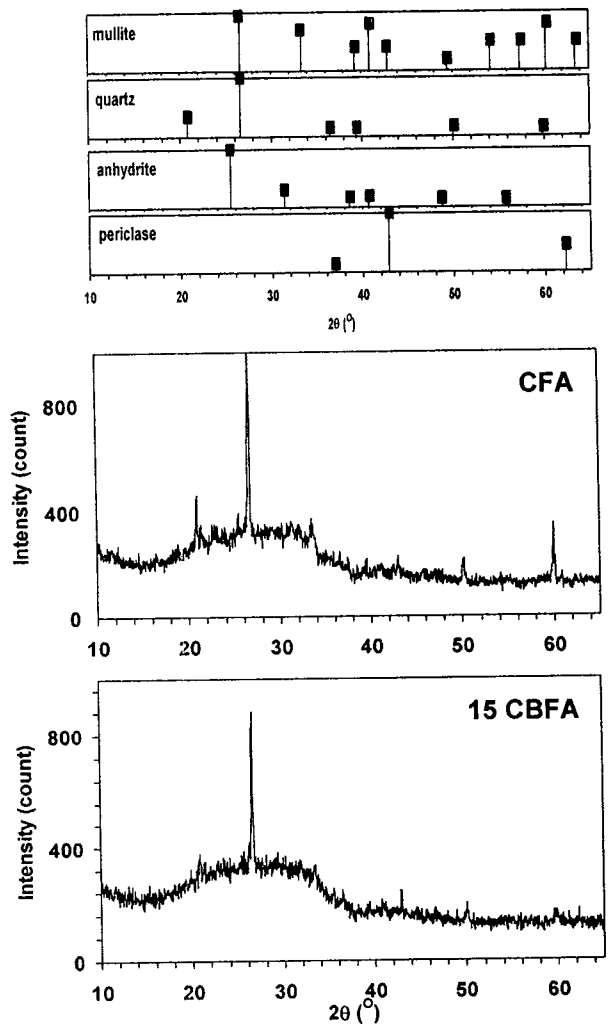

Figure 4-1: XRD spectra of CFA and 15CBFA.

4.2 Specific Gravity

The specific gravities measured for CFA, 15CBFA and 66CBFA were 2.404 ± 0.096, 2.361 ± 0.072 and 2.587 ± 0.128, respectively. The higher value obtained for 66CBFA could be attributed to a comparatively low content of porous particles (cenospheres). The cenosphere fraction of fly ash is affected by combustion temperature and fuel properties such as mineral impurities (Ghosal *et al.*, 1995; Bibby, 1977; Ngu *et al.*, 2007).

4.3 Particle Size Distribution

Figure 4-2 shows volume percent of fly ash samples with respect to particle size. Figure 4-3 depicts the cumulative particle size distribution of the fly ash samples. Both show that 15CBFA has a greater proportion of large (> 50 μm) particles than either CFA or 66CBFA which, in turn, have very similar particle size distributions. Since 15CBFA was collected with the boiler running at full load, larger particles may have been entrained in the steam being forced through the soot blowers. Conversely, at 50% load, CFA and 66CBFA would probably have cooled more rapidly, favouring formation of smaller fly ash particles. Figure 4-2 also shows that the distribution of particle size is bi-modal for all fly ash samples.

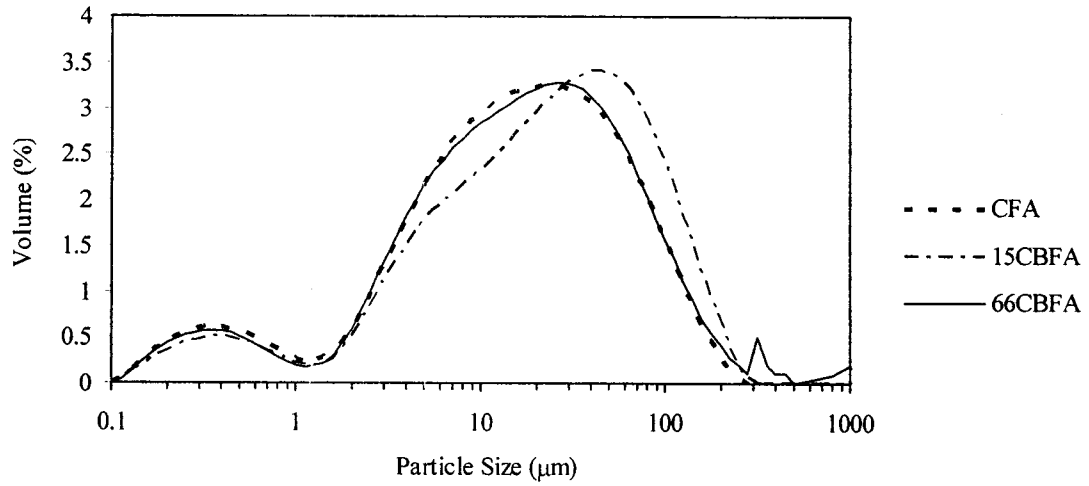

Figure 4-2: Particle size distribution of fly ash samples. Size measurements were averaged over three replicate samples, each of which was analyzed in triplicate.

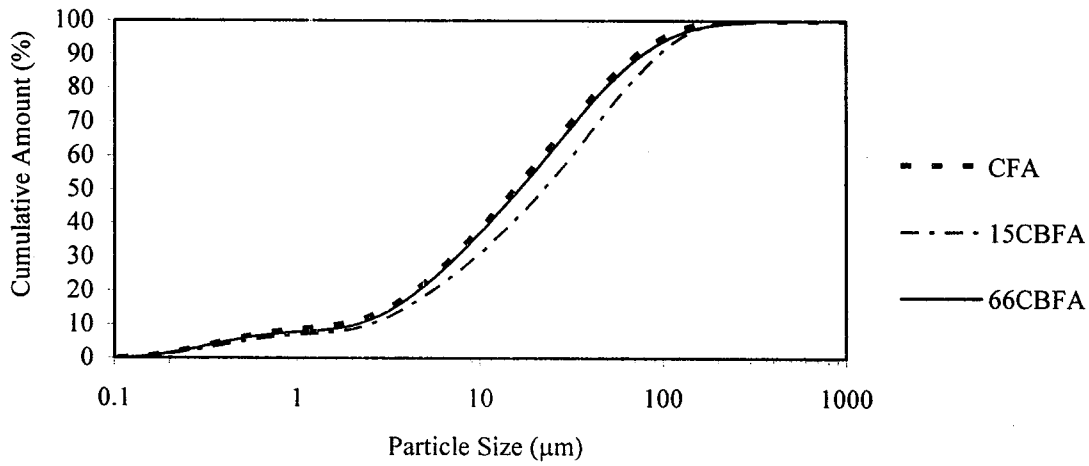

Figure 4-3: Cumulative particle size distribution of fly ash samples. Size measurements were averaged over three replicate samples, each of which was analyzed in triplicate.

4.4 Morphology and Micromineralogy

Most fly ash particles are spherical as a result of rapid cooling in the post-combustion zone of the boiler, and a significant proportion of particles are porous. In SEM images, differences in grey levels reveal compositional variations between the different particles. Light-shaded particles tend to be high in calcium, iron, magnesium, or titanium, while darker particles tend to have less of these elements and more sodium. A significant proportion of the fly ash particles are porous. Overall, CFA and CBFAs exhibit similar particle morphologies.

4.4.1 Fly Ash Powder

The following images display typical viewings of powdered stub samples on the SEM. The morphology and surface details of fly ash particles can be seen in Figures 4-4 through 4-9. The first three images, Figures 4-4, 4-5 and 4-6 show a lower magnification (x1200) of CFA, 15CBFA, and 66CBFA respectively. Subsequently, Figures 4-7, 4-8 and 4-9 show images of CFA, 15CBFA, and 66CBFA respectively, taken at higher magnification (x3000) in order to show more surface detail. The images display a wide variety of particle sizes.

The majority of particles in all fly ash samples were found to be spherical aluminosilicates (and can be seen in Figures 4-4 through 4-9). Aluminosilicate particles were abundant as porous and non-porous as well as large and small particles in all fly ashes. Even particles containing Ca, Na or Ti contain large amounts of aluminum and silicon. The particular quantitative data on these particles is discussed further in 4.4.2.

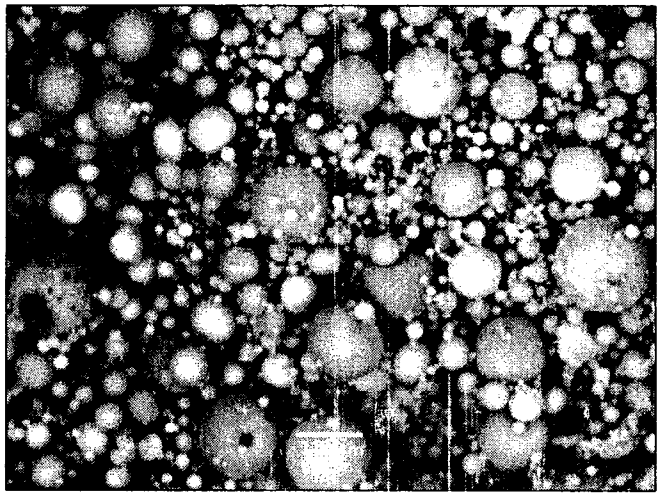

Figure 4-4: SE image of CFA powder.

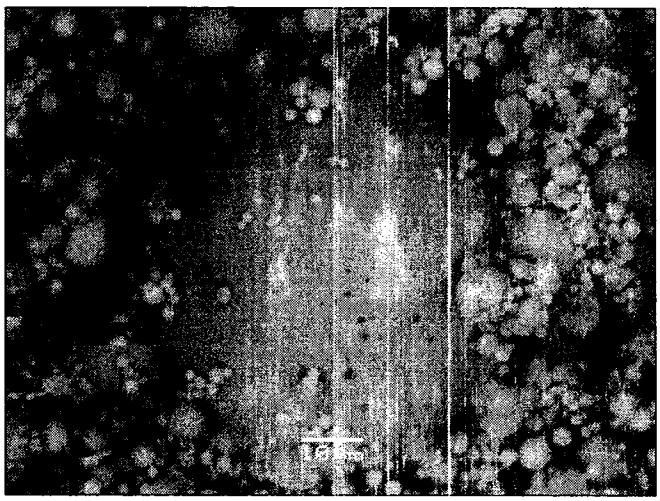

Figure 4-5: SE image of 15CBFA powder.

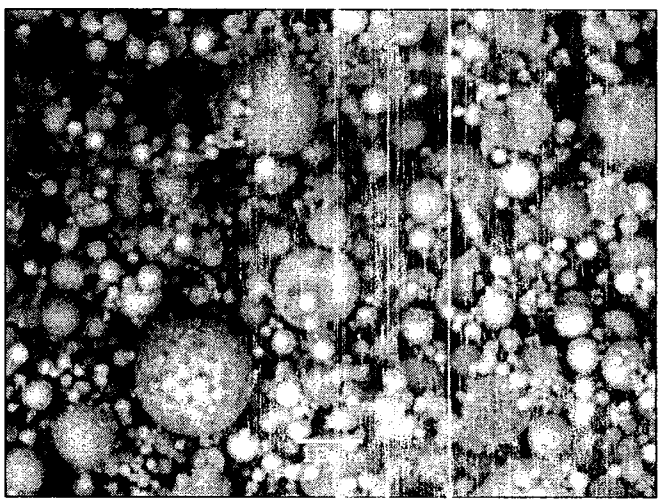

Figure 4-6: SE image of 6[illegible]CBFA powder.

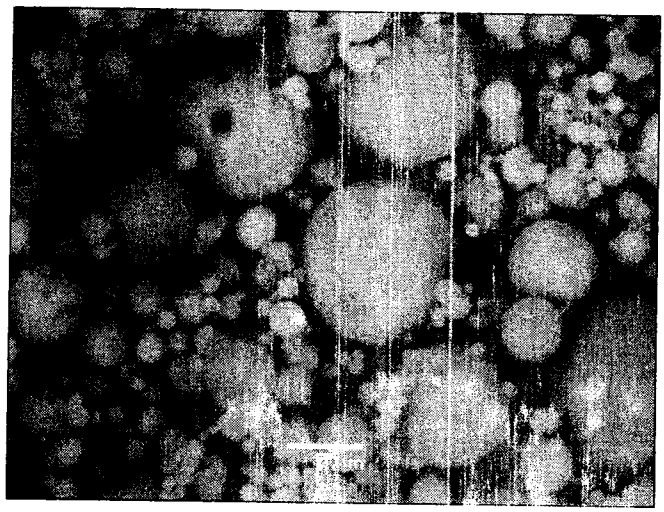

Figure 4-7: SE image of CFA powder.

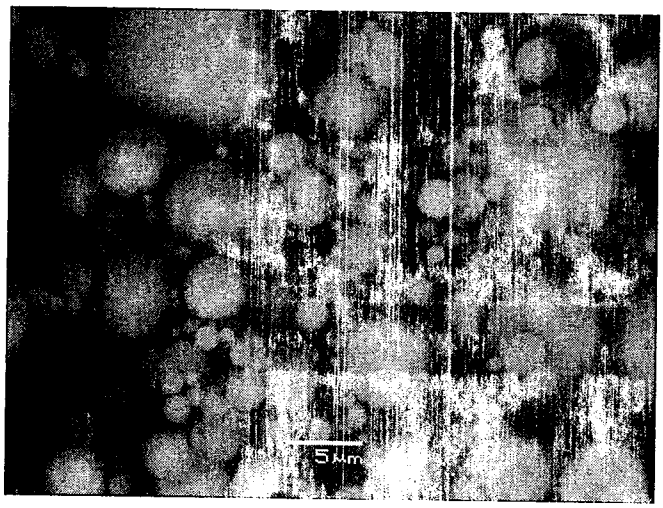

Figure 4-8: SE image of 15C FA powder.

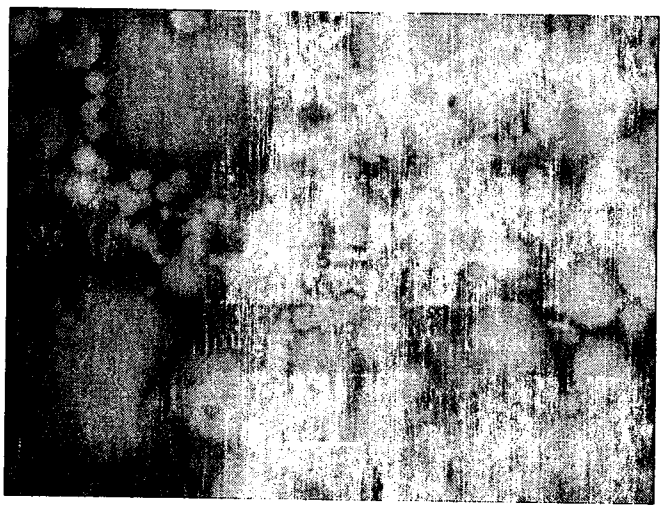

Figure 4-9: SE image of 55C FA powder

Each fly ash sample was found to contain iron-rich fly ash particles (high in iron). These particles typically display superficial surface grains or dendritic surface textures. Figures 4-10 and 4-11 show iron-rich fly ash particles in CFA and 15CBFA, respectively, at sufficient magnifications to show surface detail. The iron contents of the iron-rich particles were determined through quantitative EDS, and were determined to be 42.8 molar%, for the particle in Figure 4-10 and 32.3 molar% for the particle in Figure 4-11 (with the remainder being oxygen and some trace elements).

Some non-spherical fly ash particles were also encountered in each fly ash sample, and quantitative EDS analysis revealed that these particles were quartz as in Figure 4-12.

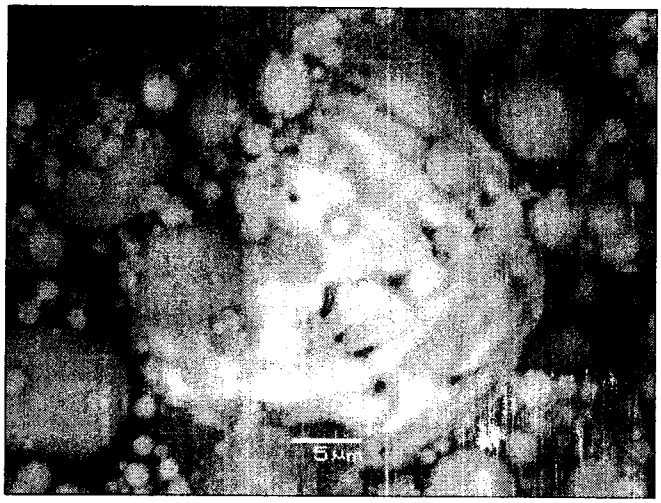

Figure 4-10: SE image of an iron-rich particle in CFA.

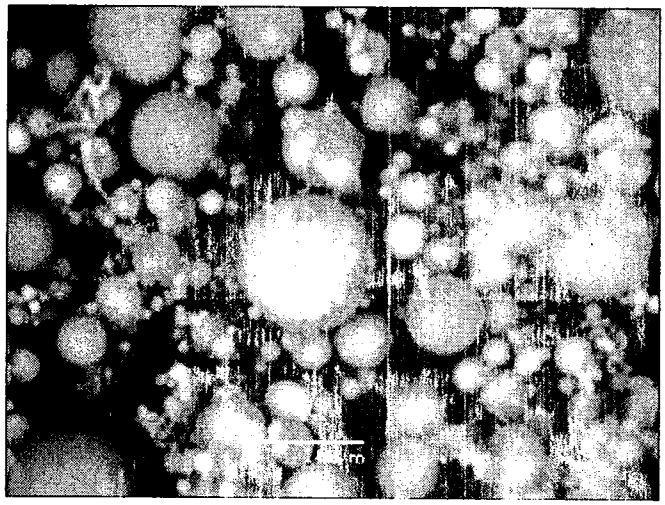

Figure 4-11: SE image of an iron-rich particle in 66CBFA.

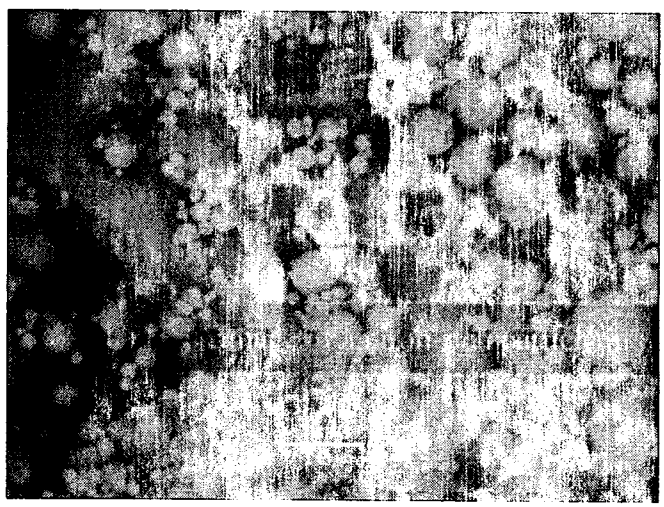

Figure 4-12: SE image of an irregularly shaped quartz particle in 15CBFA.

4.4.2 Fly Ash Polished Slices

Quantitative EDS analysis of individual fly ash particles on powdered stubs can be unreliable because it is difficult to determine which particles are porous and which are solid. Although quantitative EDS can be employed on porous particles to determine their composition, the user must make certain that the X-ray beam is not placed directly on the cavity within a particle. If the beam were positioned directly above the cavity, the beam would penetrate through to the stub surface, resulting in inaccurate quantitative data. Therefore, quantitative data was collected on polished slices of fly ash.

Figures 4-13, 4-14 and 4-15 show typical BSE images of CFA, 15CBFA and 66CBFA polished slices (at x1000 magnification), respectively. Again, differences in grey level reveal compositional variations between the different particles. Light-shaded particles tend to be high in calcium, iron, magnesium, or titanium, while darker particles tend to have less of these elements and more sodium. By capturing images of polished slices, it is possible to determine which particles are porous so that the EDS X-ray beam can be positioned to collect representative data on elemental composition.

Examination of the porous particles revealed that internal cavity sizes vary significantly. Some particles contain very small cavities relative to the size of the particle, while other particles have very thin walls. Cavities are not always located in the centre of the particle and some porous particles contain several distinct cavities (as seen for the particle near the centre of Figure 4-13). In some cases, the cavity within a porous particle contains additional smaller particles (e.g., bottom right corner of Figure 4-14).

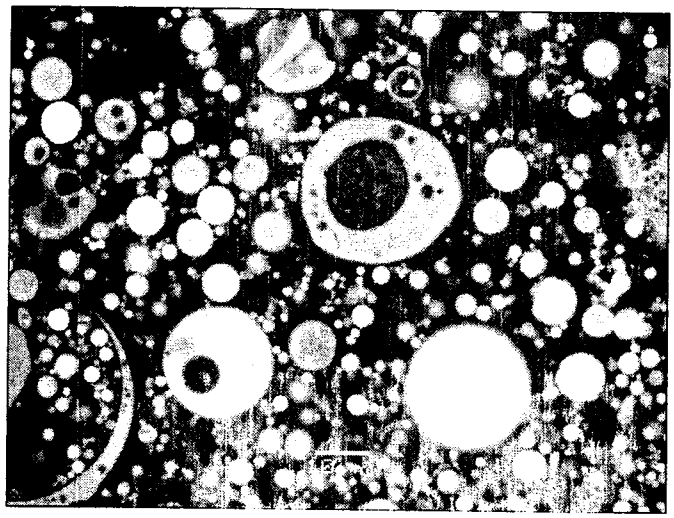

Figure 4-13: BSE image of polished CFA.

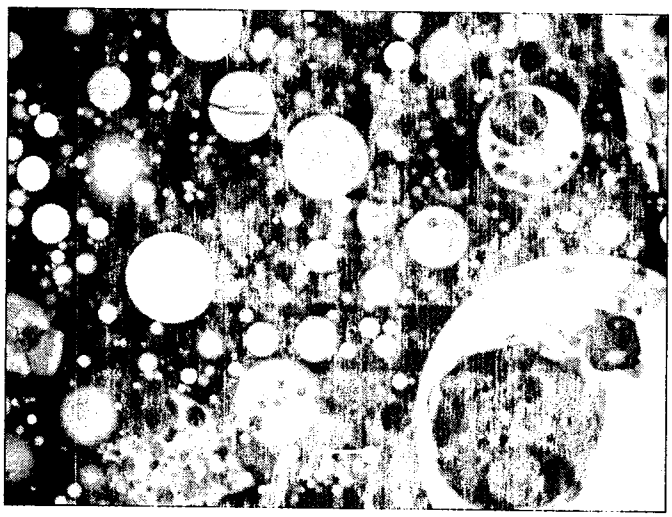

Figure 4-14: BSE image of polished 150°C FA.

Figure 4-15: BSE image of polished 350°C FA.

Select SEM images of fly ash polished slices are displayed in order to showcase some less abundant types of particles. Figure 4-16 shows a larger, non spherical particle which was determined to be quartz by EDS. Figures 4-17 and 4-18 both show bright particles with distinct surface textures. In Figure 4-17 the particle is large and porous with small repeating, textured marks, and in Figure 4-18 the particle appears to be solid with larger textured marks. These are both iron-rich particles. The Fe contents of the two particles are 55.97 molar%, and 37.84 molar%, respectively.

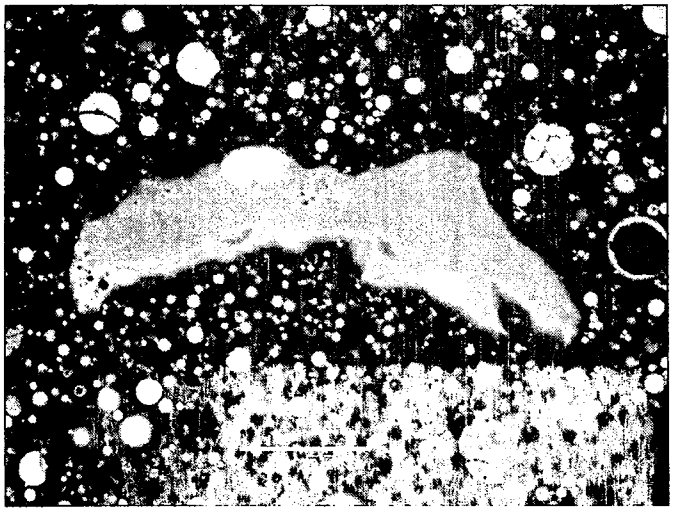

Figure 4-16: BSE image of polished [illegible] showing a quartz particle.

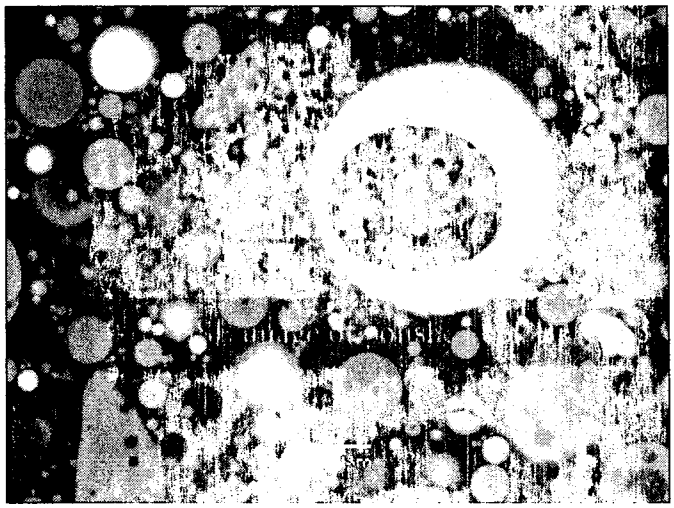

Figure 4-17: [illegible] wing an iron-rich particle.

Figure 4-18: [illegible] showing an iron-rich particle.

Over 85 quantitative EDS measurements of each fly ash were recorded from polished slice imaging and used to create compositional ternary diagrams (Figures 4-18 through 4-21). Note that ternary diagrams do not show individual concentrations, but rather the proportion of each of three elements (*e.g.*, Al, Ca and Si) when their sum is taken to be constant (100%). All ternary diagrams have Si and Al (the most abundant elements) as two of their apexes. The remaining apex is Fe, Ca, Na, or Mg. For directions on how to read a ternary diagram, refer to Appendix D.

The ternary diagrams show that the range of composition of individual particle does not markedly change with co-firing up to 62 wt% wood pellets. Aluminosilicates, represented by points close to the Si-Al binary line, were abundant in all fly ashes. The Si-Al-Fe ternary diagram (Figure 4-18) also reveals the presence of iron-rich aluminosilicate particles. Some particles have a relative Fe content as high as 90%. Calcium aluminosilicates correspond to points on tie lines connecting the aluminosilicate binary and the Ca-apex in Si-Al-Ca diagram (Figure 4-19). Most calcium aluminosilicate particles fall on tie lines having Si/Al molar ratios ranging from 1 to 2 (Figure 4-19).

Both relative Na and Mg contents had much tighter ranges (less than 25 mol%), as shown in Figures 4-20 and 4-21, respectively. The majority of fly ash particles in each fly ash sample have a relative Na content in the range of 10 to 20 mol%. Figures 4-20 and 4-21 also show that as the relative Al content increases above 50%, the relative Na content decreases to less than 10% while the relative Mg content increases up to 30 mol%. Hence, the Mg and Na content move in opposite directions as a function of Al content.

Since mineralogy of the parent coal is the dominant factor in determining the chemical distribution of the resulting fly ash (Tishmack and Burns, 2004; Wigley and Williamson, 1998), minerals present in lignite coal may be compared to the composition of individual fly ash particles. It is expected that fly ash has such a high proportion of aluminosilicate particles, since coals typically have high levels of silicate minerals present, most of which include aluminum (Tishmack and Burns, 2004). Yu. *et al.*, (1998) reported aluminosilicate content of up to 55 wt% in bituminous coals. Wigley and Williamson (1998) attribute the abundance of aluminosilicates to the reduction in mass if other minerals during volatile loss and the mineral-mineral interactions that occur during coalescence (explained in section 1.1). In some cases, the composition of fly ash particles closely resembles that of minerals found in coal. In Figures 4-18 to 4-20 there is a cluster of points at the Si-apex, which would indicate a mineral composition of quartz. Helmuth (1987) states that much of the quartz in the fly ash originates from the coal as silt- and sand-sized particles, and it remains in the ash because it survives thermal transformation during the combustion process. In Figure 4-20 there is a cluster of points with Na/Al=0.5 and Na/Si=0.5, which resembles the composition of Anorthite ($NaAl_2Si_2O_8$), which is known coal mineral (Tishmack and Burns, 2004). Fly ash particles particularly high in iron would be derived from oxides and sulfides present in coal, or may occur due to iron-rich fused material fragments separating from the main mass of mineral matter in the fuel source (see "Fusion" in section 1.1).

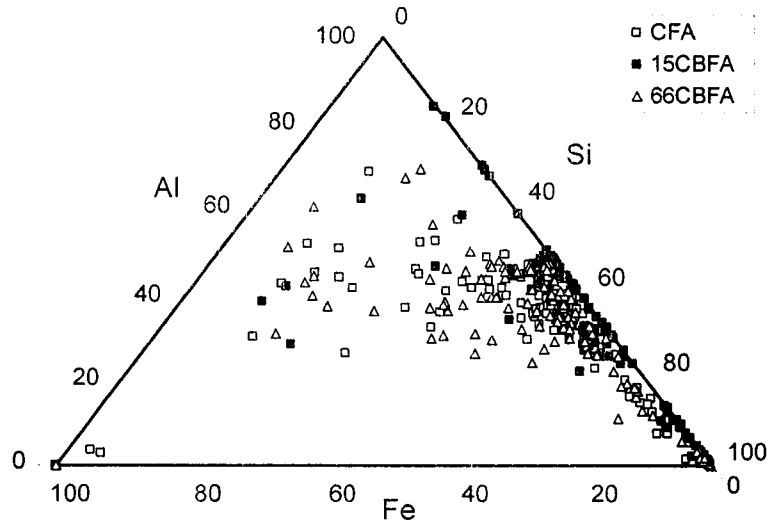

Figure 4-19: Ternary diagram (Si-Al-Fe) for fly ash samples.

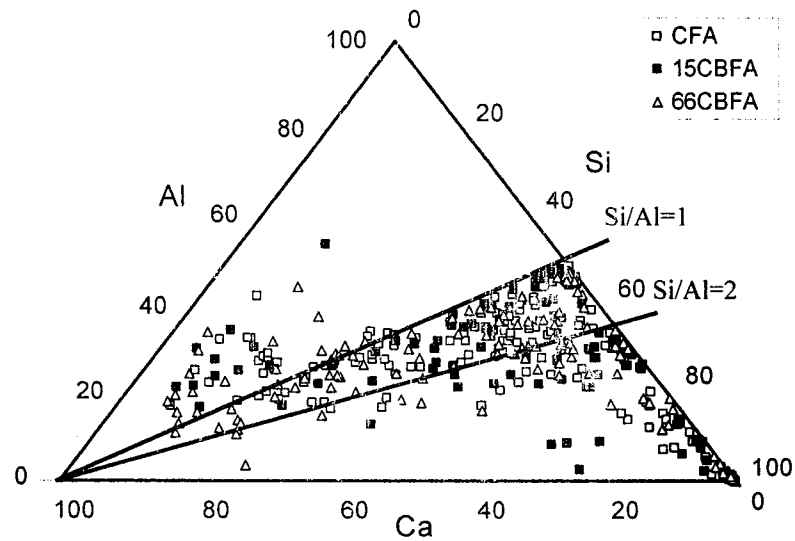

Figure 4-20: Ternary diagram (Si-Al-Ca) for fly ash samples.

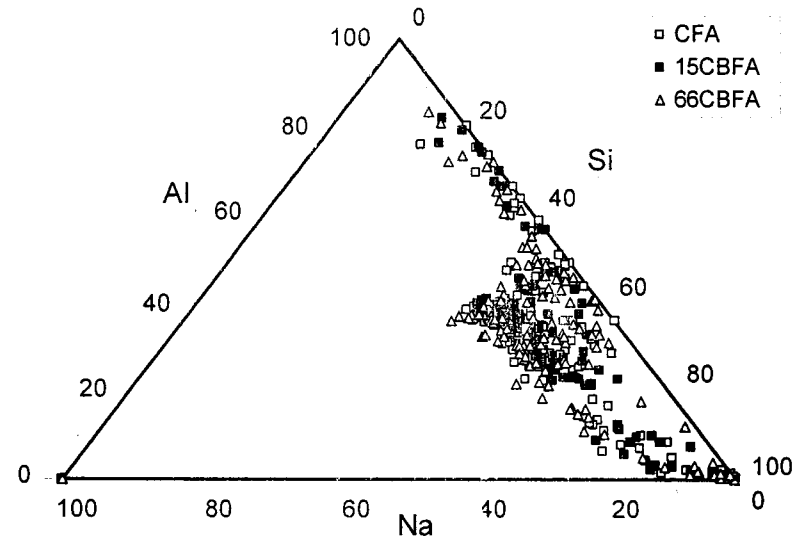

Figure 4-21: Ternary diagram (Si-Al-Na) for fly ash samples.

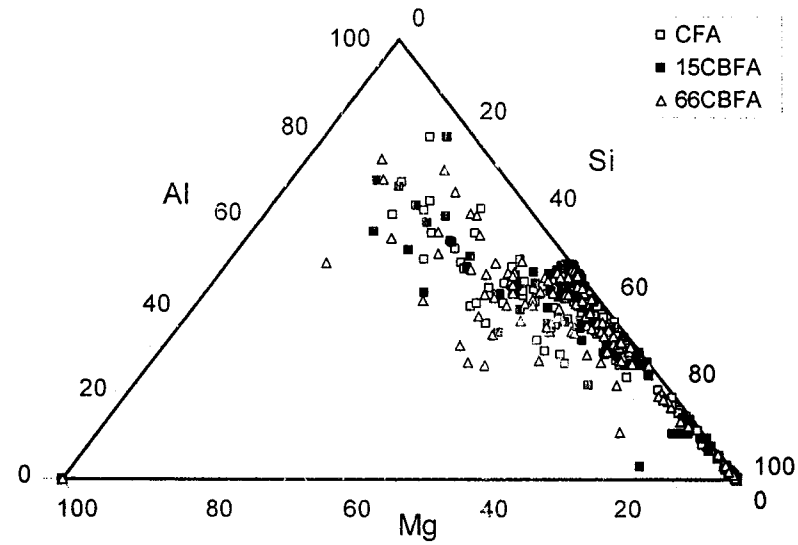

Figure 4-22: Ternary diagram (Si-Al-Mg) for fly ash samples.

Since fly ashes containing larger proportions of smaller particles have been found to contribute more to increased long term compressive strength (Burden, 2003; Samarin *et al.*, 1983; Berry and Malhotra, 1978), the compositions of large and small particles were compared. During EDS data collection, fly ash particles were classified into two size groups corresponding to diameters respectively smaller and larger than 5 μm. Ternary diagrams were completed as above but this time comparing the compositions of smaller and larger particles for each fly ash (Figures 4-22 through 4-24). Results show that both small and large particles having the same range of compositions and their distributions on the ternary diagrams are undistinguishable.

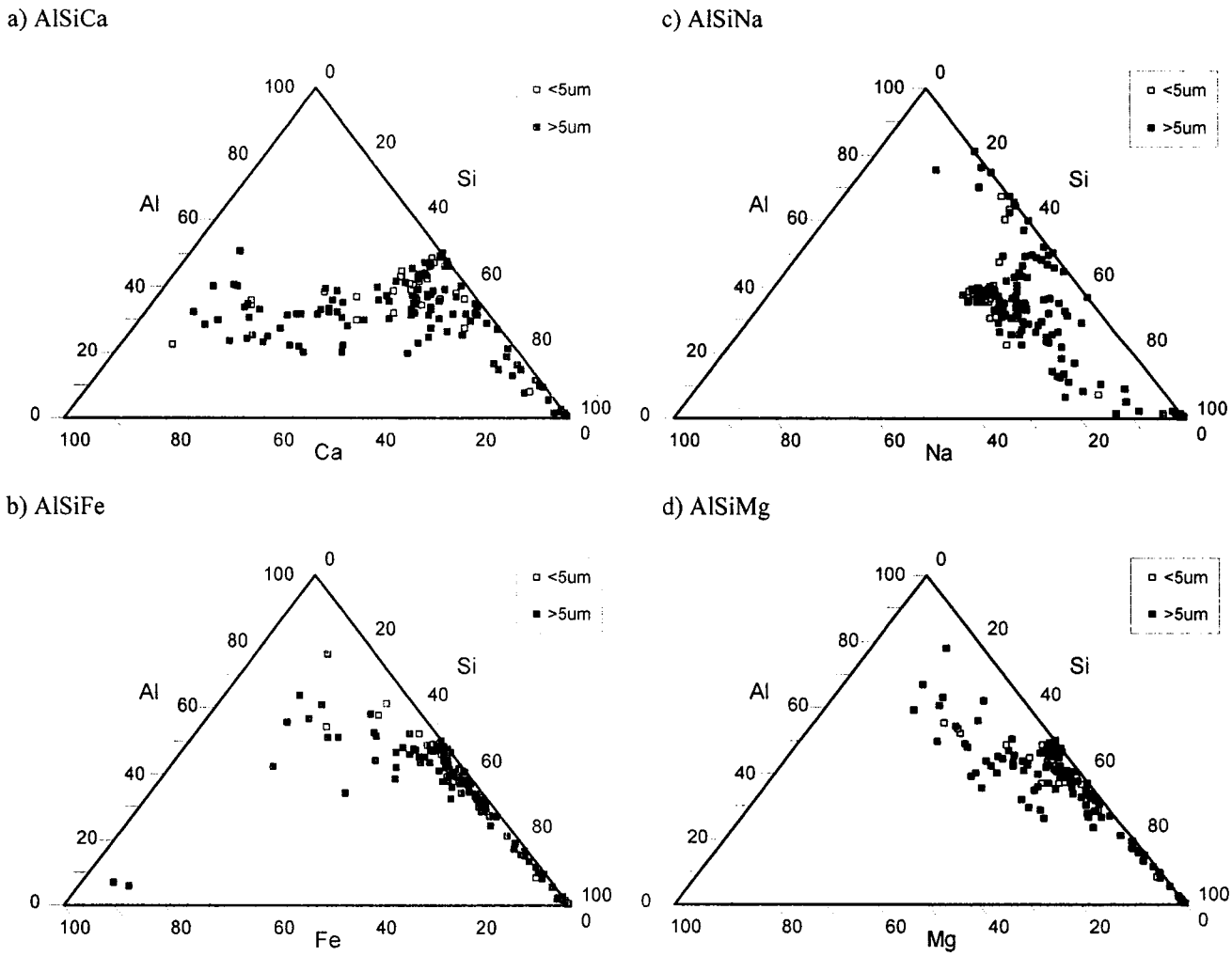

Figure 4-23: Ternary diagrams for CFA comparing the relative molar compositions of individual smaller and larger particles: a) AlSiCa, b) AlSiFe, c) AlSiNa, and d) AlSiMg.

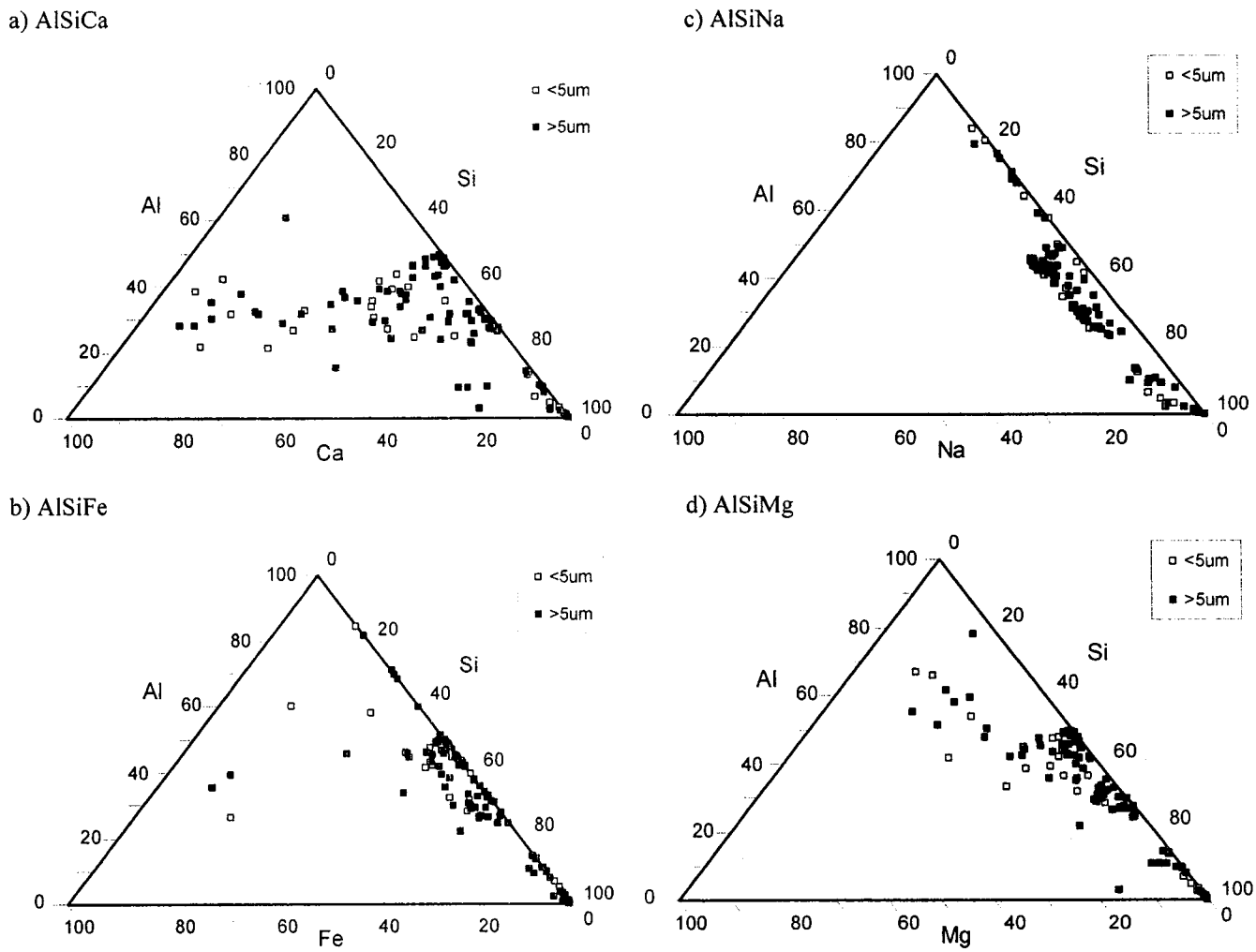

Figure 4-24: Ternary diagrams for 15CBFA comparing the relative molar compositions of individual smaller and larger particles: a) AlSiCa, b) AlSiFe, c) AlSiNa, and d) AlSiMg.

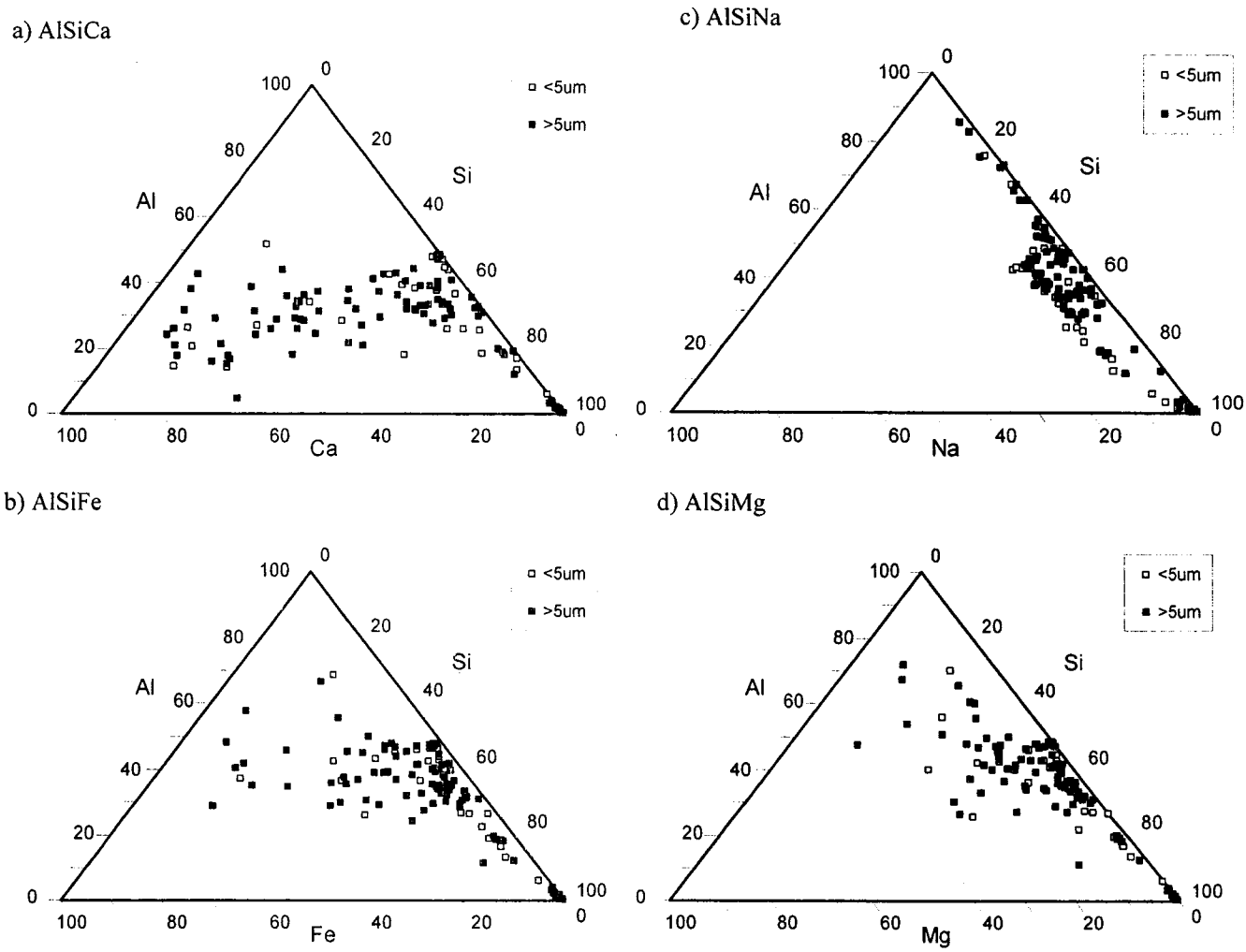

Figure 4-25: Ternary diagrams for 66CBFA comparing the relative molar compositions of individual smaller and larger particles: a) AlSiCa, b) AlSiFe, c) AlSiNa, and d) AlSiMg.

The differences in specific gravities of the fly ashes may be attributable to differences in proportions of porous particles. Ternary diagrams differentiating between porous and non-porous fly ash particles were also prepared (Figures 4-25 through 4-27) and show that porosity was not correlated with differences in particle composition, since porous and non-porous particles are similarly distributed on the ternary diagrams.

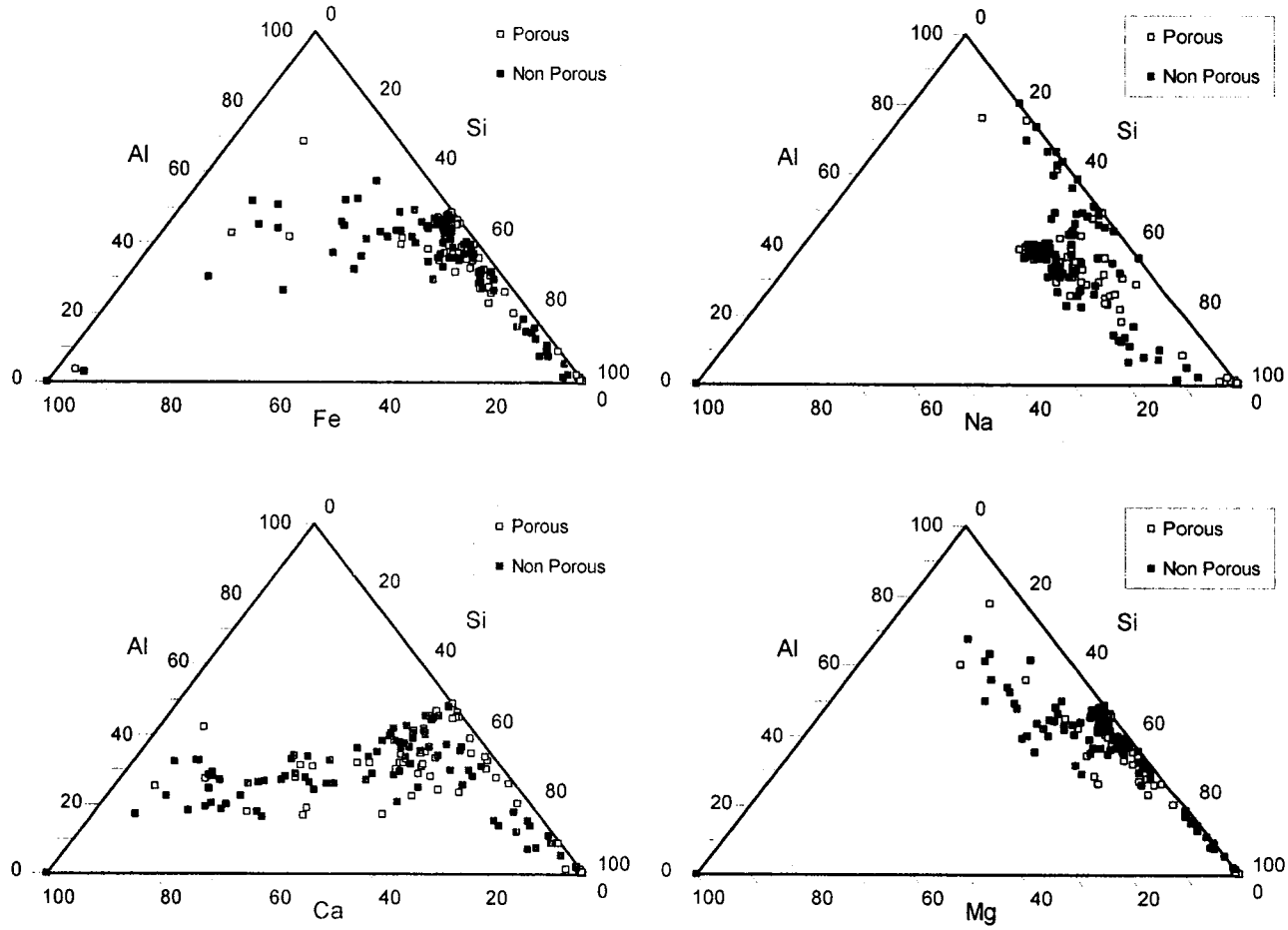

Figure 4-26: Ternary diagrams for CFA, comparing the relative molar compositions of individual porous and non-porous particles: a) AlSiCa, b) AlSiFe, c) AlSiNa, and d) AlSiMg.

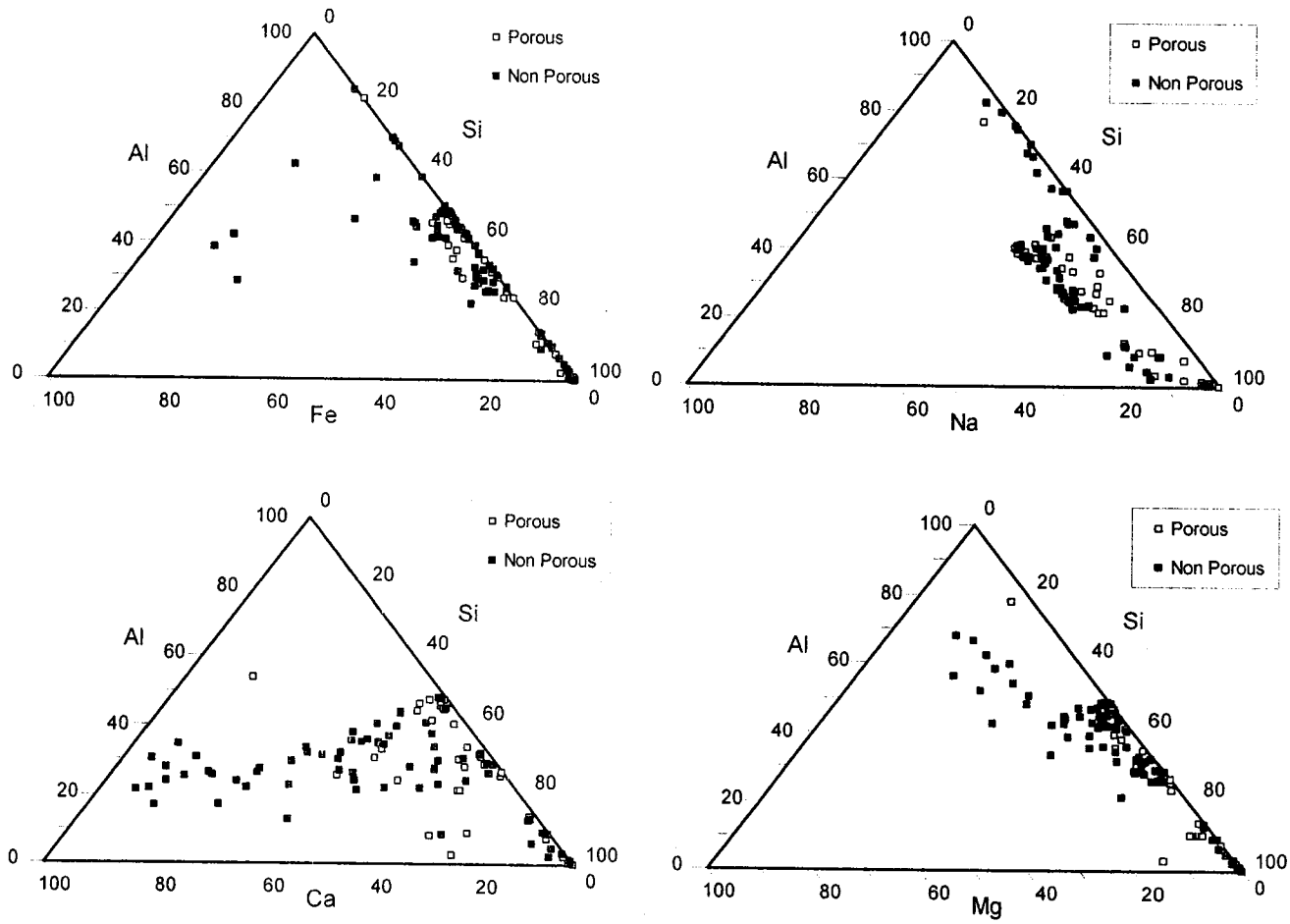

Figure 4-27: Ternary diagrams for 15CBFA, comparing the relative molar compositions of individual porous and non-porous particles: a) AlSiCa, b) AlSiFe, c) AlSiNa, and d) AlSiMg.

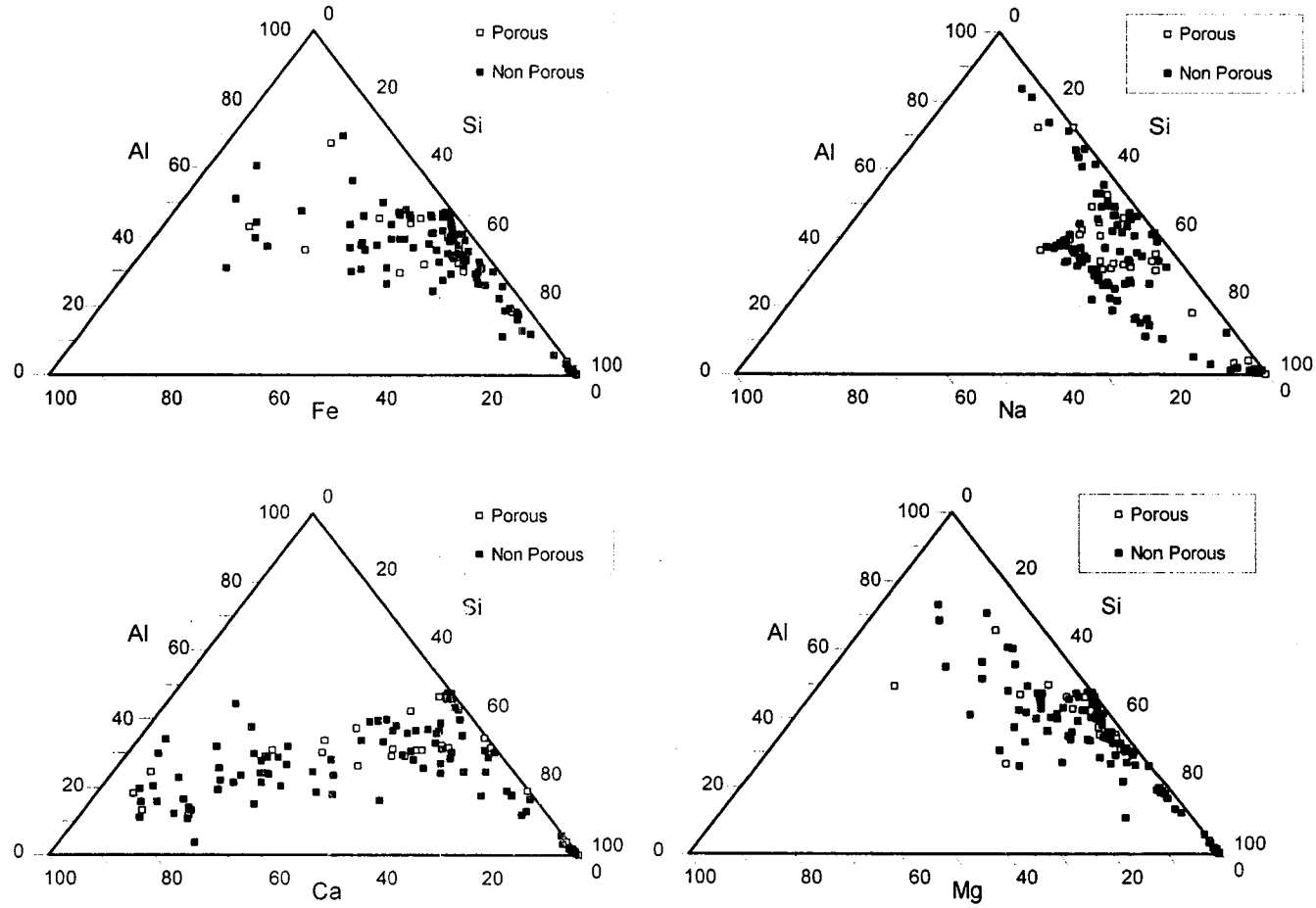

Figure 4-28: Ternary diagrams for 66CBFA, comparing the relative molar compositions of individual porous and non-porous particles: a) AlSiCa, b) AlSiFe, c) AlSiNa, and d) AlSiMg.

5.0 Effect of Fly Ash Substitution on Mortar Properties

5.1 Effect of Ash Substitution and Air Entraining Agent on Air Content of Mortars

Figures 5-1 and 5-2 show the air content of mortars containing 0, 20 and 40 wt% fly ash as a function of air entrainment agent (AEA) addition. The entrained air content in ash-free mortar samples rose from about 5 to 10 vol% upon addition of 0.6 mL/kg AEA, but did not increase further when the AEA dosage was doubled. The air content of AEA-amended mortar was totally unaffected by fly ash substitution, presumably due to its very low carbon content. However, in the absence of AEA, use of 20% ash decreased the air content by roughly 1% (Figure 5-1), whereas 40% ash caused it to increase 2-2.5% (Figure 5-2). A similar trend of air content versus mixed cement substitution by fly ash was reported by Chindaprasirt *et al.* (2005), although most other studies show a uniform decrease in air content with increasing fly ash (Bouzoubaa and Foo, 2004; Wesche, 1991; Helmuth, 1987; Wang *et al.*, 2008a; Zhang, 1996). The fly ash used in Chindaprasirt *et al.* (2005) had a similar composition to those used in the present study, lying close to the boundary between ASTM classes C and F, and having an LOI of 2.07 wt%.

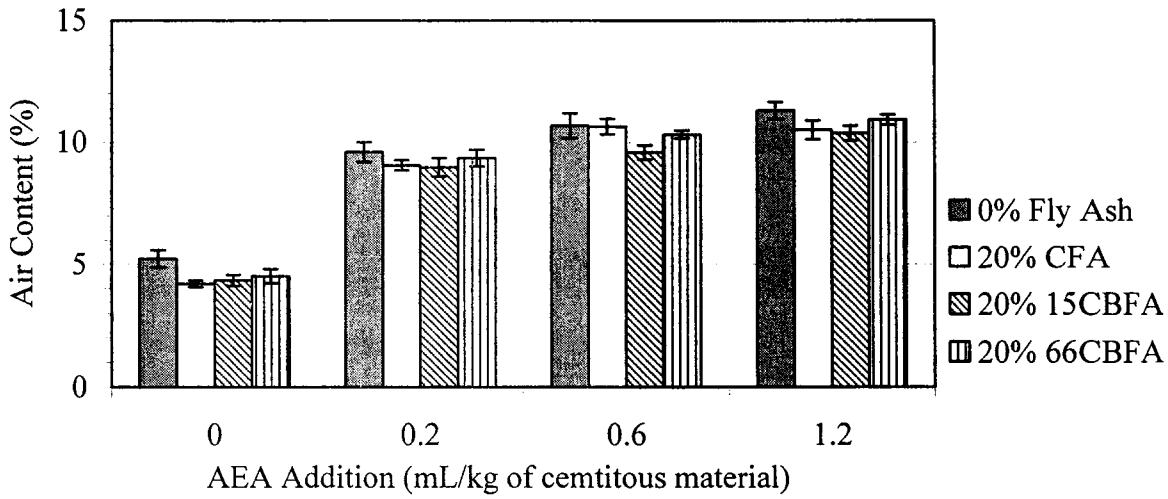

Figure 5-1: Air content of mortars containing 0 and 20 wt% fly ash. Air content was averaged from quadruplicate analyses. Error bars represent ± 1 standard deviation.

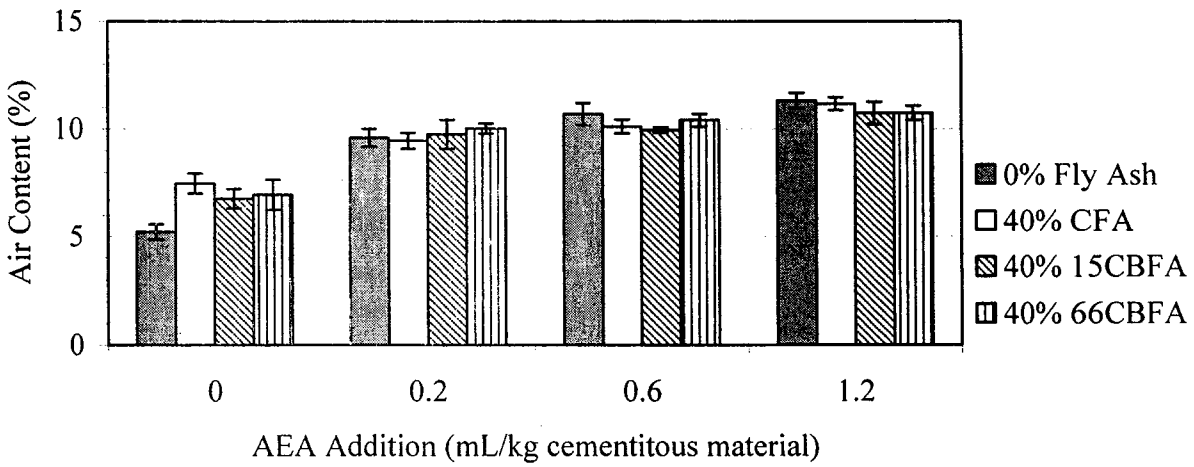

Figure 5-2: Air content of mortars containing 0 and 40 wt% fly ash. Air content was averaged from quadruplicate analyses. Error bars represent ± 1 standard deviation.

5.2 Compressive Strength Development

Table 5-1 shows compressive strength values for mortars containing 0, 20 and 40 wt% fly ash at different curing times between 1 and 365 days. Note the extremely small values for ± 1 standard deviation, indicating the reproducibility of the results. In each case, the standard deviation of quadruplicate samples was determined in order to comply with ASTM C109 (2003) reporting requirements. Although ASTM C109 (2003) recommends triplicate testing, it was found that quadruplicate testing met ASTM requirements for deviation in results for replicates in each case (Having ranges between specimens from the same mortar batch, at the same test age of less than 8.7% for three cubes, and less than 10% for four cubes (ASTM C109, 2003)).

By 7 days curing, all ash-amended mortars fulfilled ASTM requirements by achieving compressive strength which was at least 75% of ash-free mortar. By 28 days of curing time, the strength of ash-amended mortars closely approached or surpassed that of ash-free mortar. After 90 and 365 days, the compressive strength of mortars containing fly ash was significantly higher than that of ash-free mortar.

Table 5-1: Compressive strength of mortars containing 0, 20 and 40 wt% fly ash up to 365 days of curing.

Time (d)	Compressive Strength (MPa) ± 1 Standard Deviation						
	0%	20 wt%			40 wt%		
	Fly Ash	CFA	15CBFA	66CBFA	CFA	15CBFA	66CBFA
1	14.67±1.60	12.37±0.68	9.77±0.28	12.38±0.34	9.16±0.50	7.73±1.06	9.27±0.52
3	25.14±0.68	22.01±1.26	22.99±0.38	23.88±0.50	19.32±1.22	16.32±2.30	19.00±1.20
7	36.24±0.00	26.28±0.82	27.79±1.60	28.41±0.58	24.41±1.25	19.20±1.38	25.34±1.86
28	37.41±0.72	40.57±1.48	34.71±2.84	42.04±1.90	41.64±1.82	34.49±3.50	39.96±3.38
90	41.39±0.70	47.23±0.24	45.30±2.04	47.37±2.56	45.50±1.30	41.78±3.14	46.99±2.24
365	42.28±2.66	49.30±3.96	48.84±1.74	-[a]	46.84±0.20	45.61±2.80	-

a: "-" indicates mortars containing 66CBFA had not reached 365 days of curing.

Figures 5-3 and 5-5 show the strength development of specified mortars up to 28 days of curing (as prescribed by ASTM C618 (2003)). Figures 5-4 and 5-6 show the strength development of the same mortars as Figures 5-3 and 5-5 up to 365 days of curing. The strength of the ash-free mortar increased much faster than that of the other specimens over the first 7 days, but thereafter increased very slowly. These observations are consistent with previous reports (Washa and Withey, 1953; Lamond, 1983; Samarin *et al.*, 1983; Costa and Massazza, 1983; Abdun-Nur, 1961; Pasko and Larson, 1962; Ipatti, 1998; Wang *et al.*, 2007) and are explained by the slow pozzolanic reaction of fly ashes.

Mortars containing the same percent cement substitution by fly ash initially gained strength at the same rate. At day 28, however, the mortars containing CFA or 66CBFA were 6-17% stronger than mortars containing 15CBFA. Since the bulk composition of all fly ashes was similar, this phenomenon may have been caused by differences in their particle size distributions. This trend continues through to 365 days, where the 15CBFA-amended mortars have slightly lower compressive strength than CFA-amended mortars for the same percent substitution, but with less of a disparity (Table 5-1). 66CBFA-amended mortars were not tested for 365 day compressive strength as they have yet to reach 365 days of curing, however since the compressive strength development of 66CBFA-amended mortars was very similar to that of CFA-amended mortars they would be expected to have similar 365 day compressive strengths as well. Indeed, the CFA and 66CBFA had a larger proportion of small (< 30 μm) particles and thus a larger reactive surface area (see Section 4.3), which may have enhanced the pozzolanic reaction rate compared to mortars containing 15CFA. Nevertheless, all fly

ashes met ASTM requirement C 618 (2003), that is, the 28-day compressive strength of mortars containing fly ash exceeded 75% that of mortar containing no fly ash. At 90 days of curing, the compressive strength of fly ash amended mortars met or exceeded the strength of ash-free mortar.

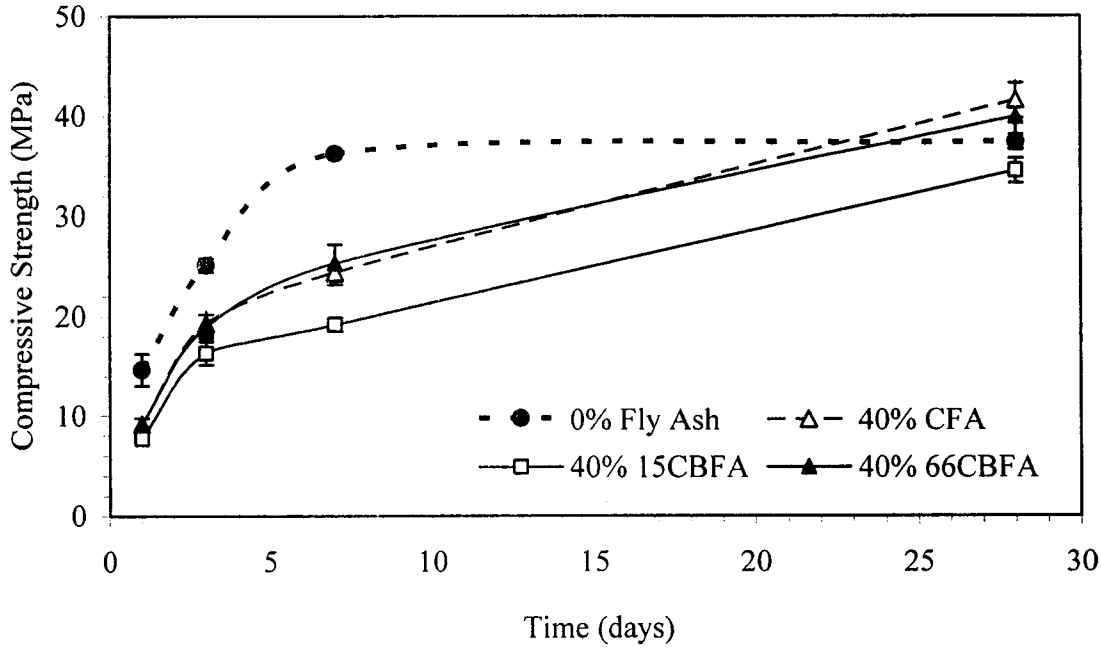

Figure 5-3: Compressive strength development up to 28 days curing for mortars having 0 or 20 wt% fly ash substitution. Compressive strength was averaged from quadruplicate analyses. Error bars represent ± 1 standard deviation.

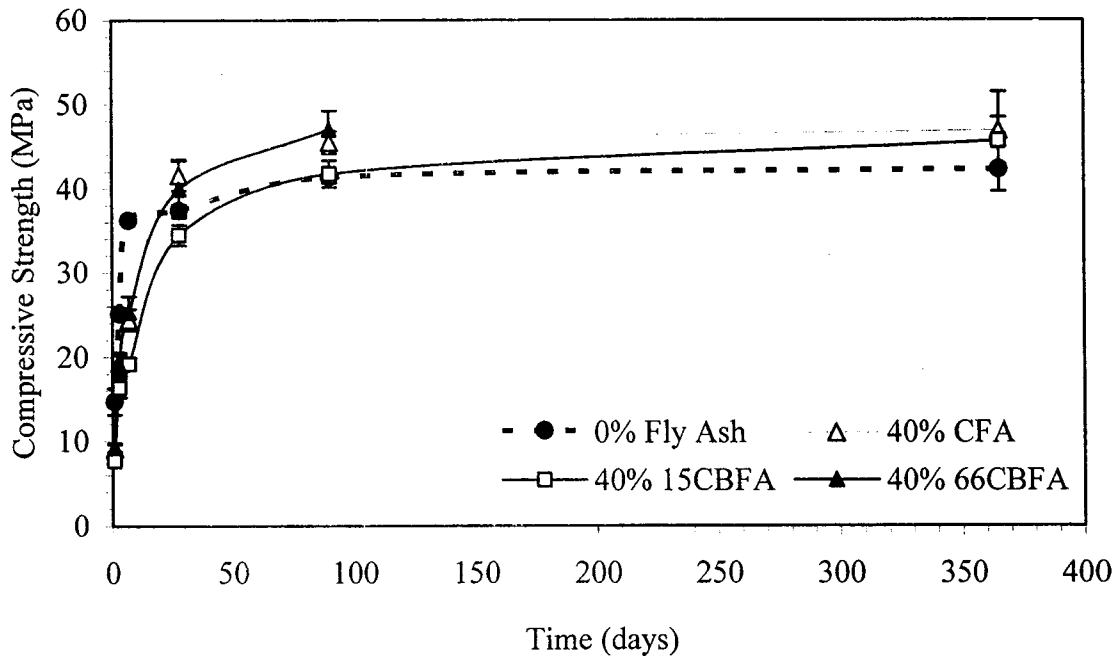

Figure 5-4: Compressive strength development up to 365 days curing for mortars having 0 or 20 wt% fly ash substitution. Compressive strength was averaged from quadruplicate analyses. Error bars represent ± 1 standard deviation

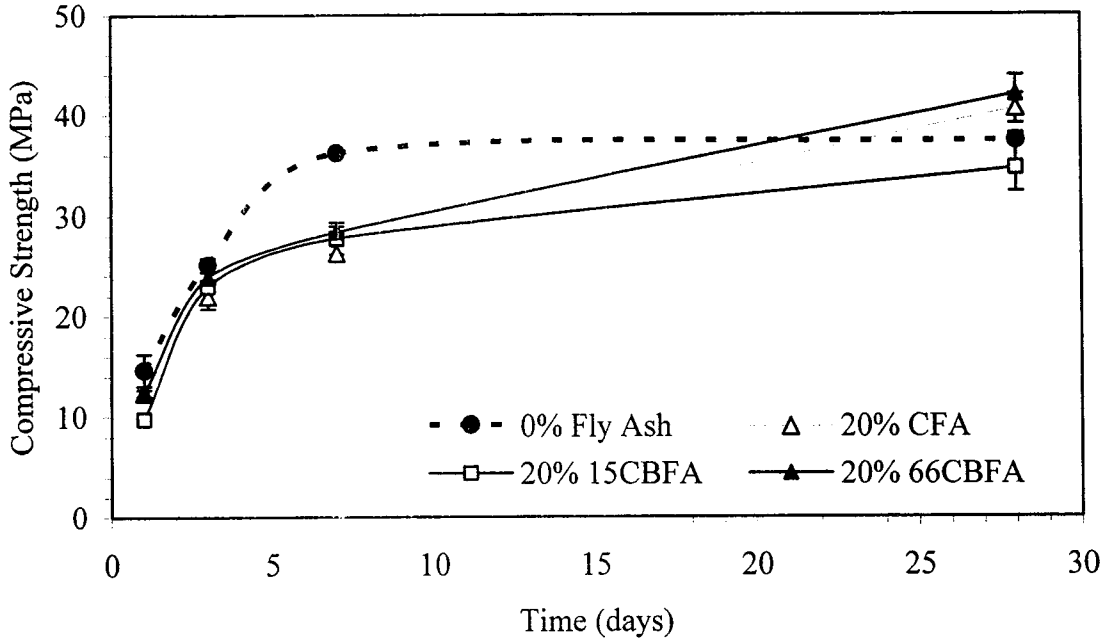

Figure 5-5: Compressive strength development up to 28 days curing for mortars having 0 or 40 wt% fly ash substitution. Compressive strength was averaged from quadruplicate analyses. Error bars represent ± 1 standard deviation.

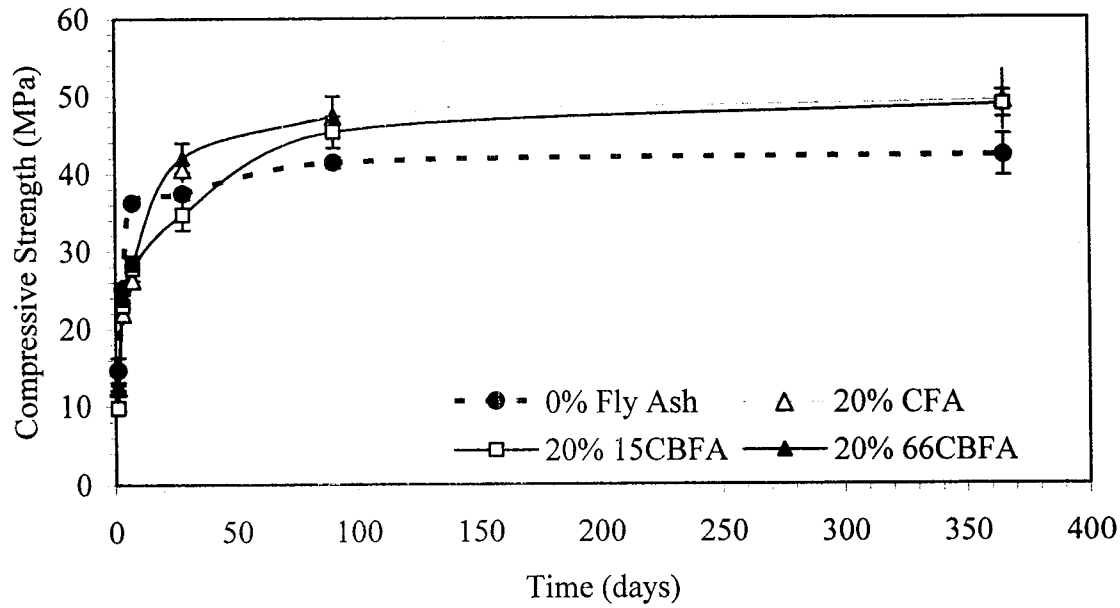

Figure 5-6: Compressive strength development up to 365 days curing for mortars having 0 or 40 wt% fly ash substitution. Compressive strength was averaged from quadruplicate analyses. Error bars represent ± 1 standard deviation

5.3 Resistance to Freezing and Thawing

The air contents of all mortars used in resistance to freeze-thaw analysis were within the 2 to 6 vol% range that is prescribed for the determination of strength and durability (Ipatti, 1998; Wang *et al.*, 2008a). The air content of each mortar is presented in Figure 5-1.

The variations in average dimension, mass, and compressive strength of mortar cubes as they were subjected to repeated freeze-thaw cycles are shown in Figures 5-5, 5-6 and 5-7, respectively. The first two parameters decreased slightly upon repeated cycling for all mortars. The compressive strength loss after 140 cycles was found to range from 40 to 46% for all mortars. No significant differences were observed between ash-free mortars and mortars containing, 20 wt% CFA or 15CBFA with respect to dimensions, mass or compressive strength. Thus, amending mortar with 20 wt% CFA or 15CBFA had no significant effect on resistance to freeze-thaw. This is mostly attributed to the fact that all three mortars had similar air contents (Figure 5-1) and is consistent with other studies (Berry, 1978; Wang *et al.*, 2008a; Brown, 1976), which also found that specimens with controlled air content had the same durability to rapid freeze-thaw.

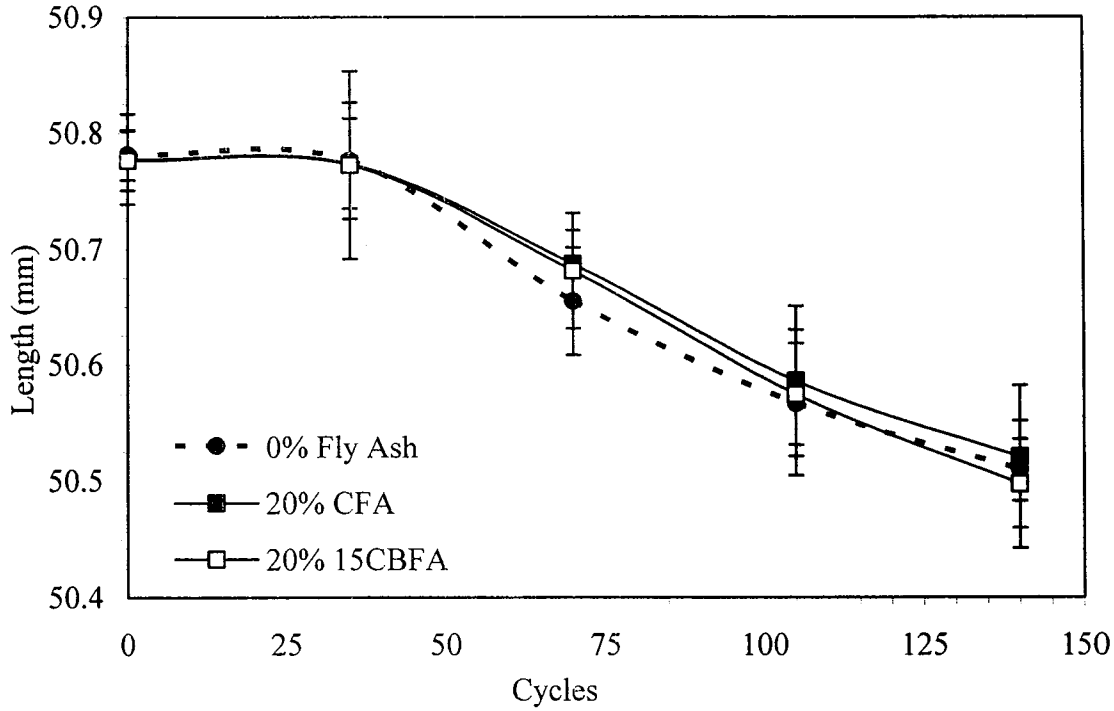

Figure 5-7: Average length of mortar cubes subjected to repeated freeze-thaw cycles. Error bars represent 1 standard deviation.

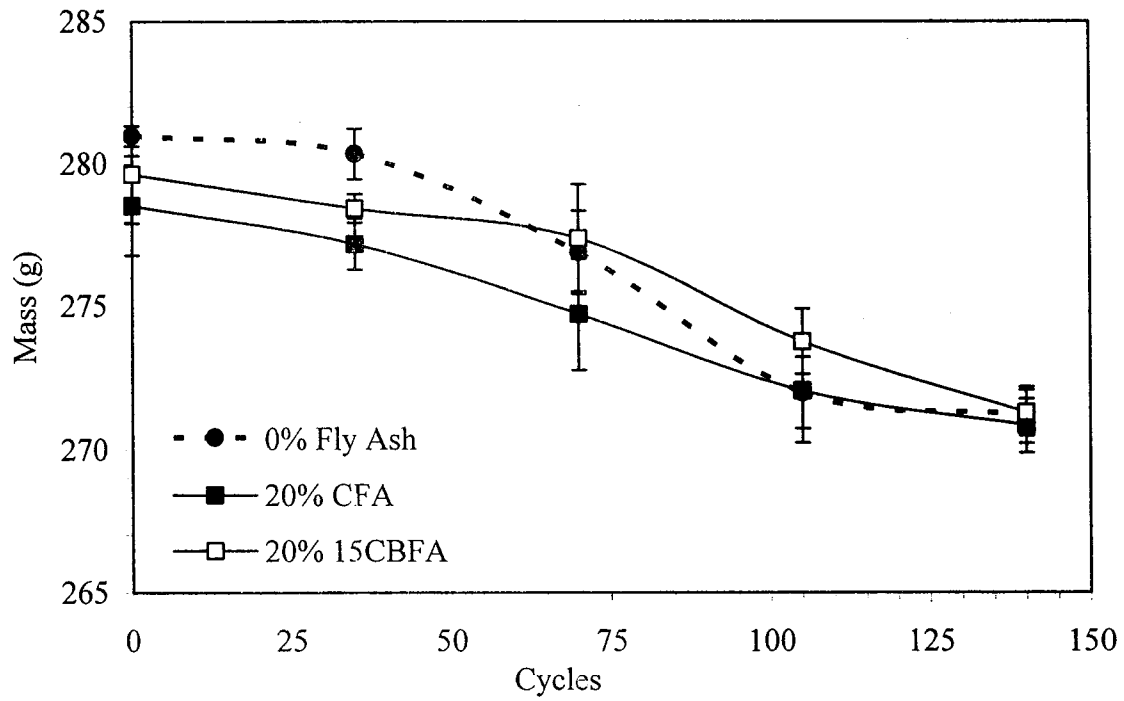

Figure 5-8: Average mass of mortar cubes subjected to repeated freeze-thaw cycles. Mass was averaged from quadruplicate analyses. Error bars represent ± 1 standard deviation.

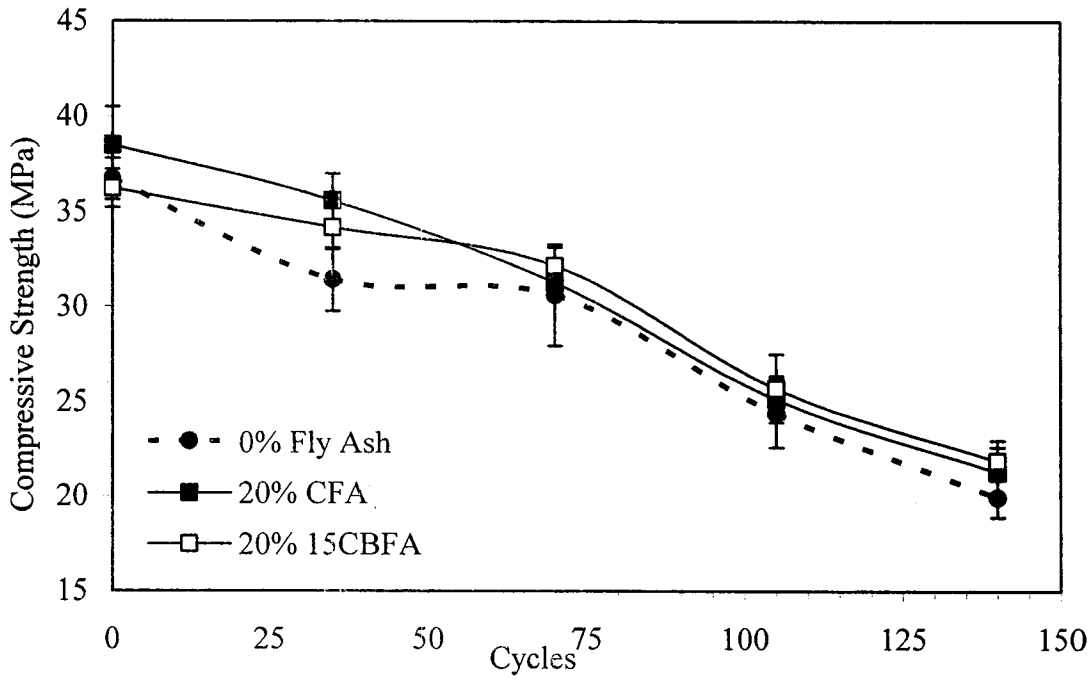

Figure 5-9: Average compressive strength of mortar cubes subjected to repeated freeze-thaw cycles. Compressive strength was averaged from quadruplicate analyses. Error bars represent ± 0.5 standard deviation.

5.4 Scanning Electron Microscope Image Analyses of Mortars

Figures 5-8 and 5-9 show typical back scattered electron images of mortar containing fly ash. Partly reacted fly ash particles are recognizable by their spherical shapes. They generally consist of an un-reacted core surrounded by a layer of smooth-textured hydration products rich in calcium and silicon. In some cases, fly ash particles had completely reacted and only a spherical layer of hydration products remained. This material is designated "fly ash inner-CSH" because its morphology is similar to that of the inner-CSH layers surrounding partly un-hydrated cement grains. Fly ash inner-CSH consists mainly of Ca and Si with an average molar Ca/Si ratio of 2.22 ±0.73, as determined from 38 independent EDS measurements (Appendix C). Other elements

occurring in fly ash inner CSH include Al>Fe>Mg≈Na. This composition is similar to that of cement inner-CSH where the Ca/Si ratio is 2.35 ±0.64, also with Al>Fe present (but very little Mg or Na). The fly ash inner-CSH layers are either in direct contact with the un-reacted core (*e.g.*, see the fly ash particle on the left hand side of Figure 5-8) or separated by a thin gap from the un-reacted core.

Much of the void space that was originally filled with water is occupied by calcium hydroxide (CH) crystals, irregularly textured CSH termed "outer-CSH" to distinguish it from the inner-CSH associated with cement or fly ash particles, and other hydration products collectively termed "dense hydration product" (DHP). CH is easily identified by its uniform texture and light grey colour in BSE images. The edges of sand particles were sometimes covered with a CH build-up (e.g., bottom of Figure 5-9). The observed features of CH (irregular masses varying in size and build ups on sand grains) are similar to those reported by Diamond (2004) for concrete samples. Outer-CSH has an average Ca/Si molar ratio of 1.96 ± 0.35 as determined from 65 independent EDS measurements (Appendix C), which is slightly higher than the range of 0.5 to 1.7 provided by Wang (2008c). DHP consists of smooth-textured, irregularly shaped particles (*e.g.*, see DHP particle near the left top corner of Figure 5-8), varying widely in size and composition (generally with Ca>Si>Al>Fe≈S≈Na and often approaching that of ettringite ($Ca_6Al_2(SO_4)_3(OH)_{12}\cdot 26H_2O$). There are no distinguishable differences between the DHP found in CFA- and CBFA-amended mortars.

Using EDS analysis, the Ca/Si molar ratio was determined for a number of points situated along lines that transect individual CFA and 15CBFA particles along with their shells of inner-CSH (Figures 5-10 to 5-12). The comparatively high Ca/Si ratio of the fly

ash inner-CSH shell suggests that it is formed by reaction of fly ash with Ca ions in the interstitial fluid which originate from cement or CH dissolution.

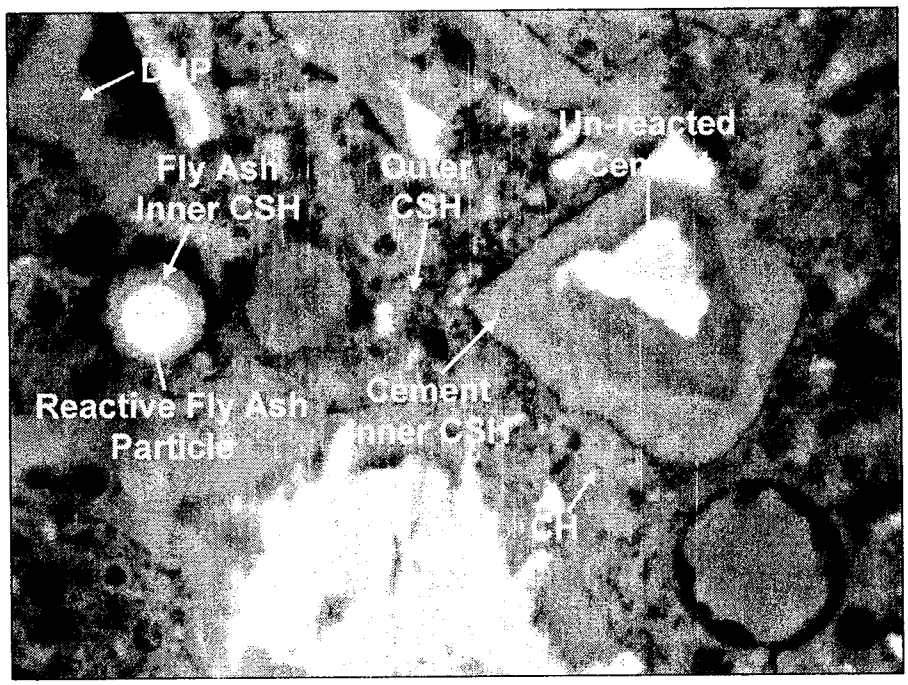

Figure 5-10: BSE image of 20% CFA-amended mortar cured for 28 days

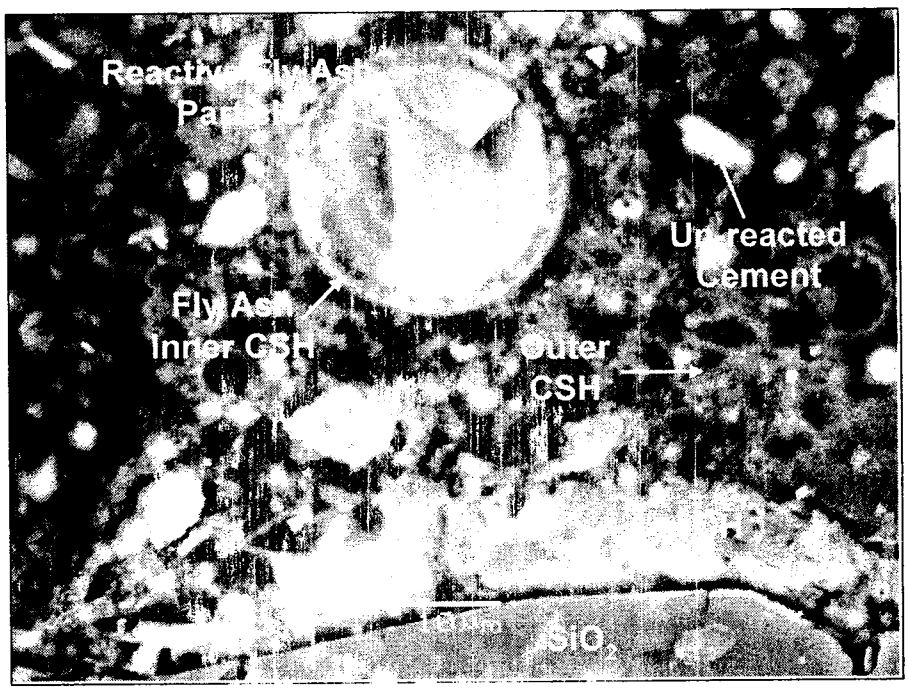

Figure 5-11: BSE image of [illegible] 15CBFA-amended mortar cured for 28 days

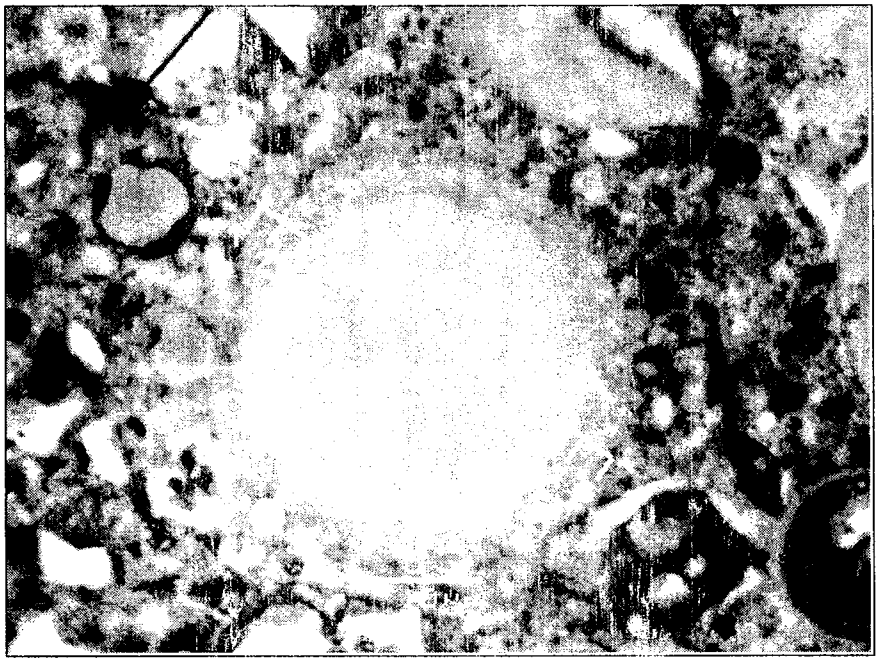

Figure 5-12: BSE image of reacted fly ash particle in 20% CFA-amended mortar, showing positions at which EDS analysis was carried out. Sites 4, 5 and 6 are in the un-reacted core of a CFA particle that is encased by a shell of fly ash inner-CSH.

Figure 5-13: BSE image of reacted fly ash particle in 20% 15CBFA-amended mortar, showing positions at which EDS analysis was carried out. Sites 4 and 5 are in the un-reacted core of a 15CBFA particle that is encased by a shell of fly ash inner-CSH.

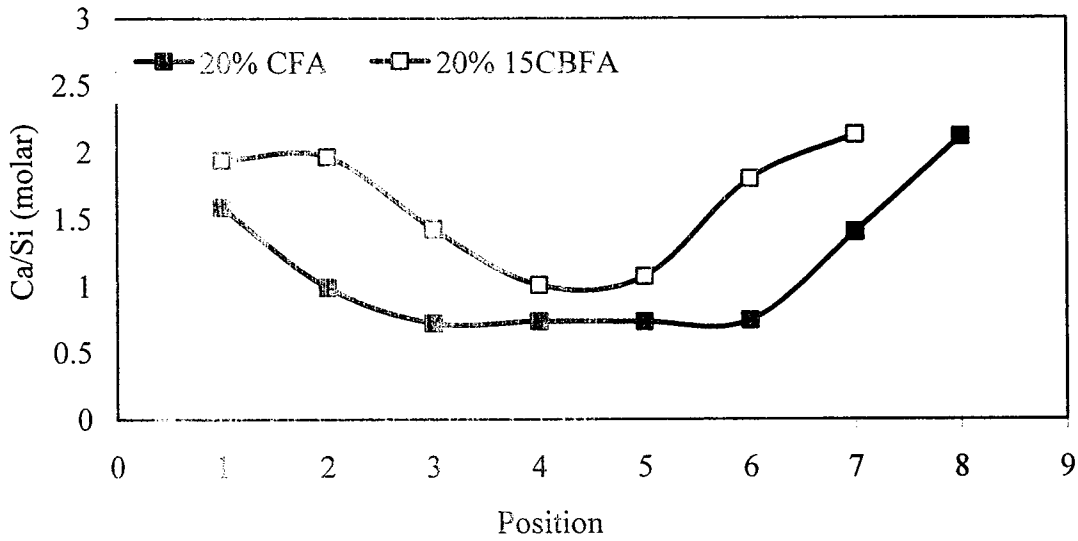

Figure 5-14: Ca/Si molar ratio profile for reacted CFA and 15CBFA particles in Figures 5-10 and 5-11.

6.0 Summary and Conclusions

This chapter provides a summary of the main results obtained from the characterization of CFA, 15CBFA and 66CBFA, as well as the effect of their substitution for cement in cement mortars.

6.1 Characterization of Fly Ash

1. Co-combustion of lignite coal with up to 62 wt% wood pellets did not markedly change the bulk composition of fly ash or the composition of individual fly ash particles, owing to the very low ash content of wood pellets. All fly ashes contained less than 1 wt% carbon and thus complied with ASTM regulations regarding carbon content. Concentrations of toxic metals and other minor elements in all fly ashes were within the ranges reported for other coal fly ashes.
2. Combustion conditions (*e.g.*, loading) affected the particle size distribution of fly ash, with higher loads increasing the proportion of larger particles.
3. Both large and small particles as well as porous and non-porous particles have a broad range of individual particle composition, with no distinguishable differences between small and large or porous and non-porous within a fly ash sample.

6.2 Effect of Fly Ash Substitution on Mortar Properties

1. Increasing the amount of cement substituted by fly ash decreased the amount of water required to maintain constant consistency, with the type of fly ash having no effect.
2. Substitution of cement with up to 40% fly ash from coal or wood-coal combustion did not affect the entrained air content of mortar containing $\geq$ 0.6 mL/kg AEA because of the low carbon content of the fly ashes. In the absence of AEA, however, use of 20% ash decreased the air content by roughly 1%, whereas 40% ash caused it to increase 2-2.5%.
3. The compressive strength of mortars in which up to 40% of cement is substituted by co-combustion fly ash exceeded 75% that of ash-free mortars by 28 days, and approached or even surpassed the compressive strength of ash-free mortars after 90 days of curing. Hence, all co-combustion fly ashes met ASTM C 618 strength requirements. Fly ash that contained a higher proportion of large (> 50 μm) particles exhibited the lowest 28-day strength.
4. Amending mortar with 20 wt% CFA or 15CBFA had no effect on its durability following repeated freeze-thaw cycles when air content was kept constant.
5. No micromineralogical differences were observed between hydrated CFA- and CBFA-amended mortars. Backscattered electron microscope images of all fly ash types show products from the reaction of fly ash with Ca ions in the interstitial fluid which originate from cement or CH dissolution.

6.3 Overall Conclusions

Characterization of fly ashes from the combustion of coal and of the co-combustion of coal with wood pellets has shown that small disparities between fly ashes (mostly limited to their particle size distribution) result from the combustion conditions (i.e., loading), and not from the introduction of biomass into the process. This lack of effect of wood pellets on the fly ash chemical and physical properties is explained by the fact that the ash content of wood pellets is marginal compared to that of lignite coal. The study of the effects of fly ash substitution on mortar physical properties has revealed that all the tested fly ashes are appropriate to use in blended mortars and concrete.

6.4 Future Research

The main recommendation for future research is to collect representative samples from the combustion of (100%) biomass from the generating station and run the same suite of analyses. Without the large ash content of coal, the properties of the fly ash would be expectedly different.

Further studies on the use of common cement admixtures may be beneficial, specifically the use of an accelerator in mortars containing fly ash in order to enhance early strength development (to counteract the retarding effect of fly ash). Studies on such admixtures could even include testing of chloride and non-chloride based accelerators, since fly ash-amended mortars have been found to have superior durability in chloride-rich environments (Johnson *et al.*, 2008).

Appendix A: Raw Data

A1 Specific Gravities of Fly Ashes

The following is raw data collected during the determination of specific gravity for each fly ash. Table A1 shows recorded values for triplicate testing, as well as the average, which was the reported value for specific gravity of each fly ash.

$$SpecificGravity = \frac{M_{FA}}{V_K}$$

Where M_{FA} = mass of fly ash (to replace removed kerosene)

V_K = volume of kerosene removed = 25 mL

Table A1: Specific gravity analysis results for fly ash samples.

Sample	M_{FA1}	M_{FA2}	M_{FA3}	Specific Gravity (± 1 standard deviation)
[a]CFA	62.34	57.54	60.40	2.404±0.096
15CBFA	58.06	57.89	61.12	2.361±0.072
66CBFA	61.379	67.808	64.804	2.587±0.128

a. Sample Calculation for CFA $SpecificGravity = \frac{\left(\frac{62.34+57.54+60.40}{3}\right)}{25} = 2.404 \pm 0.096 gcm^{-3}$

A2 Water Requirement Testing

The following are examples of raw data used to determine water requirements. Water requirement is determined by the amount of water added which results in the same diameter increase during a flow table test as an ash-free mortar. Table A1 shows the results for the ash-free mortar, which was used to obtain a target diameter increase of 53%. Therefore ash-amended mortars having diameter increase of 48 to 58% are considered to have the same consistency as the ash-free mortar. Table A2 shows raw data used in developing the mix proportioning of mortars, as shown in Table 4-3.

$$DiameterIncrease = \frac{D_{FT} - 2\left(\frac{\sum_{i=1}^{8} n_i}{8}\right) - D_M}{D_M}$$

Where D_{FT} = diameter of flow table = 25.5 cm

n_i = distance between the edge of the table and the edge of the mortar after flow test is complete.

D_M = diameter of mold (which was a frustrum of a cone) = 10 cm

Table A2: Flow table results for ash-free mortar.

Sample	Water (mL)	n_1 (cm)	n_2 (cm)	n_3 (cm)	n_4 (cm)	n_5 (cm)	n_6 (cm)	n_7 (cm)	n_8 (cm)	Diameter Increase (%)
[a] 0% Fly ash	242	4.45	5.05	5.25	5.55	5.50	5.20	4.75	4.40	54.6
0% Fly ash	242	4.65	5.10	5.40	5.30	5.10	5.25	4.95	4.65	54.0
0% Fly ash	242	5.10	5.00	5.15	5.45	5.30	5.20	5.30	5.40	50.0

a. Sample Calculation for 0% Fly ash

$$DiameterIncrease = \frac{25.5 - 2\left(\frac{4.45+5.05+2.25+5.55+5.50+5.20+4.75+4.40}{8}\right) - 10}{10} = 54.6$$

Table A3: Flow table results used for mix proportioning of ash-amended mortars.

Sample	Water (mL)	n_1 (cm)	n_2 (cm)	n_3 (cm)	n_4 (cm)	n_5 (cm)	n_6 (cm)	n_7 (cm)	n_8 (cm)	Diameter Increase (%)	Pass? (Y/N)
20% CFA	220	5.20	5.85	5.90	5.45	5.20	5.50	5.25	5.05	46.5	N
20% CFA	228	5.70	5.45	4.75	4.70	4.95	4.75	5.35	5.50	52.1	Y
20% CFA	228	5.50	4.85	4.60	4.80	4.80	4.65	4.90	4.70	58.0	Y
20% 15CBFA	228	5.00	5.35	5.00	4.70	4.50	5.25	5.35	5.20	54.1	Y
20% 15CBFA	228	4.85	5.50	4.70	4.90	4.70	4.90	4.90	4.75	57.0	Y
20% 66CBFA	228	4.90	4.75	4.85	5.00	5.10	5.15	5.00	5.10	55.4	Y
20% 66CBFA	228	5.10	5.20	5.20	5.4	5.20	5.00	4.90	5.00	52.5	Y
40% CFA	218	4.50	4.60	4.50	4.50	4.20	4.40	4.50	4.40	66.0	N
40% CFA	200	5.20	5.20	5.05	5.10	5.35	5.25	4.90	4.95	52.5	Y
40% CFA	200	4.80	4.90	4.70	4.90	5.10	5.30	5.30	5.0	55.0	Y
40% 15CBFA	200	4.85	4.65	4.65	4.80	5.25	5.20	5.0	4.80	57.0	Y
40% 15CBFA	200	4.90	4.70	4.75	5.05	5.30	5.75	5.25	4.90	53.5	Y
40% 66CBFA	200	4.90	5.20	5.10	4.80	4.75	5.00	5.10	4.80	56.0	Y
40% 66CBFA	200	5.20	5.30	5.10	4.80	4.75	5.20	5.00	5.10	54.1	Y

A2 Air Content Analysis

Mix proportioning for mortars was developed through water requirement testing and use of ASTM C109 (2003). Table A4 shows determination of W_c for mortars and Tables A5-1 to A5-4 show results to determine W_a as well as air content calculations.

$$AC = 100\left[1 - \frac{W_a}{W_c}\right]$$

Where AC = air content (%)

W_a = actual mass/unit volume as determined by test method (shown below)

W_c = theoretical mass/unit volume, calculated on an air-free basis (shown below)

$$W_a = \frac{m_{Mortar+Measure} - m_{Measure}}{V_{Measure}}$$

Where $m_{Mortar+Measure}$ = mass of mortar and the measure (g)

$m_{Measure}$ = mass of measure (g)

$V_{Measure}$ = volume of measure = 400 cm^{-3}

$$W_c = \frac{m_C + m_{FA} + m_S + m_W}{\frac{m_C}{SG_C} + \frac{m_{FA}}{SG_{FA}} \frac{m_{sand}}{SG_S} + \frac{m_W}{1}}$$

Where m_C = mass of cement = 500 g

m_{FA} = mass of fly ash (g)

m_S = mass of graded sand = 1375 g

m_W = mass of water (g)

SG_C = specific gravity of cement = 3.15 (ASMT C185, 2003)

SG_{FA} = specific gravity of fly ash (as previously determined)

SG_S = specific gravity of sand = 2.65 (ASTM C185, 2003)

Table A4: Determination of W_c for each mortar.

Sample	SG_{FA} (g cm^{-3})	m_{FA} (g)	m_W (g)	W_c (g cm^{-3})
[a] 0% Fly Ash	-	-	242	2.302
20% CFA	2.404	100	228	2.297
40% CFA		200	200	2.312
20% 15CBFA	2.361	100	228	2.295
40% 15CBFA		200	200	2.309
20% 66CBFA	2.587	100	228	2.305
40% 66CBFA		200	200	2.328

a. Sample Calculation for 0% Fly Ash $W_c = \dfrac{500g + 1375g + 228g}{\dfrac{500g}{3.15gcm^{-3}} + \dfrac{1375g}{2.65gcm^{-3}} + \dfrac{242g}{1gcm^{-3}}} = 2.302gcm^{-3}$

Table A5-1: Determination of W_a for ash-free mortar

Mortar	AEA (mL)	$m_{Measure}$ (g)	$m_{Measure+Mortar}$ (g)	W_a (g cm^{-3})	Air Content (%)	Air Content (Average) (± 1 standard deviation) (%)
[a]0% Fly ash	0	[a]739.08	1616.22	2.193	4.74	5.22±0.34
		739.12	1611.6	2.181	5.26	
		739.12	1608.35	2.173	5.60	
		739.08	1610.93	2.18	5.30	
	0.1	739.1	1566.96	2.07	10.08	9.59±0.40
		739.1	1571.05	2.08	9.64	
		739.09	1576.12	2.093	9.08	
	0.3	739.09	1571.98	2.082	9.56	10.69±0.50
		739.11	1566.72	2.069	10.12	
		739.11	1556.12	2.043	11.25	
		739.12	1559.37	2.051	10.90	
		739.12	1563.59	2.061	10.47	
	0.6	739.1	1555.91	2.042	11.29	11.32±0.36
		739.1	1559.27	2.05	10.95	
		739.12	1551.34	2.031	11.77	
		739.12	1556.13	2.043	11.25	

a. Sample Calculation for 0% Fly Ash, 0 AEA:

$$W_a = \frac{1616.22g - 739.08g}{400cm^3} = 2.193gcm^{-3} \qquad AC = 100\left[1 - \frac{2.193gcm^{-3}}{2.302gcm^{-3}}\right] = 4.74\%$$

Table A5-2: Determination of W_a for CFA-amended mortar

Mortar	AEA (mL)	$m_{Measure}$ (g)	$m_{Measure+Mortar}$ (g)	W_a (g cm^{-3})	Air Content (%)	Air Content (Average) (± 1 standard deviation) (%)
20% CFA	0	739.08	1620.59	2.204	4.05	4.19±0.14
		739.08	1618.87	2.199	4.27	
		739.1	1618.04	2.197	4.35	
		739.1	1620.26	2.203	4.09	
	0.1	739.1	1575.39	2.091	8.97	9.06±0.20
		739.1	1573.67	2.086	9.19	
		739.12	1577.02	2.095	8.79	
		739.12	1572.8	2.084	9.27	
	0.3	739.1	1562.4	2.058	10.40	10.66±0.32
		739.1	1561.77	2.057	10.45	
		739.11	1559.8	2.052	10.67	
		739.11	1555.9	2.042	11.10	
	0.6	739.12	1557.9	2.047	10.88	10.51±0.38
		739.12	1561.77	2.057	10.45	
		739.11	1566.08	2.067	10.01	
		739.11	1559.4	2.051	10.71	
40% CFA	0	739.1	1593.85	2.137	7.57	7.46±0.46
		739.1	1589.46	2.126	8.04	
		739.12	1599.48	2.151	6.96	
		739.12	1596.88	2.144	7.27	
	0.1	739.12	1575.6	2.091	9.56	9.44±0.36
		739.12	1577.12	2.095	9.39	
		739.11	1580.98	2.105	8.95	
		739.11	1572.9	2.084	9.86	
	0.3	739.12	1573.55	2.086	9.78	10.09±0.30
		739.12	1570.8	2.079	10.08	
		739.1	1571.32	2.081	9.99	
		739.1	1566.76	2.069	10.51	
	0.6	739.11	1562.87	2.059	10.94	11.16±0.30
		739.11	1556.78	2.044	11.59	
		739.1	1561.29	2.055	11.12	
		739.1	1562.2	2.058	10.99	

Table A5-3: Determination of W_a for 15CBFA-amended mortar

Mortar	AEA (mL)	$m_{Measure}$ (g)	$m_{Measure+Mortar}$ (g)	W_a (g cm^{-3})	Air Content (%)	Air Content (Average) (± 1 standard deviation) (%)
20% 15CBFA	0	739.07	1615.13	2.19	4.58	4.34±0.22
		739.07	1616.19	2.193	4.44	
		739.08	1618.07	2.197	4.27	
		739.08	1619.82	2.202	4.05	
	0.1	739.1	1578.83	2.099	8.54	8.95±0.38
		739.1	1573.3	2.086	9.11	
		739.12	1576.12	2.093	8.80	
		739.12	1571.01	2.08	9.37	
	0.3	739.11	1572.36	2.083	9.24	9.59±0.30
		739.11	1568.47	2.073	9.67	
		739.12	1570.01	2.077	9.50	
		739.12	1565.9	2.067	9.93	
	0.6	739.1	1565.77	2.067	9.93	10.39±0.30
		739.1	1561.16	2.055	10.46	
		739.12	1559.88	2.052	10.59	
		739.12	1560.09	2.052	10.59	
40% 15CBFA	0	739.11	1599.43	2.151	6.84	6.80±0.46
		739.11	1601.93	2.157	6.58	
		739.08	1594.34	2.138	7.41	
		739.08	1604.02	2.162	6.37	
	0.1	739.1	1575.66	2.091	9.44	9.77±0.66
		739.1	1565.06	2.065	10.57	
		739.12	1578.98	2.1	9.05	
		739.12	1570.29	2.078	10.00	
	0.3	739.11	1570.52	2.079	9.96	9.97±0.12
		739.11	1570.81	2.079	9.96	
		739.1	1571.72	2.082	9.83	
		739.1	1569.09	2.075	10.13	
	0.6	739.07	1563.17	2.06	10.78	10.75±0.52
		739.07	1569.59	2.076	10.09	
		739.11	1557.79	2.047	11.35	
		739.11	1562.99	2.06	10.78	

Table A5-4: Determination of W_a for 66CBFA-amended mortar

Mortar	AEA (mL)	$m_{Measure}$ (g)	$m_{Measure+Mortar}$ (g)	W_a (g cm^{-3})	Air Content (%)	Air Content (Average) (± 1 standard deviation) (%)
20% 66CBFA	0	739.11	1616.08	2.192	4.90	4.53±0.28
		739.11	1620.34	2.203	4.43	
		739.09	1618.75	2.199	4.60	
	0.1	739.09	1622.34	2.208	4.21	9.37±0.32
		739.12	1574.32	2.088	9.41	
		739.12	1570.75	2.079	9.80	
		739.1	1575.88	2.092	9.24	
	0.3	739.1	1578.02	2.097	9.02	10.34±0.16
		739.1	1567.43	2.071	10.15	
		739.1	1566.21	2.068	10.28	
		739.1	1563.82	2.062	10.54	
	0.6	739.1	1565.33	2.066	10.37	11.53±0.20
		739.12	1557.25	2.045	11.28	
		739.12	1554.26	2.038	11.58	
		739.11	1555.02	2.04	11.50	
		739.11	1552.63	2.034	11.76	
40% 66CBFA	0	739.13	1603.65	2.161	7.17	6.97±0.70
		739.13	1597.23	2.145	7.86	
		739.1	1609.23	2.175	6.57	
	0.1	739.1	1611.78	2.182	6.27	10.03±0.22
		739.11	1579.77	2.102	9.71	
		739.11	1574.89	2.089	10.27	
		739.1	1577.18	2.095	10.01	
	0.3	739.1	1575.79	2.092	10.14	10.43±0.28
		739.12	1576.72	2.094	10.05	
		739.12	1570.82	2.079	10.70	
		739.11	1571.39	2.081	10.61	
	0.6	739.11	1574.03	2.087	10.35	10.76±0.32
		739.11	1570	2.077	10.78	
		739.11	1567.3	2.07	11.08	
		739.09	1574.4	2.088	10.31	
		739.09	1568.9	2.075	10.87	

A3 Compressive Strength Development

Below are raw data for quadruplicate analysis of compressive strength development. Raw data is reported as pounds of force required to fracture specimen. Table A6-1 shows results for ash-free mortar and CFA-amended mortars, and Table A6-2 shows results for 15CBFA-amended and 66CBFA-amended mortars.

$$CS = \frac{P}{A} \qquad [4\text{-}3]$$

Where CS = compressive strength of specimen (MPa)

P = force to fracture (reported in lb_f and converted: $1lb_f = 4.45x10^{-6}$ Mega N)

A = area of specimen = 4 in^2 = 0.00258 m^2

Table A6-1: Compressive strength results for ash-free mortar and CFA-amended mortar.

Mortar	Curing Time (d)	Force to Fracture Trials (lb_f)				Compressive Strength Trials (MPa)				Compressive Strength (Average) (± 1 standard deviation) (MPa)
		1	2	3	4	1	2	3	4	
0% Fly Ash	1	9864.4	8127.2	8289	7770.1	17.00	14.01	14.29	13.39	14.67±1.60
	3	15230	14852	14589	14306	26.25	25.6	25.15	24.66	25.14±0.68
	7	19660	21133	22279	-	33.89	36.43	38.4	-	36.24±2.26
	28	22071	22129	21759	21228	38.04	38.14	37.51	36.59	37.41±0.72
	90	23858	23479	24456	24101	41.12	40.47	42.15	41.54	41.39±0.70
	365	23496	22989	24123	26479	40.5	39.63	41.58	45.64	42.28±2.66
20% CFA	1	7239.2	-	7538.1	6760.5	12.48	-	12.99	11.65	12.37±0.78
	3	12431	11937	13089	13609	21.43	20.58	22.56	23.46	22.01±1.26
	7	15877	14875	15327	14895	27.37	25.64	26.42	25.67	26.28±0.82
	28	23198	24522	22898	-	39.99	42.27	39.47	-	40.57±1.48
	90	27547	27372	27277	24006	47.48	47.18	47.02	41.38	47.23±2.94
	365	30000	26000	29800	26700	51.71	44.82	51.37	46.02	49.30±3.56
40% CFA	1	5618	5449	4949.3	5240.2	9.68	9.39	8.53	9.03	9.16±0.50
	3	11200	12069	11225	10348	19.31	20.8	19.35	17.84	19.32±1.22
	7	14587	13149	14793	14123	25.14	22.66	25.5	24.34	24.41±1.26
	28	-	25362	23702	23405	-	43.72	40.85	40.34	41.64±1.82
	90	27359	26643	25783	25793	47.16	45.92	44.44	44.46	45.50±1.30
	365	26200	24100	28000	30400	45.16	41.54	48.26	52.40	46.84±4.61

Note: " – " indicates a result not used in average calculations due to it being far removed from the other results.

Table A6-2: Compressive strength results for 15CBFA-amended and 66CBFA-amended mortars.

Mortar	Curing Time (d)	Force to Fracture Trials (lb_f)				Compressive Strength Trials (MPa)				Compressive Strength (Average) (± 1 standard deviation) (MPa)
		1	2	3	4	1	2	3	4	
20% 15CBFA	1	-	5557.4	5596.6	5854.7	-	9.58	9.65	10.09	9.77±0.28
	3	13067	13570	13262	13458	22.52	23.39	22.86	23.2	22.99±0.38
	7	17505	15566	15779	15639	30.17	26.83	27.2	26.96	27.79±2.60
	28	20801	18117	21967	19663	35.85	31.23	37.86	33.89	34.71±2.84
	90	27533	26284	24697	26608	47.46	45.31	42.57	45.86	45.30±2.04
	365	28100	29014.5	27003	29221	48.44	50.01	46.54	50.37	48.84±1.74
40% 15CBFA	1	4481.9	4112.1	4478.7	4870.6	7.73	7.09	7.72	8.4	7.73±0.54
	3	9596.9	10275	9353	8657.9	16.54	17.71	16.12	14.92	16.32±1.16
	7	-	11441	11290	10680	-	19.72	19.46	18.41	19.20±0.70
	28	20469	19686	21114	18765	35.28	33.93	36.39	32.35	34.49±1.74
	90	23655	24767	23300	25230	40.77	42.69	40.16	43.49	41.78±1.56
	365	28889	25913	25565	25477	49.8	44.67	44.07	43.91	45.61±2.80
20% 66CBFA	1	-	6158.3	7192.9	6986.4	12.71	-	12.4	12.04	12.38±0.34
	3	13684	13538	14053	14150	23.59	23.34	24.22	24.39	23.88±0.50
	7	16897	16107	16344	16590	29.13	27.76	28.17	28.6	28.41±0.58
	28	25303	25086	24287	22880	43.61	43.24	41.86	39.44	42.04±1.90
	90	26773	25738	28847	28562	46.15	44.36	49.72	49.23	47.37±2.56
40% 66CBFA	1	5068.8	5185.7	5601.1	5665.7	8.74	8.94	9.65	9.77	9.27±0.52
	3	11663	11569	10242	10629	20.1	19.94	17.65	18.32	19.00±1.20
	7	-	15915	13768	13812	26.38	-	23.73	23.81	25.34±1.86
	28	23824	21911	21335	25652	41.07	37.77	36.77	44.22	39.96±3.38
	90	29064	26010	27240	26725	50.1	44.83	46.95	46.07	46.99±2.24

Note: " – " indicates a result not used in average calculations due to it being far removed from the other results.

A4 Resistance to Freeze-Thaw

A4.1 Length Change over Cycles

Table A7 shows raw data recorded for length during resistance to freeze-thaw analysis. The dimension of the cube was determined by taking two measurements of each cube using a calliper. The reported length of a cube side is an average of two measurements of four cubes for each mortar type at the specified time.

Table A7: Length measurements as a function of freeze-thaw cycles.

Mortar	Cycle	Cube Side Measurements (mm)								Length of Cube (Average) (± 1 standard deviation) (mm)
		1		2		3		4		
0% Fly Ash	0	50.78	50.80	50.75	50.79	50.78	50.81	50.75	50.79	50.781±0.022
	35	50.83	50.86	50.76	50.78	50.73	50.75	50.71	50.79	50.776±0.050
	70	50.58	50.68	50.68	50.69	50.64	50.59	50.70	50.68	50.655±0.046
	105	50.47	50.58	50.57	50.60	50.59	50.52	50.53	50.68	50.568±0.062
	140	50.51	50.55	50.54	50.49	50.49	50.48	50.49	50.53	50.510±0.026
20% CFA	0	50.71	50.78	50.83	50.74	50.81	50.80	50.76	50.79	50.778±0.040
	35	50.80	50.83	50.79	50.76	50.71	50.79	50.78	50.73	50.774±0.038
	70	50.68	50.70	50.73	50.69	50.68	50.71	50.63	50.68	50.688±0.030
	105	50.54	50.60	50.51	50.62	50.67	50.59	50.50	50.66	50.586±0.064
	140	50.52	50.47	50.50	50.55	50.48	50.49	50.50	50.66	50.521±0.062
20% 15CBFA	0	50.75	50.76	50.79	50.75	50.80	50.76	50.78	50.82	50.776±0.026
	35	50.80	50.77	50.73	50.68	50.66	50.79	50.89	50.86	50.773±0.080
	70	50.63	50.59	50.71	50.67	50.70	50.69	50.72	50.74	50.681±0.050
	105	50.56	50.59	50.49	50.57	50.63	50.60	50.61	50.55	50.575±0.044
	140	50.39	50.38	50.41	50.40	50.39	50.37	50.39	50.51	50.498±0.054

A4.2 Mass Change over Cycles

Table A8 shows raw data recorded for quadruplicate analysis of mass during resistance to freeze-thaw analysis.

Table A8: Length measurements as a function of freeze-thaw cycles.

Mortar	Cycles	Mass of Cube (g)				Mass of Cube (Average) (± 1 standard deviation) (g)
		1	2	3	4	
0% Fly Ash	0	280.54	281.30	281.24	280.83	280.98±0.36
	35	280.60	279.30	281.40	280.10	280.35±0.88
	70	277.50	275.20	278.60	276.30	276.90±1.47
	105	273.20	272.80	271.40	270.50	271.98±1.25
	140	271.30	272.40	271.10	270.00	271.20 ±0.98
20% CFA	0	279.99	276.35	279.88	277.95	278.54±1.74
	35	276.80	276.20	278.30	277.50	277.20±0.91
	70	273.80	273.30	277.60	274.20	274.73±1.95
	105	270.00	271.10	273.90	273.20	272.05±1.81
	140	271.20	269.70	271.90	270.50	270.83±0.94
20% 15CBFA	0	277.52	279.88	281.65	279.46	279.63±1.69
	35	278.50	277.90	278.30	279.10	278.45±0.50
	70	278.10	279.60	275.20	276.70	277.40±1.86
	105	275.20	272.40	273.80	273.70	273.78±1.04
	140	271.80	270.50	272.10	270.70	271.28±0.80

A4.3 Compressive Strength over Cycles

Table A9 shows raw data recorded for quadruplicate analysis of compressive strength during resistance to freeze-thaw analysis. Calculations are as explained in A3.

Table A9: Compressive strength measurements as a function of freeze-thaw cycles.

Mortar	Cycles	Force to Fracture Trials (lb_f)				Compressive Strength Trials (MPa)				Compressive Strength (Average) (± 1 standard deviation) (MPa)
		1	2	3	4	1	2	3	4	
0% Fly Ash	0	20377.0	21801.0	21507.0	21500.0	35.12	37.58	37.07	37.06	36.71±1.08
	35	17865.0	19588.0	18209.0	17289.0	30.79	33.76	31.39	29.80	31.44±1.68
	70	18260.0	16010.0	18998.2	15037.0	31.47	27.60	32.75	25.92	29.43±3.20
	105	15662.0	13998.0	13740.2	13230.0	27.00	24.13	23.68	22.80	24.40±1.81
	140	11762.0	12341.0	11447.0	10694.0	20.27	21.27	19.73	18.43	19.93±1.18
20% CFA	0	22936.0	22611.0	20632.0	23180.0	39.53	38.97	35.56	39.96	38.51±2.00
	35	19911.0	20489.0	-	21523.0	34.32	35.32	-	37.10	35.58±6.28
	70	17643.0	18593.0	18689.0	17634.0	30.41	32.05	32.21	30.40	31.27±1.00
	105	15340.0	-	13936.0	14473.0	26.44	-	24.02	24.95	25.137±3.40
	140	11420.0	12733.0	11648.0	13531.0	19.68	21.95	20.08	23.32	25.26±1.69
20% 15CBFA	0	21684.0	20646.0	18948.0	20708.0	37.38	35.59	32.66	35.69	36.22±1.96
	35	19054.0	20684.0	19851.0	19721.0	32.84	35.65	34.22	33.99	34.18±1.15
	70	18940.0	17833.0	18764.2	19092.0	32.65	30.74	32.34	32.91	32.16±1.29
	105	13672.0	14493.0	15489.0	16001.0	23.57	24.98	26.70	27.58	25.71±1.80
	140	12526.0	12679.0	13261.0	12223.0	21.59	21.85	22.86	21.07	21.843±0.75

Note: " – " indicates a result not used in average calculations due to it being far removed from the other results.

Appendix B: SEM/EDS Analysis of Fly Ash Thin Slices

B1 EDS Data

In Appendix B, information is presented which describes the excel spreadsheets used to construct the ternary diagrams shown in Chapter 4. Quantitative elemental analysis of each fly ash section was carried out by X-ray energy dispersive spectrometry (EDS) with an Oxford Link ISIS system, using calibration standards: garnet for Al, Fe, Mg and Si; orthoclase for K and Na; wollastonite for Ca; and barium sulfate for Ba and S. EDS analysis of thin slices of fly ash particles allowed to quantify more accurately the mineral phases present of each fly ash were recorded and input into Microsoft Excel files (explained below). The Microsoft excel files are available on CD attached at the back of this thesis. The following section titles match the titles of the excel files on the CD:

Overall Ternary Diagrams

Figures 4-19 through 4-22 were constructed in this Microsoft Excel File. The first three worksheets represent the raw data collected for each fly ash and are labelled *Thin Slice CFA, Thin Slice 15CBFA,* and *Thin Slice 66CBFA* respectively. In each work sheet:

- Rows 4 to 26 show raw data which were input into excel:
    - During EDS acquisition, particles were recorded as <5μm or >5μm, with particles <5μm denoted by an "x" in row 3 above the particle.
    - During EDS acquisition, particles were recorded as *Porous* or *Non-Porous* and sorted accordingly under headings in row 4.

- In some cases, more than one EDS measurement was made in an image. Row 5 shows the title of the SEM images to which the particles belong *(Ex. ATCOALFA1)*.
- Row 6 contains letters, for each of which one EDS measurement was taken. EDS quantitative data are recorded in the cells underneath these letters in weight %.
- Cells A7 to A24 list elements which were quantified by EDS.
- Row 25 shows the Element Total, as determined by EDS.

- The data presented in rows 4 to 26 were then normalized and shown in rows 29 to 50 in the same manner as above.
- In order to construct ternary diagrams, the normalized data for Si, Al, Ca, Fe, Na, and Mg were extracted and displayed in rows 54 to 202 for *Thin Slice CFA,* 54 to 164 for *Thin Slice 15CBFA,* and 54 to 179 for *Thin Slice 66CBFA.* Each row represents data for one particle.
  - Headings are shown in row 54, with elements in columns C to H.
  - Ternary diagrams require the sum of three constituents to be taken as constant (100% in this case), so the data must be normalized again with only the three components which will be used in the ternary diagram. Therefore, columns J to M show the summation of the three components used for each ternary diagram.
  - An "x" in column A denotes particles <5μm and an "x" in column B denotes porous particles.

- Since it is desirable to present ternary diagrams in terms of molar composition, the data presented in rows 54 to 202 for *Thin Slice CFA,* 54 to 164 for *Thin Slice 15CBFA,* and 54 to 179 for *Thin Slice 66CBFA* were converted from weight % into molar % by taking the quotient of the weight % and the molar mass of each element (listed in row 54).
- This data was then used to construct ternary diagrams in subsequent work sheets (one for each ternary diagram).

CFA Molar Thin Slices, 15CBFA Molar Thin Slices, and 66CBFA Molar Thin Slices

Figures 4-23 to 4-28 were constructed from these Microsoft Excel Files, with one file for each type of fly ash. These files show the same information as explained for *Overall Ternary Diagrams,* however there are many more worksheets.

In the first work sheet in each file, the work sheet differs when the data are displayed for ternary diagram construction, by being sorted according to size (with particles <5μm at the top of the data). This makes it easier to subsequently construct ternary diagrams (in the following 4 worksheets: *SiAlCa(Size), SiAlFe(Size), SiAlNa(Size)* and *SiAlMg(Size)*), comparing small and large particles for the fly ash in the file.

The second worksheet (*Thin Slice CFA, Thin Slice 15CBFA or Thin Slice 66CBFA)* is a copy of the first (the same as *Overall Ternary Diagrams*) but with the data sorted according to porous or non-porous in rows containing data to construct ternary diagrams. The following four worksheets (*SiAlCa(P-NP), SiAlFe(P-NP), SiAlNa(P-NP)* and *SiAlMg(P-NP)*), comparing show ternary diagrams constructed to display the composition of porous and non-porous particles.

B2 Additional SEM Images

CFA

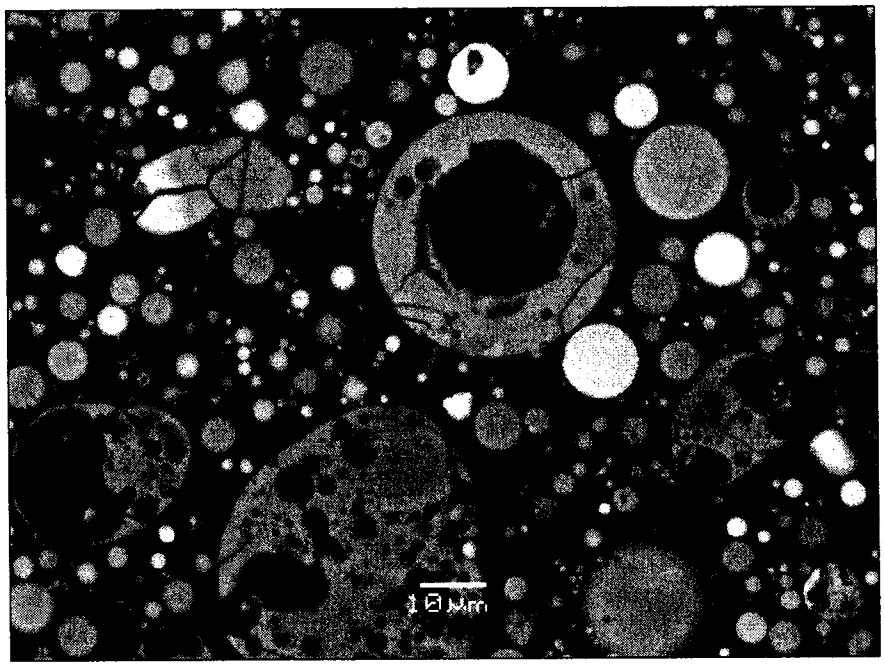

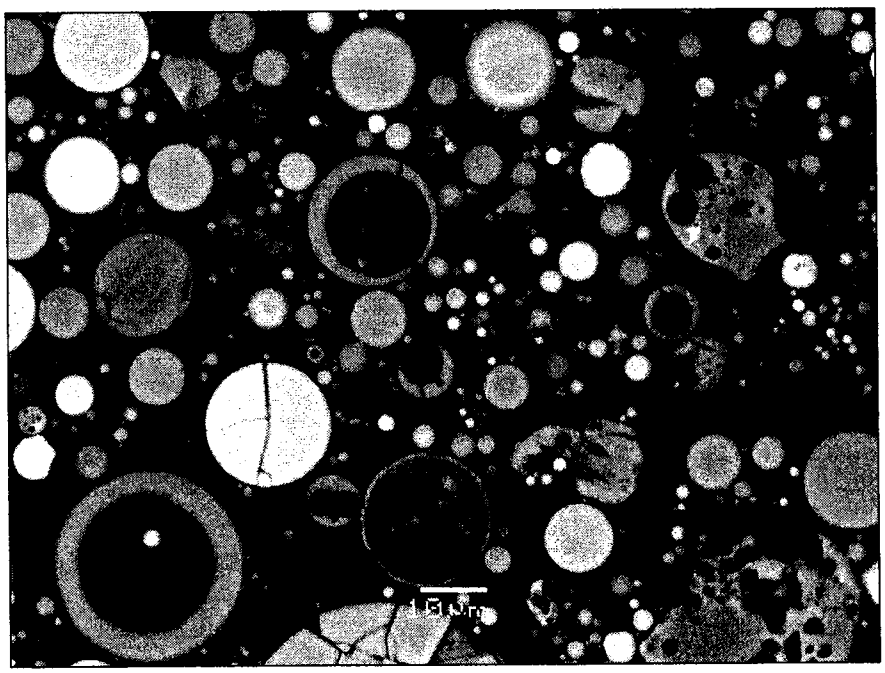

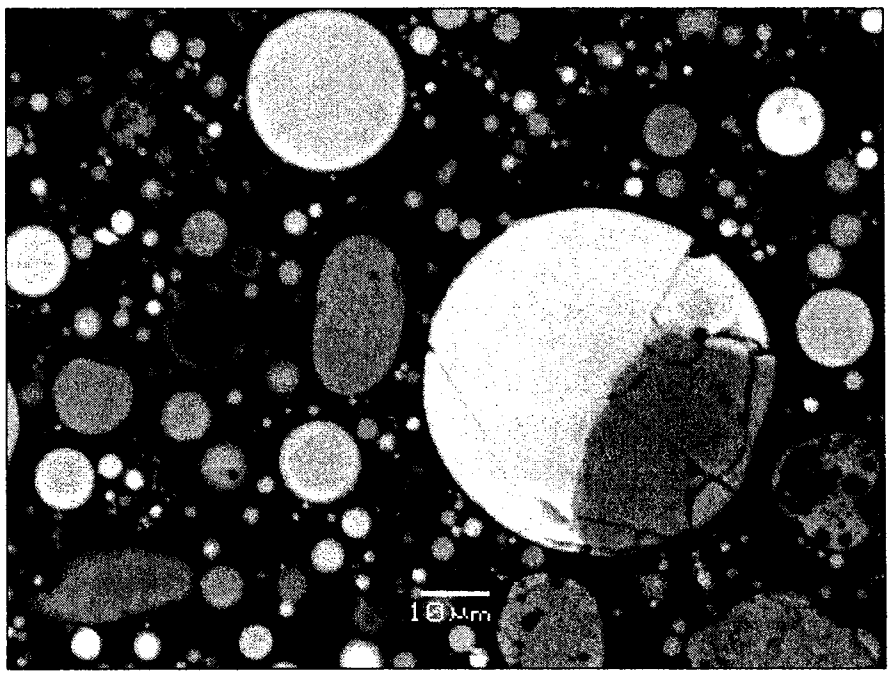
10 μm

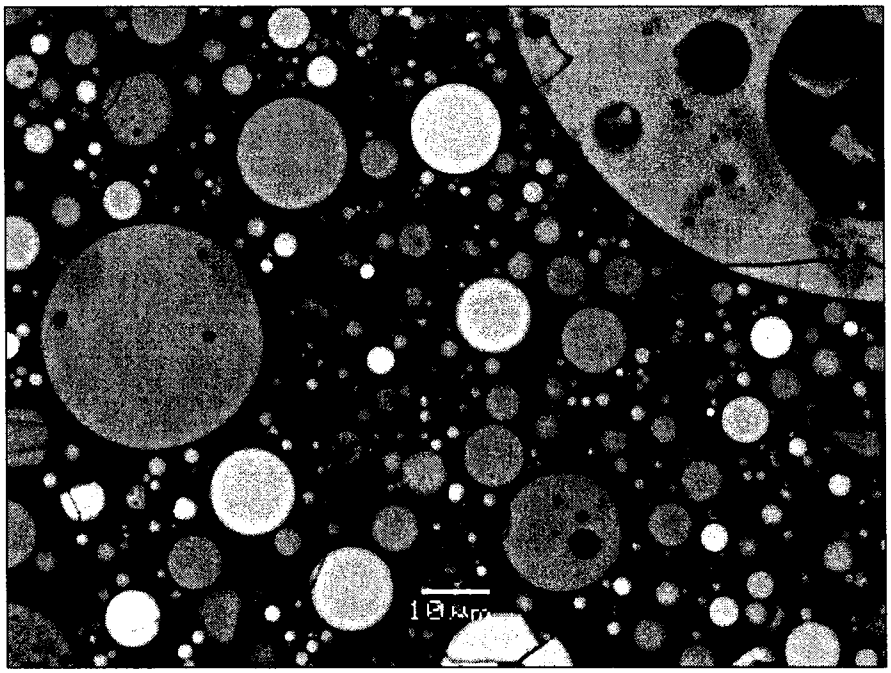
10 μm

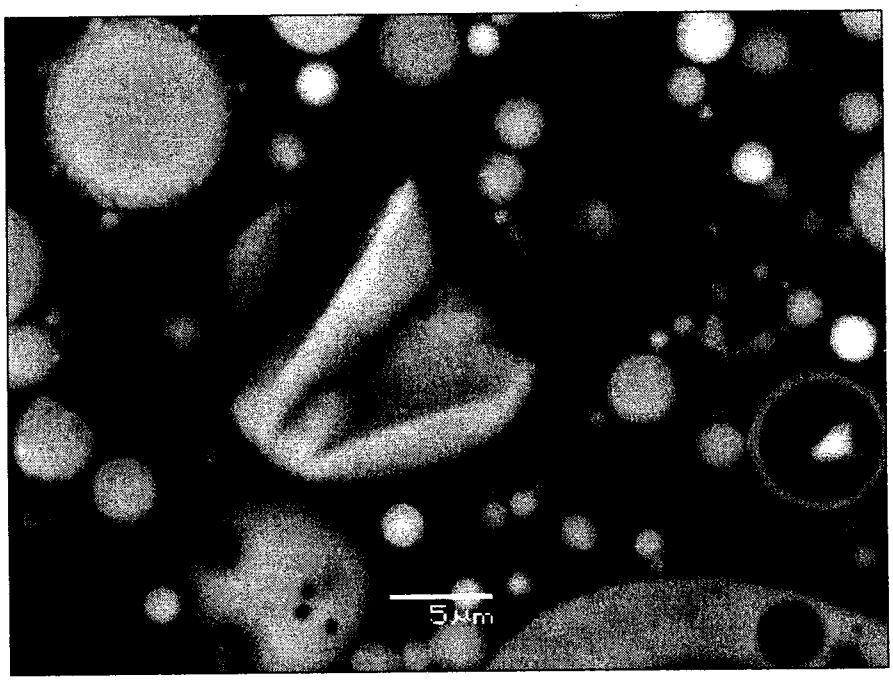
5 µm

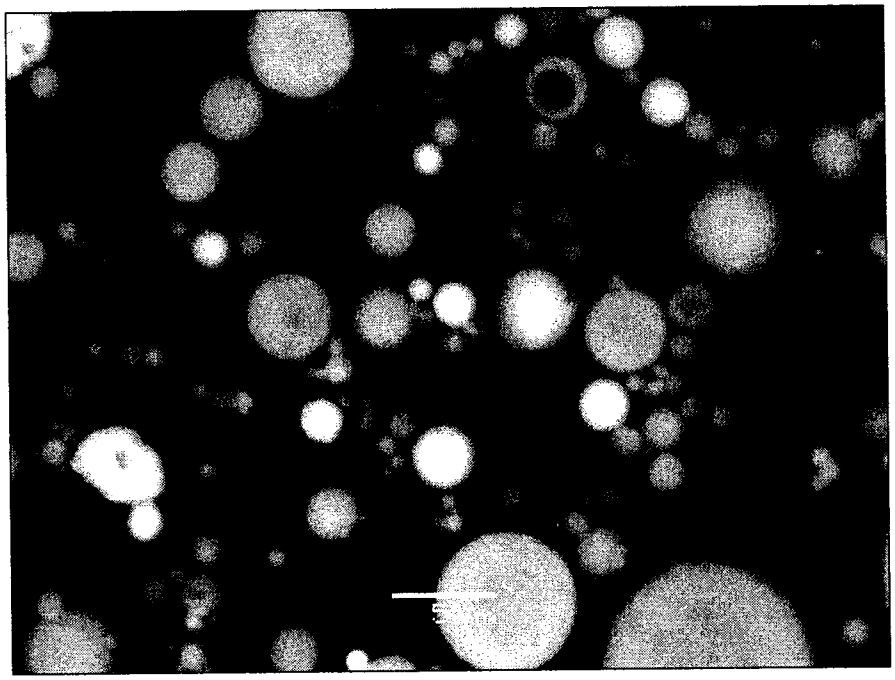

15CBFA

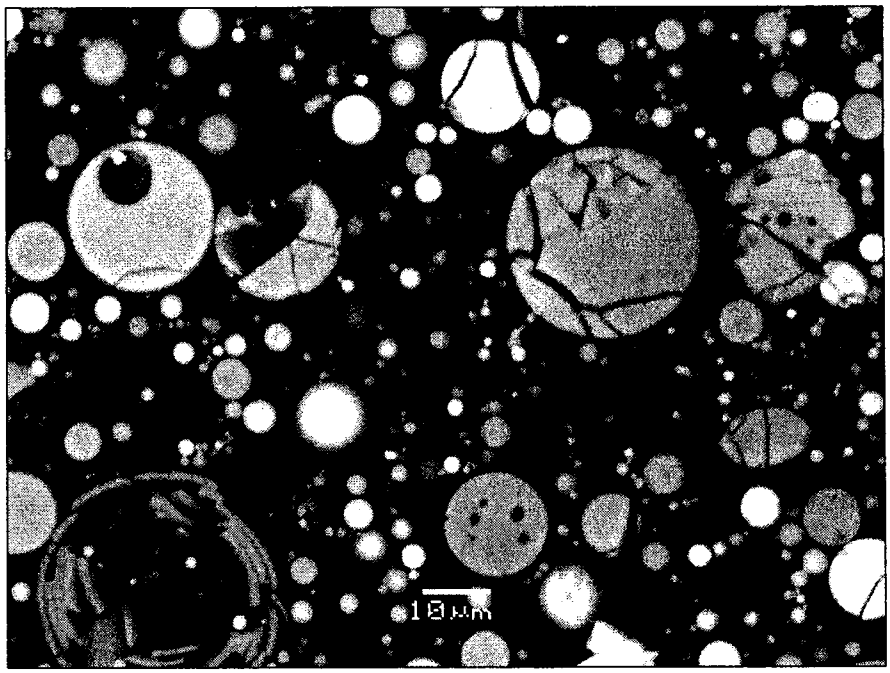

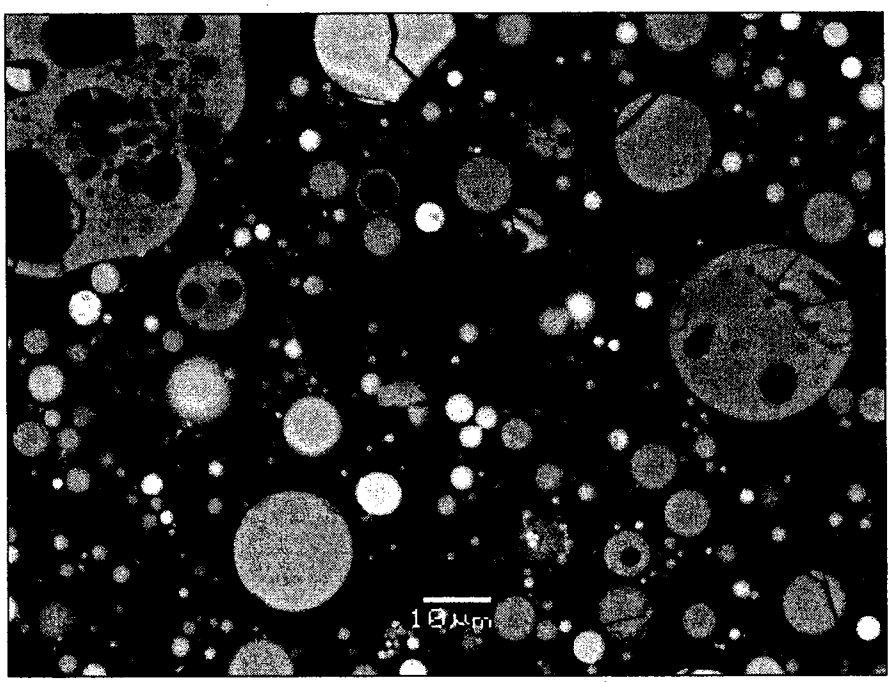

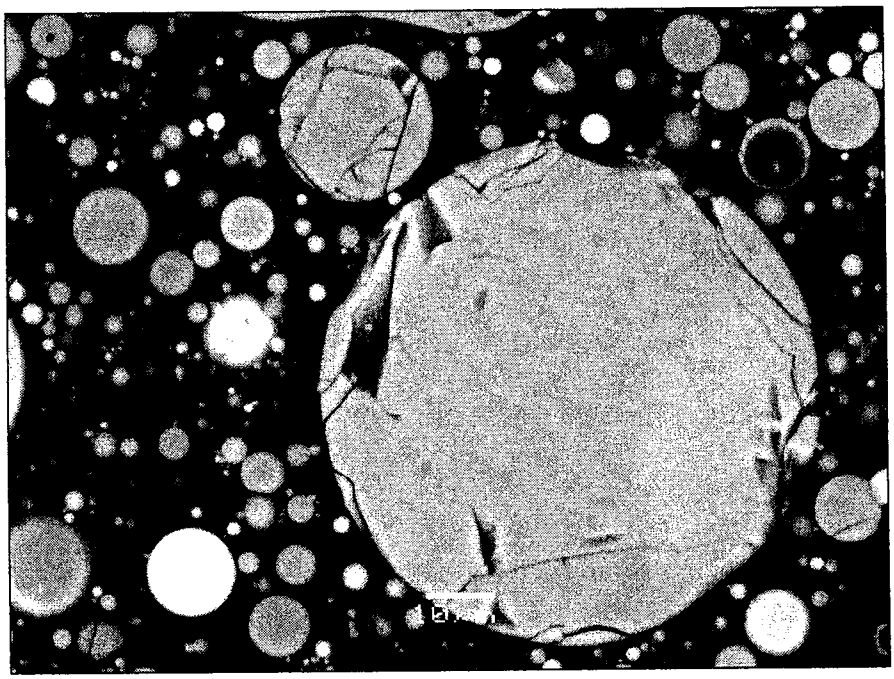

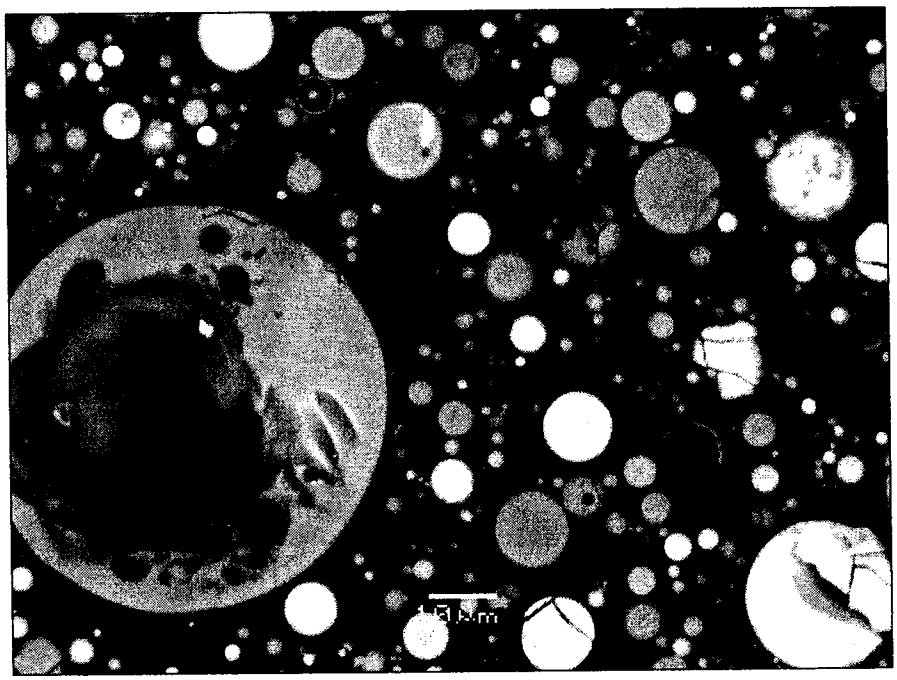

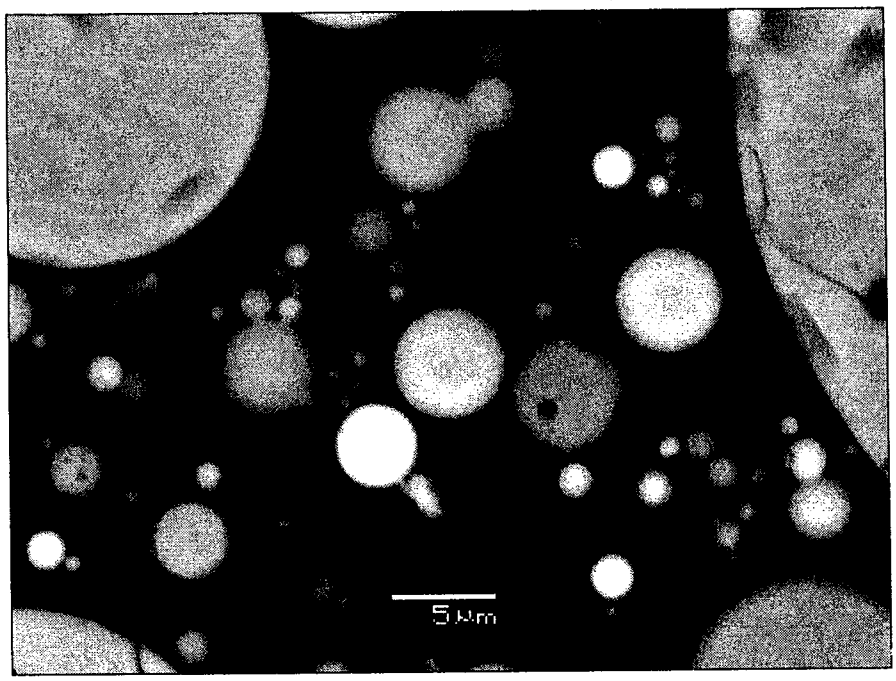
5 μm

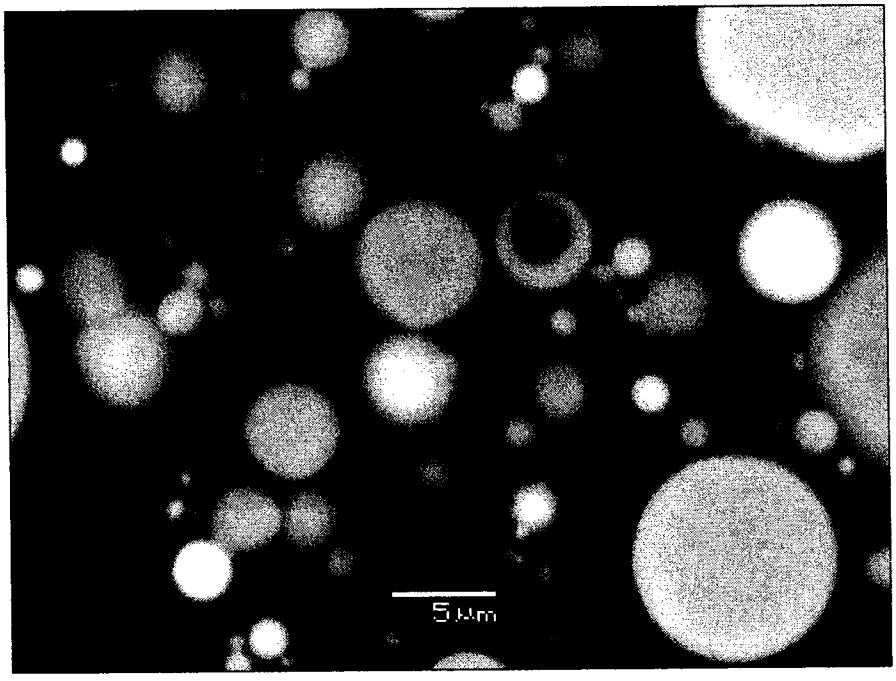
5 μm

66CBFA

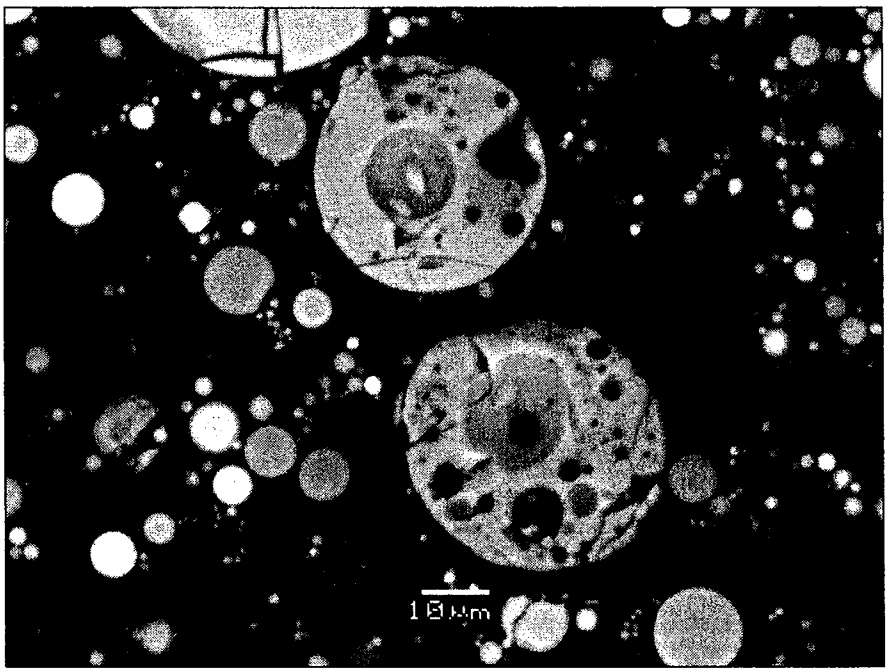

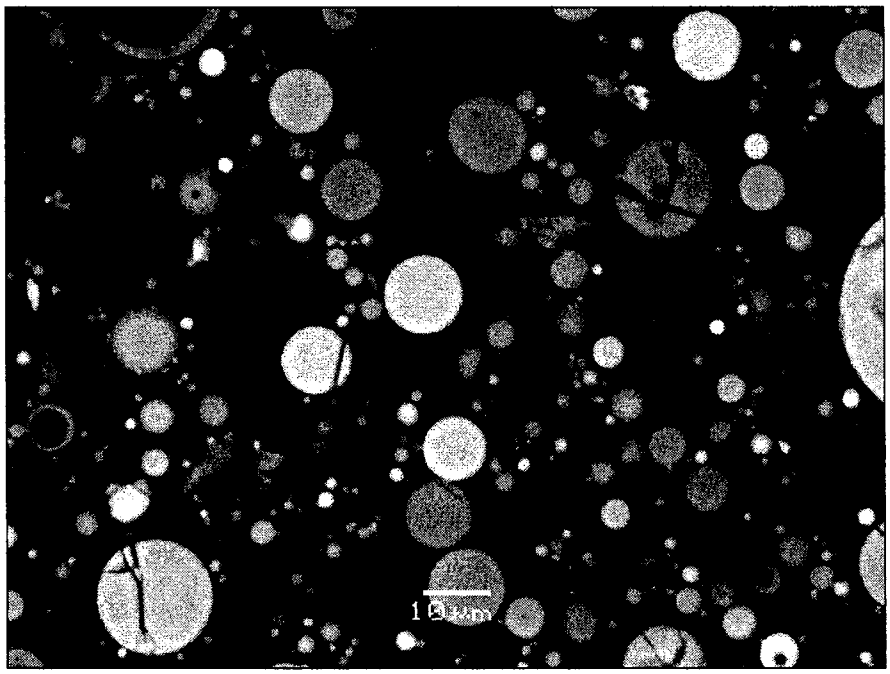

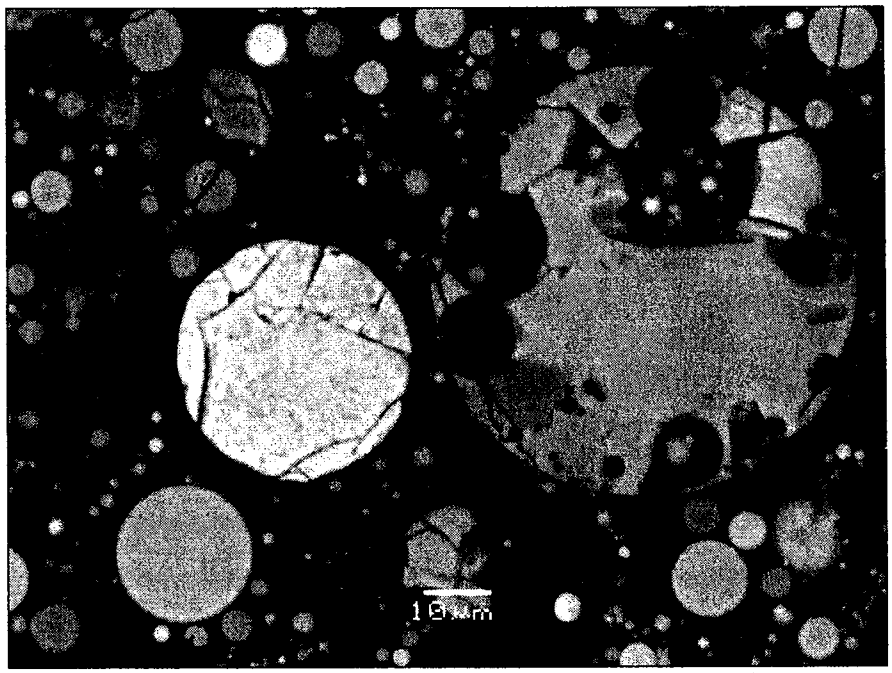
10 µm

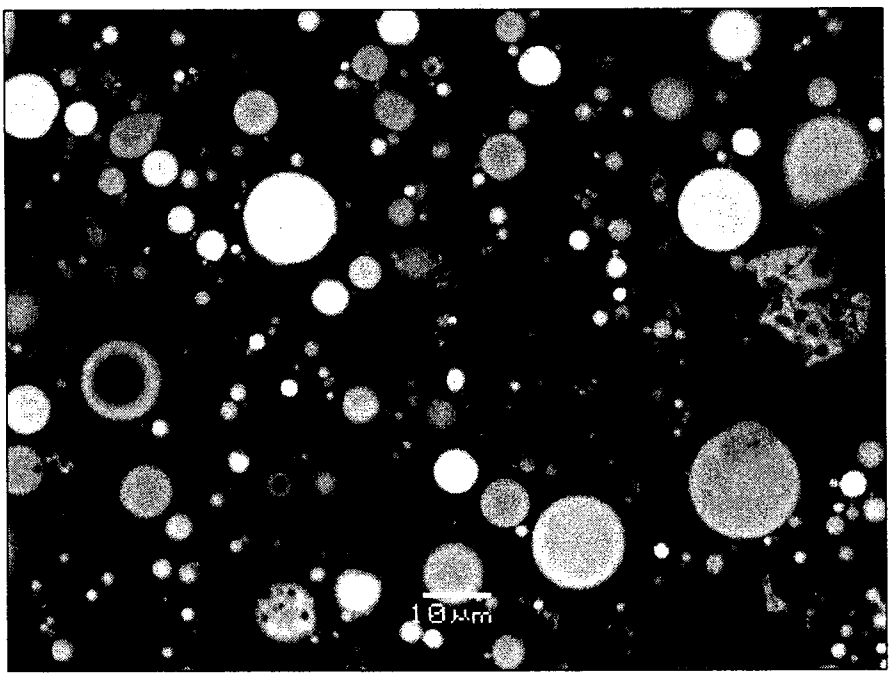
10 µm

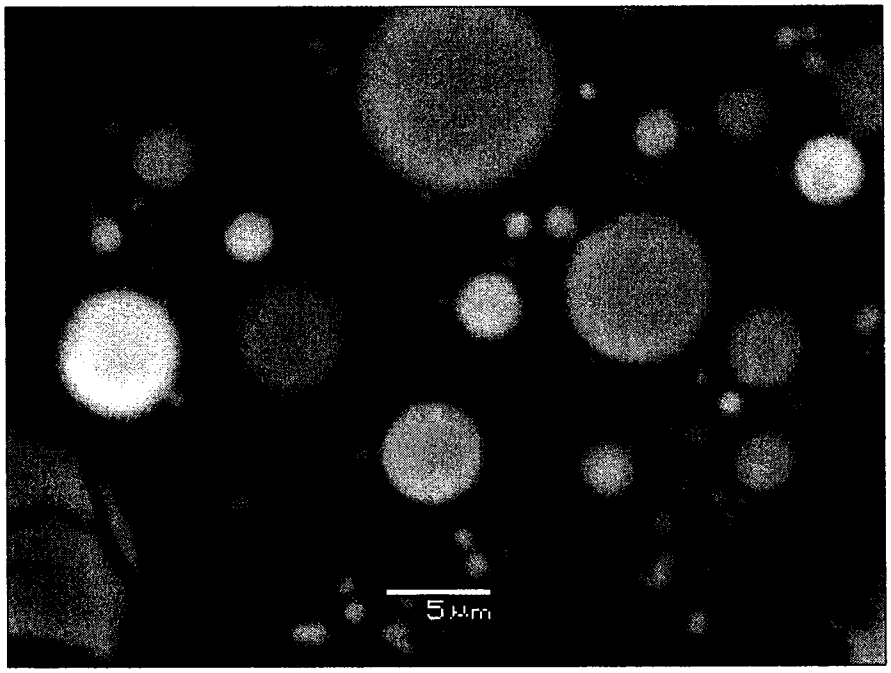
5 μm

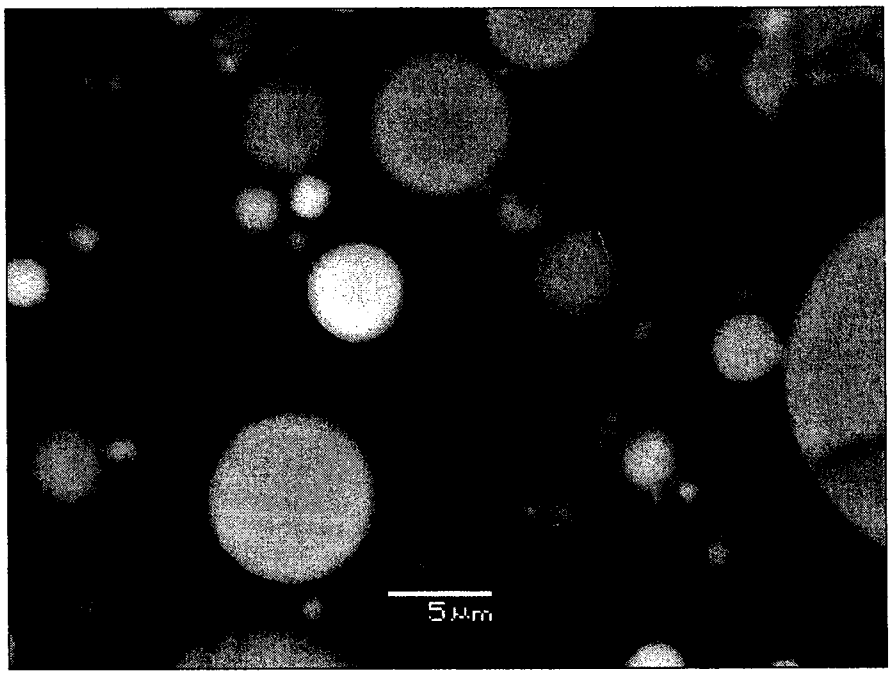
5 μm

Appendix C: SEM/EDS Analysis of Mortar Thin Slices

C1 EDS Data

In Appendix C, information is presented which describes the excel spreadsheets used to compile SEM/EDS analysis completed on cement mortars in Chapter 5. Quantitative elemental analysis of mortar thin sections was carried out by X-ray energy dispersive spectrometry (EDS) with an Oxford Link ISIS system, using calibration standards: garnet for Al, Fe, Mg and Si; orthoclase for K and Na; wollastonite for Ca; and barium sulfate for Ba and S. EDS analysis of thin slices of mortars allowed to quantify more accurately the composition of phases present in each mortar (Fly ash inner CSH, cement CSH, outer CSH, sand and non-sand CH, and dense hydration products (DHP)) as explained in section 5.4. EDS data were recorded and input into Microsoft Excel files (explained below). The Microsoft excel files are available on CD attached at the back of this thesis. The following section titles match the titles of the excel files on the CD:

SEM 0%FA CM - 28days

This excel file contains EDS data collected from a thin slice of ash-free mortar at 28 days curing. The worksheets are titled: *Cement Inner CSH, Outer CSH,* and *CH.* Similar to the spreadsheets explained in Appendix B, elements for which EDS performed quantitative measurements are listed in column A. Row 2 shows the title of the image on which the EDS was performed, and row 3 shows the individual point. In the first worksheet, *Cement Inner CSH,* row one titles "Cement centres" and "Inner CSH" in order to distinguish the

EDS performed on un-reacted cores of cement particles and the CSH belonging to a particular particle of cement which has undergone hydration reactions.

SEM 20%CFA – 28 days and SEM 20%15CBFA – 28days

These files are similar to SEM 0%FA – 28 days, except with a few additional worksheets. The samples on which SEM-EDS was performed were mortars containing 20% CFA or 15CBFA which had been cured for 28 days (the same slices from which BSE images in Figures 5-10 to 5-13 were taken). The worksheets are titled: *CFA Inner CSH, (or 15CBFA Inner CSH), Cement Inner CSH, Outer CSH, Sand CSH, non-sand CSH* and *DHP*. As explained above, elements for which EDS performed quantitative measurements are listed in column A. Row 2 shows the title of the image on which the EDS was performed, and row 3 shows the individual point. Again, in *Cement Inner CSH,* row one titles "Cement centres" and "Inner CSH" in order to distinguish the EDS performed on un-reacted cores of cement particles and the CSH belonging to a particular particle of cement which has undergone hydration reactions, as is the same for *CFA Inner CSH*, in which row 1 distinguishes between the un-reacted core of a fly ash particle and the fly ash inner-CSH which has formed around it due to pozzolanic reactions.

In SEM 20%CFA – 28 days, the final worksheet is titled *Profiles.* This worksheet contains EDS data collected from images shown in Figures 5-12 and 5-13. Rows 3 through 11 show raw EDS data collected at positions 1 to 8 in Figure 5-12 (in weight %) of Ca, Si and finally column C calculates the Ca/Si ratio. In Rows 16 through 23, the raw data (in weight%) is converted to a molar% by taking the quotient of the reported

weight% (in rows 3 through 11) and the respective molar mass of Ca or Si. Again, Column C calculated the Ca/Si molar ratio, and is used for plotting Figure 5-14.

The same information is given for the 15CBFA particle shown in Figure 5-13 in rows 28 to 35 and 38 to 45.

C2 Additional SEM Images of Cement Mortars

Ash-free Mortar, Cured for 28 Days

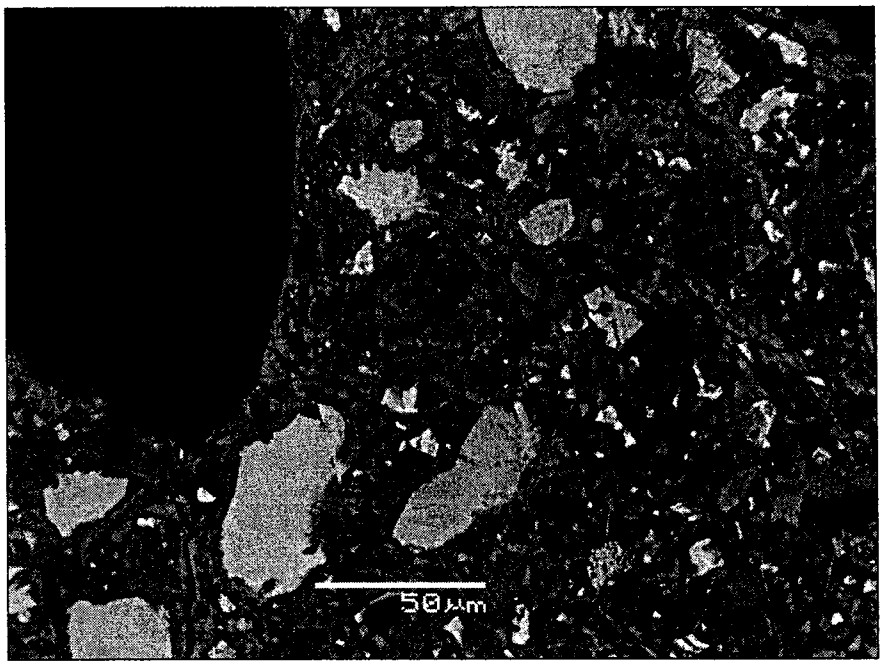

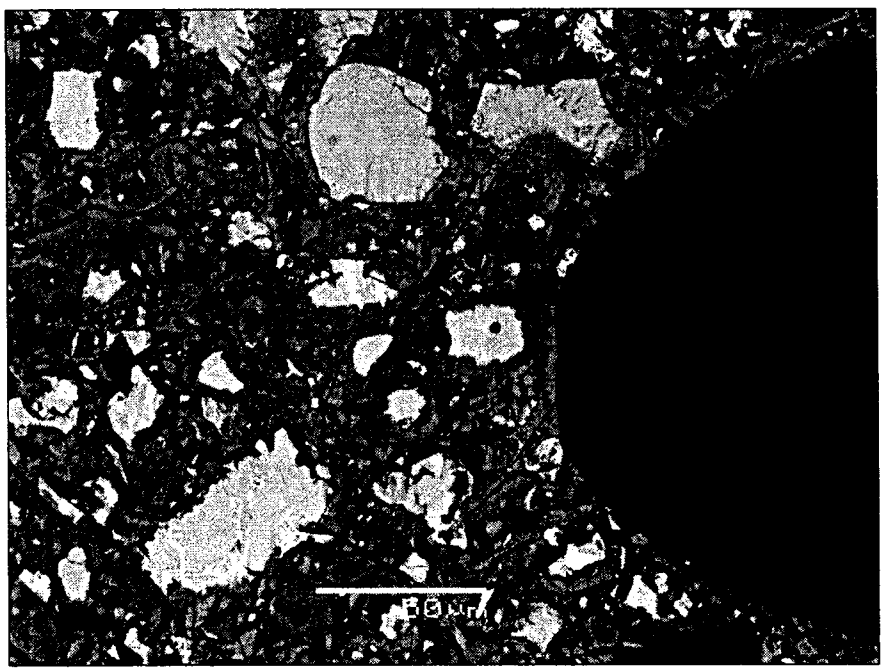

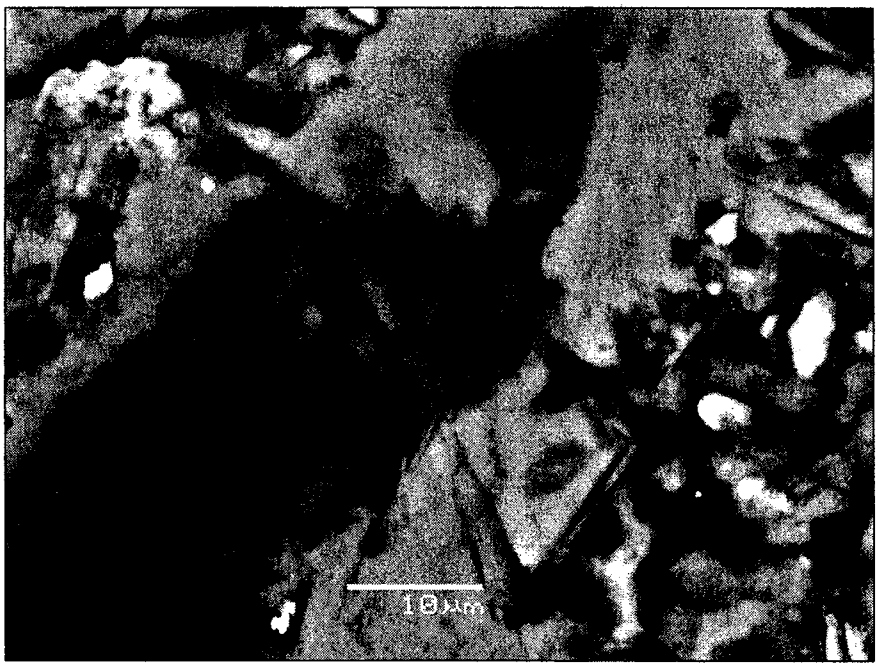
10μm

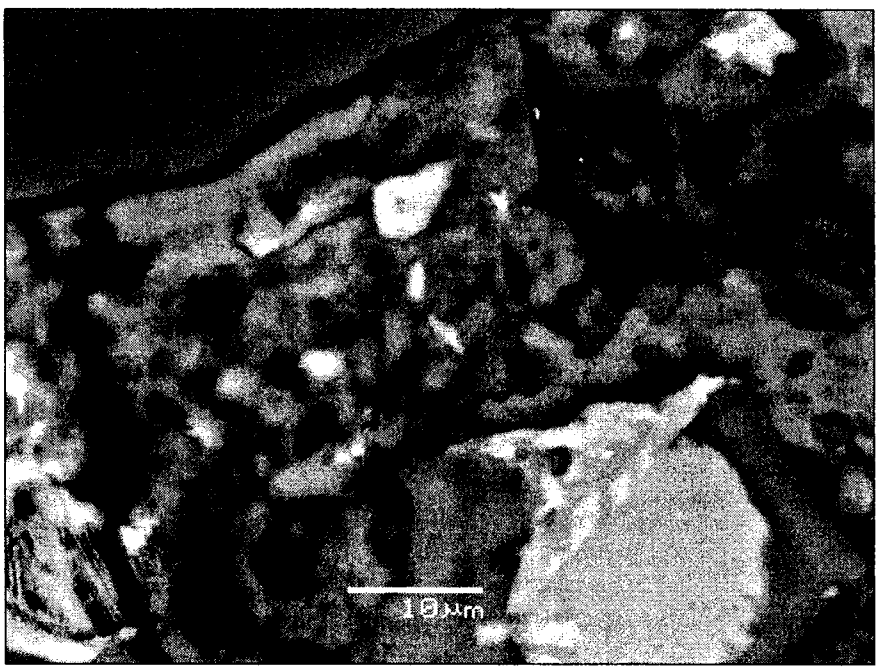
10μm

20% CFA Mortar, Cured for 28 Days

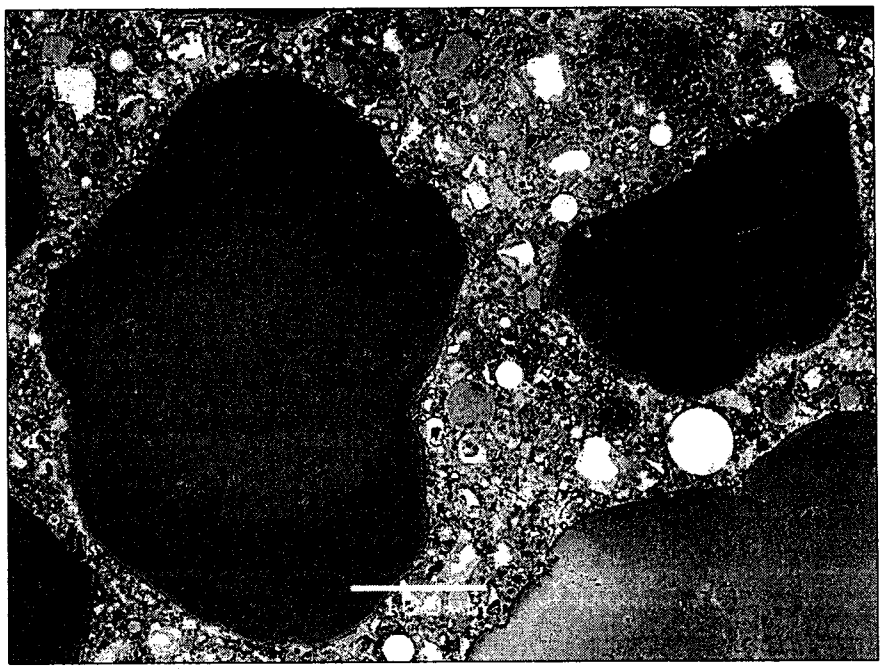

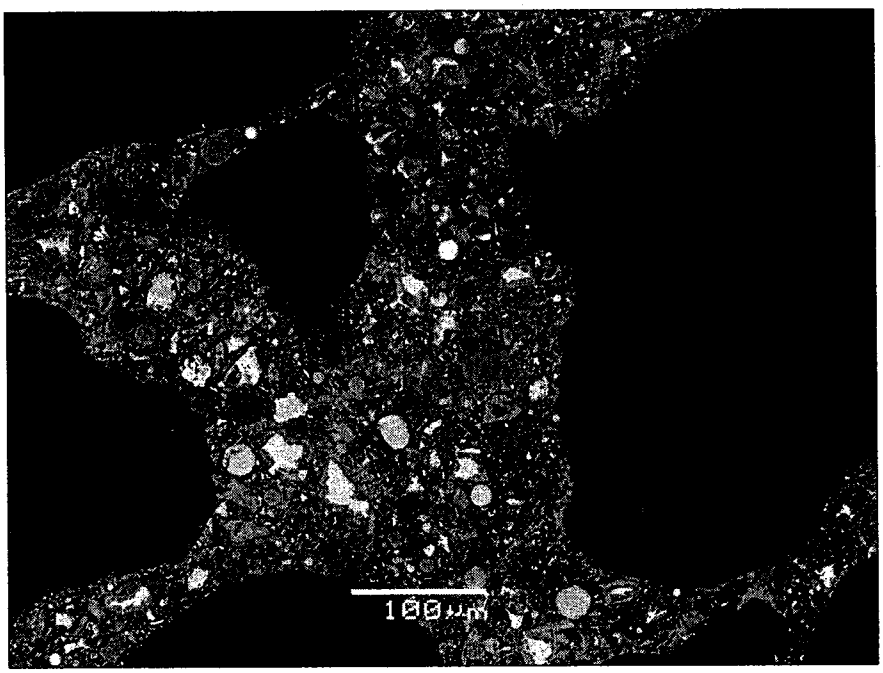

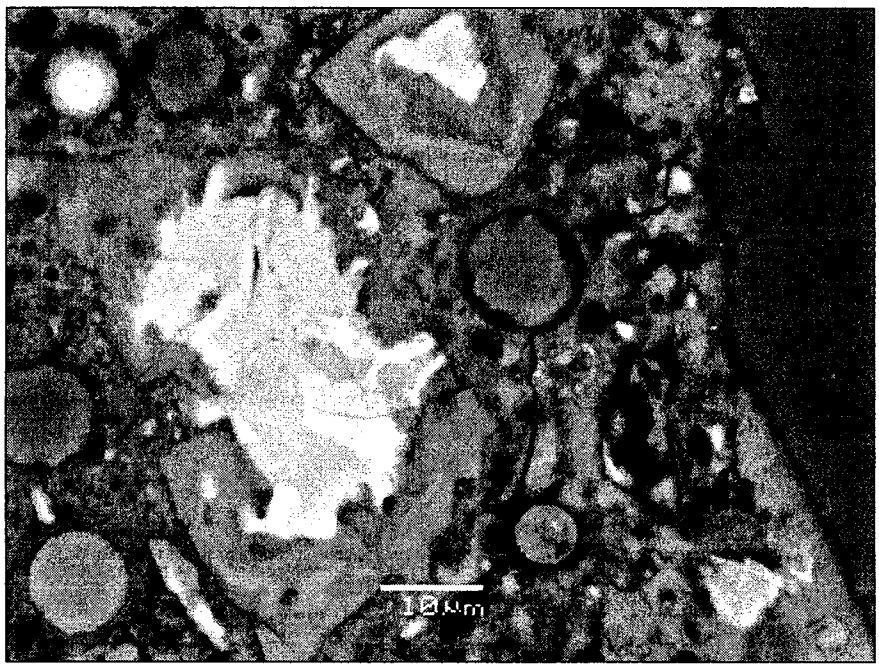
10μm

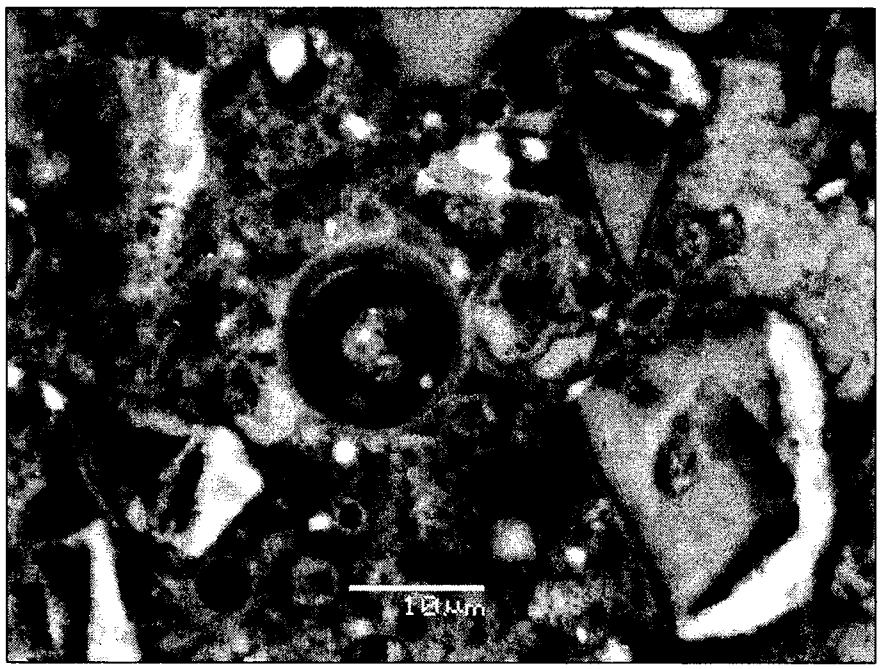
10μm

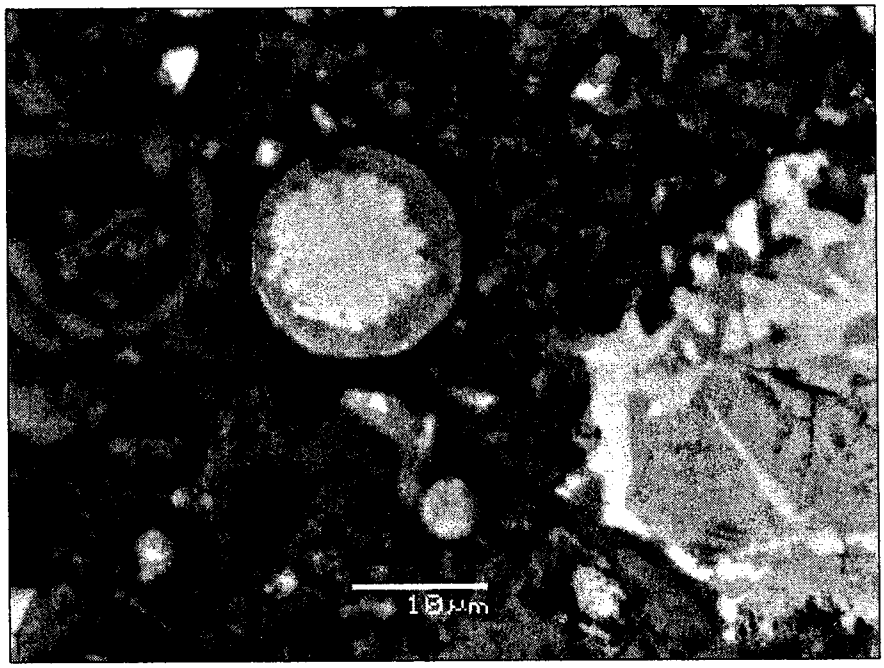
10μm

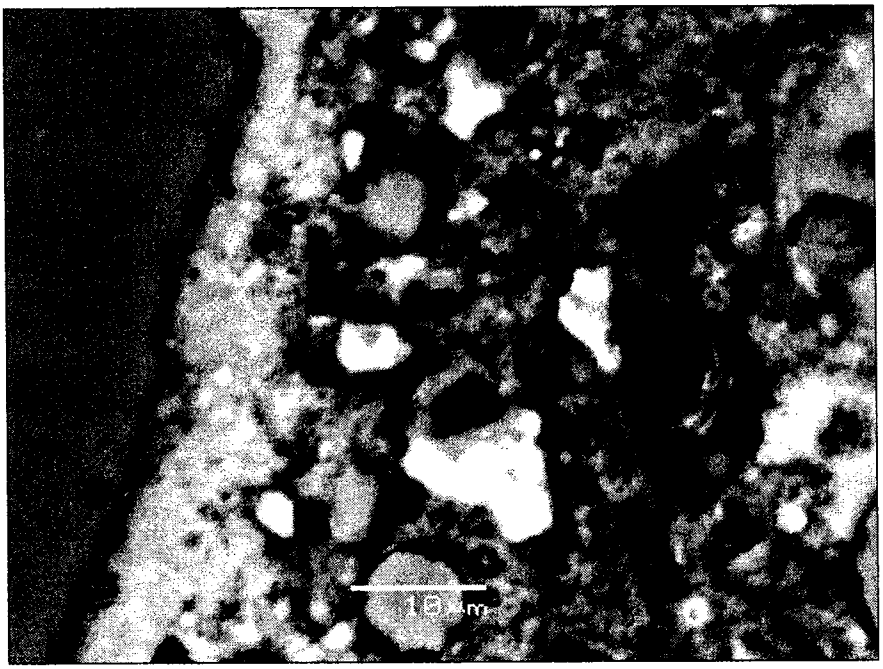
10μm

20% 15CFA Mortar, Cured for 28 Days

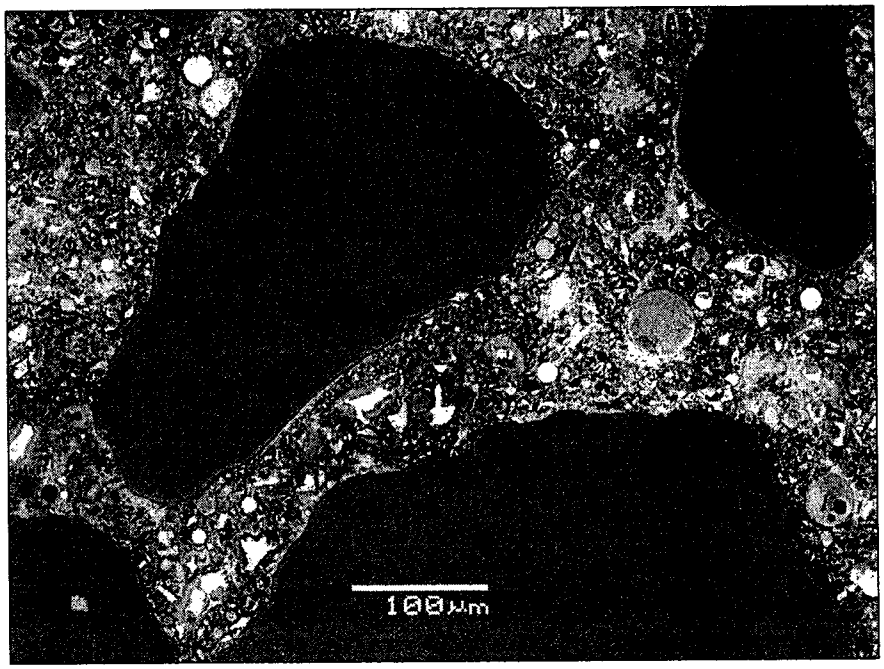

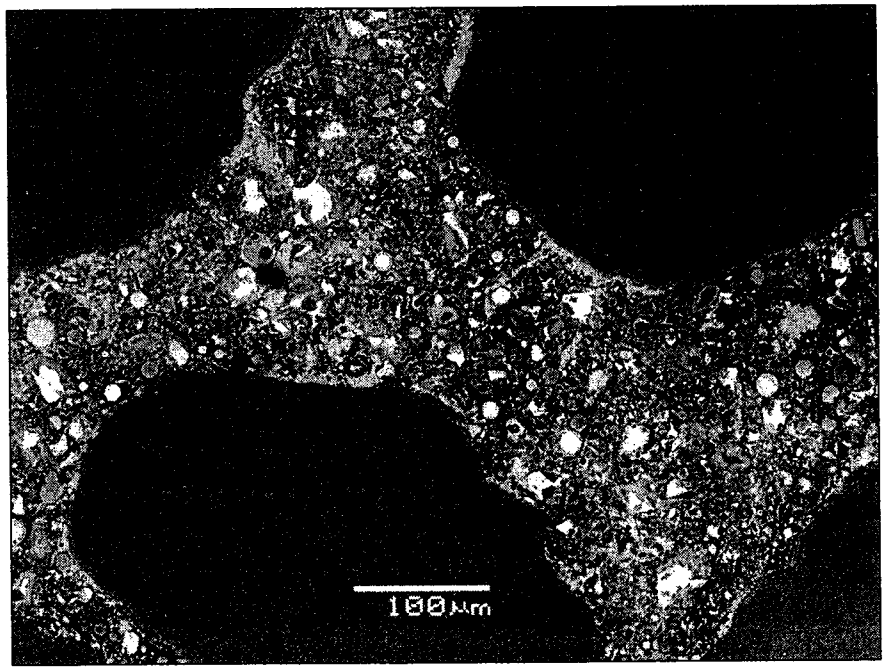

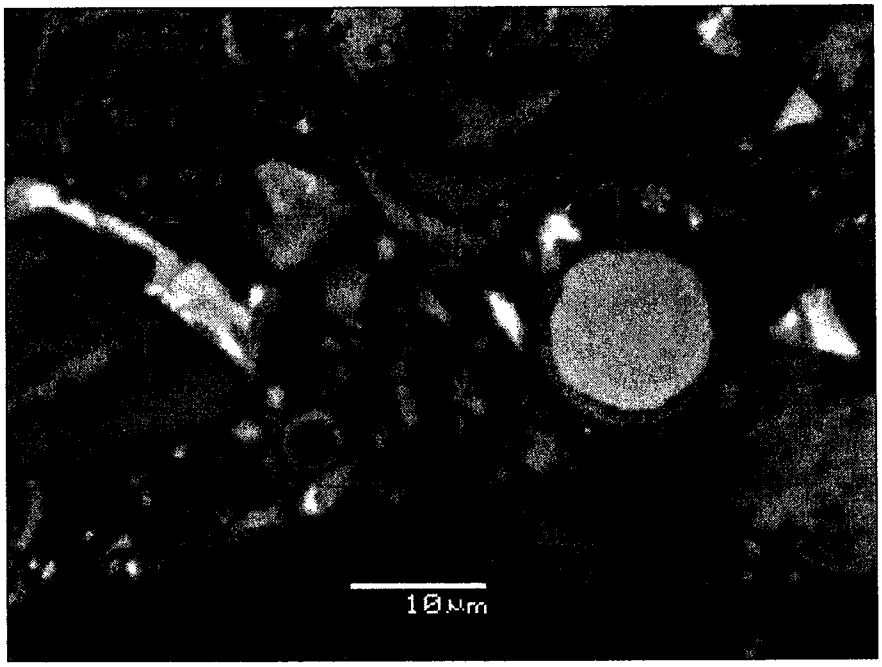
10μm

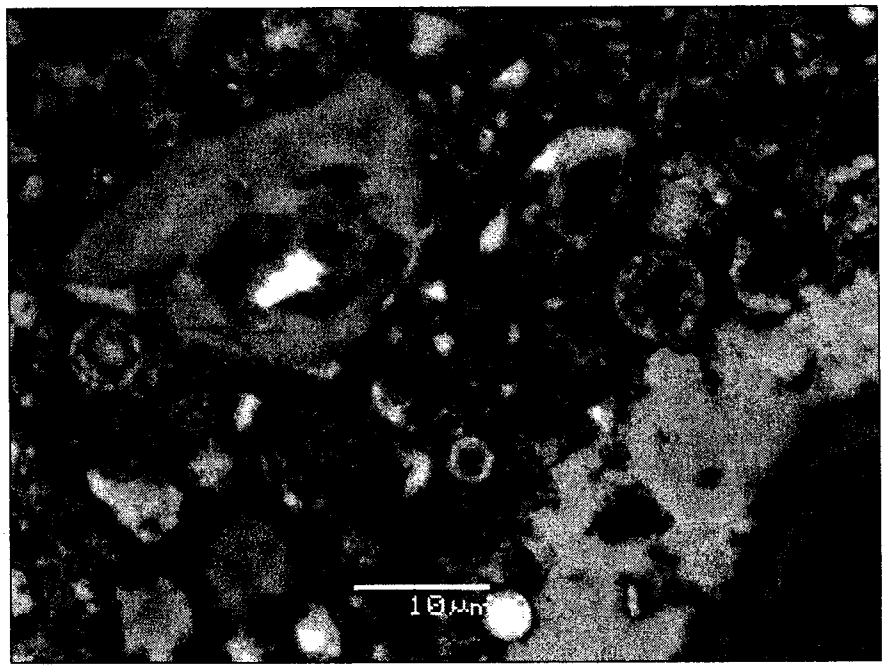
10μm

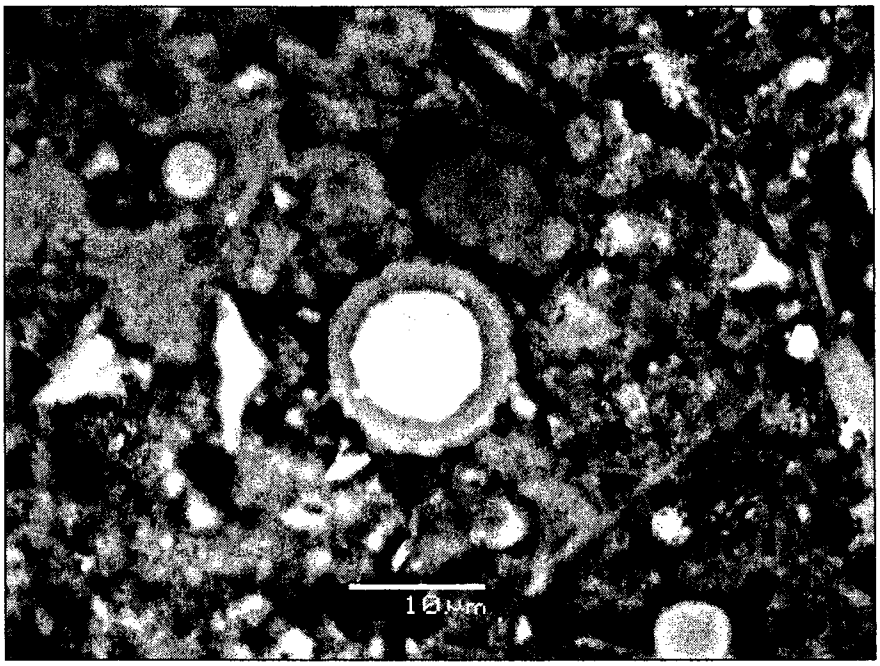
10μm

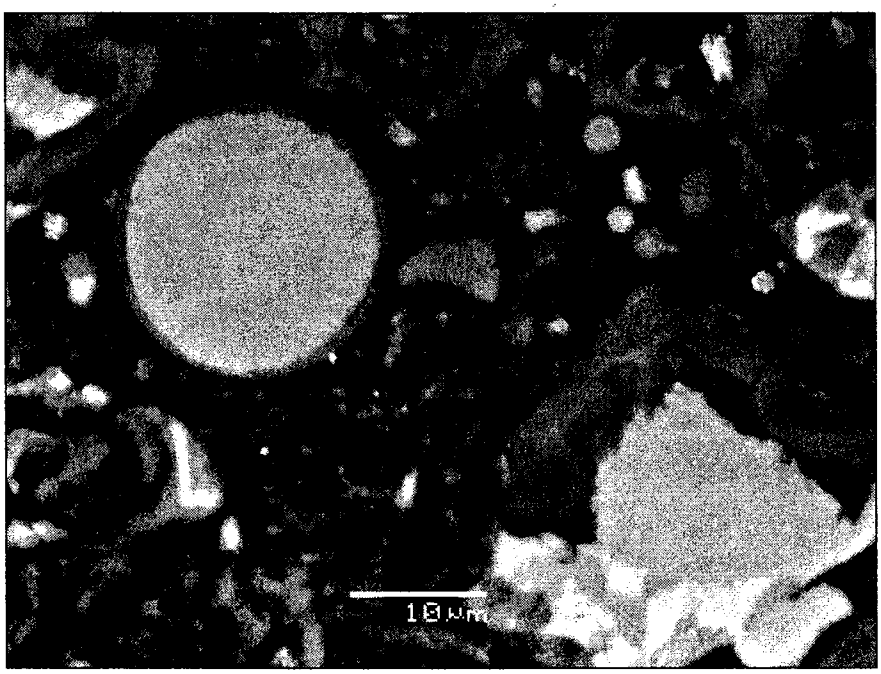
10μm

Appendix D: How to Read a Ternary Diagram

A ternary diagram is a triangular figure, with each of the corners (apexes) representing a composition (such as Al, Si and Fe). Ternary diagrams do not show individual concentrations, but rather the proportion of each of three elements when their sum is taken to be constant (100%).

The following image has only the skeleton of the triangular diagram as we concentrate on the Al concentration. The Al axis is on the left side of the triangle. The Al-apex, or the point representing 100% relative Al concentration, is at the top of the triangle. The bottom of the triangle represents 0% Al. The horizontal lines represent constant percentages of Al. To read the Al concentration corresponding to a point on the diagram, a line would be projected out to the left.

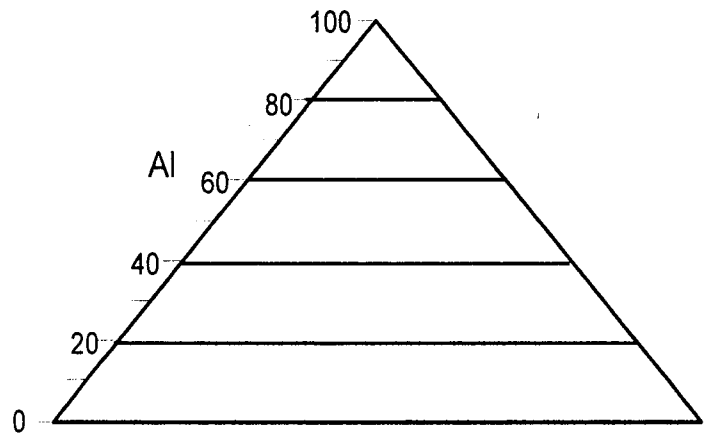

The Si-apex is at the lower right corner of the triangle and represents 100% Si. A percent abundance scale is made of Si along the right side of the triangle by the placement of lines parallel to the left side of the triangle, which represents 0% Si. To find the %Si of a point in the diagram, a line is projected along these diagonal lines and the right side of the triangle becomes the scale for percent abundance of Si.

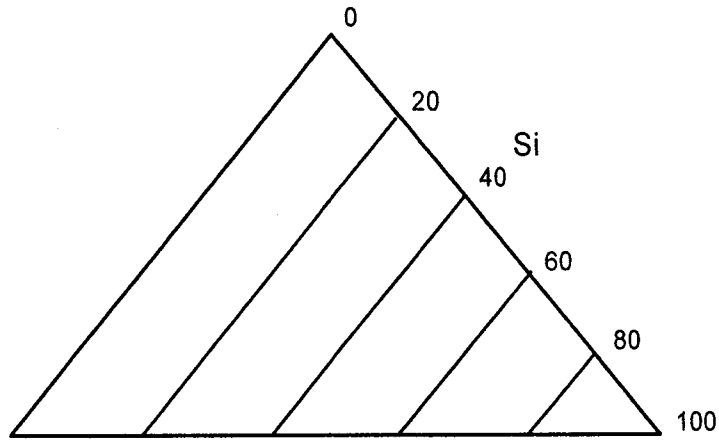

The Fe-apex is at the lower left corner of the triangle and represents 100% Fe. A percent abundance scale is made of Fe along the bottom of the triangle by the placement of lines parallel to the right side of the triangle, which represents 0% Fe. To find the %Fe for a data point in the diagram, a line is projected along these diagonal lines and the right side of the triangle becomes the scale for percent abundance of Fe.

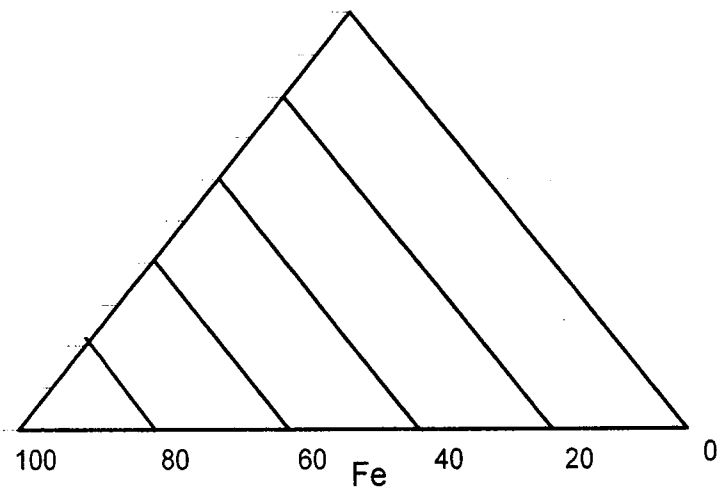

Below is a diagram in which all three above diagrams are superimposed to show the full ternary diagram. A point is also placed on the diagram in order to exemplify how to read the composition of this point.

The arrows follow the lines established in the previous images to reveal a composition of 40% Al, 20% Si and 40% Fe.

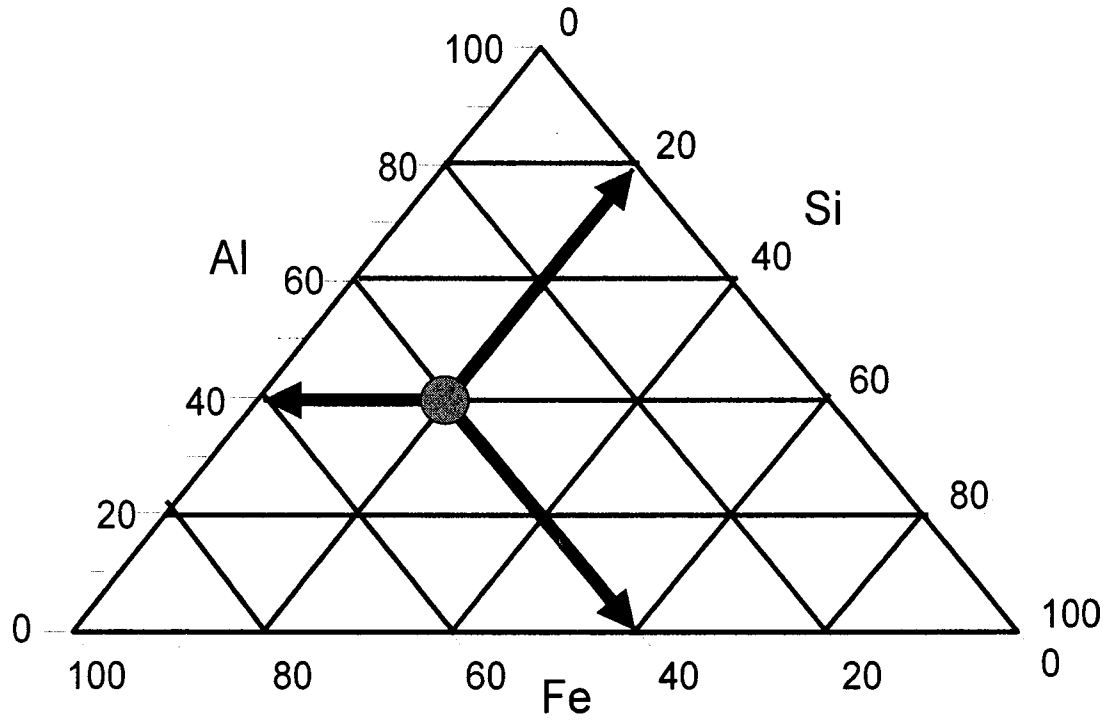

References

Abdun-Nur EA. Fly-ash in concrete: an evaluation. Bulletin No. 284, Highway Research Board, Washington DC, USA. 1961.

Adriano DC, Page AL, Elseewi AA, Chang AC, Straughan I. Utilization of fly ash and other coal residues in terrestrial ecosystems: a review. Journal of Environmental Quality 1980; 9:333-344.

Ahmad A, Alam MM. Utilization of fly ash and *Paecilomyces lilacinus* for the control of *Meloidogyne incognita.* International Journal Nemitol 1997; 162-164.

Alba N, Gasso A, Lacorte T, Baldasano JM. Characterization of municipal solid waste incineration residue from facilities with different air pollution control systems. Journal of Air Waste Management Association 1997; 47:1170-1179.

American Association of State Highway and Transportation Officials (AASHTO). Mineral filler for bituminous paving mixtures. AASHTO Designation M17-83, Part I Specifications. 1986.

American Association of State Highway and Transportation Officials (AASHTO). Guidelines and guide specifications for using pozzolanic stabilized mixture (base course of subbase) and fly ash for in-place subgrade soil modifications. AASHTO Task Force Report 28, Washington DC, USA. 1999.

American Coal Ash Association (ACAA). Coal fly ash in pozzolanic stabilized stabilized mixtures for flexible pavement systems. Flexible Pavement Manual. American Coal Ash Association, Washington DC, USA. 1991.

American Coal Ash Association (ACAA). Fly ash facts for highway engineers. US Department of Transportation 2003; FHWA-IF-03-019.

American Concrete Institute Committee 201 (ACIC). Durability of concrete in service, Chapt. I, freezing and thawing; Proceedings American Concrete Institute 1962; 59:1771-1784.

American Concrete Institute (ACI). Controlled low strength materials. ACI229R. Farmington Hills MI, USA. 1999.

American Concrete Pavement Association (ACPA). Slab stabilization guidelines for concrete pavements. ACPA Technical Bulletin 018P. 1994.

American Cube Mold (ACM). Unpublished: Comparison Study. Twinsburgh, OH, USA. 1994.

American Society of Civil Engineers (ASCE). Fly ash for soil improvement. ASCE Geotechnical Special Publication 36, New York NY, USA. 1999.

American Society for Testing and Materials. Concrete and Aggregates. West Conshohocken, PA, USA. 2003; Vol 04.02,

C 109/C 109M-02 Standard Test for Compressive Strength of Hydraulic Cement Mortars (Using 2-in or [50mm] Cube Specimens)

C 114-03 Standard Test Methods for Chemical Analysis of Hydraulic Cement

C 150-03 Standard Specification for Portland Cement

C 185-02 Standard Test Method for Air Content of Hydraulic Cement Mortar

C 191-03 Standard Test Methods for Time of Setting of Hydraulic Cement by Vicat Needle

C 260-03 Standard Specification for Air-Entraining Admixtures for Concrete

C 266-03 Standard Test Method for Time of Setting of Hydraulic-Cement Paste Paste by Gillmore Needles

C 311-03 Standard Test Methods for Sampling and Testing Fly Ash or Natural Pozzolans for Use in Portland-Cement Concrete

C403/C403M-03 Standard Test Method for Time of Setting of Concrete Mixtures by Penetration Resistance

C 595-03 Standard Specification for Blended Hydraulic Cements

C 618-03 Standard Specification for Coal Fly-ash and Raw or Calcined Natural Pozzolan for Use in Concrete

C 666/C 666M-03 Standard Test Method for Resistance of Concrete to Rapid Freezing and Thawing

C 778-03 Standard Specification for Standard Sand

C 1437-01 Standard Test Method for Flow of Hydraulic Cement Mortar

ASTM Committee III-H. Co-operative tests of fly-ash as an admixture in portland cement concrete. Proceedings ASTM 1962; 62: 314-348.

Aubert JE, Husson B, Vaquier A. Use of municipal solid waste incineration fly ash in concrete. Cement Concrete Research 2004; 34:957-963.

Barth EF, De Percin P, Arozarene MM, Zieleniewski JL, Dosani M, Maxey HR, Hokanson SA, Pryately CA, Whipple T, Kravitz R, Cullinane MJ, Jones LW, Malone PG. Stabilization and solidification of hazardous wastes. Noyes Data Co. NJ, USA. 1990.

Berry EE. Fly-ash for use in concrete part I – a critical review of the chemical, physical and pozzolanic properties of fly-ash. Canmet Report, Minerals Research Program (Ottawa, Canada) 1976; 76-25.

Berry EE, Malhotra VM. Fly-ash for use in concrete part II – a critical review of the effects of fly-ash on the properties of concrete. Canmet Report, Minerals Research Program (Ottawa, Canada) 1978; 78-16.

Bibby D. Composition and variation of pulverized fuel ash obtained from the combustion of sub-bituminous coals, New Zealand, Fuel 1977; 56:427–31.

Blanco F, Garcia P, Mateos P, Ayala J. Characteristics and properties of lightweight concrete manufactured with cenospheres. Cement and Concrete Research 2000; 30-11:1715-1722.

Bloem DL. Effect of fly-ash in concrete. National Ready Mixed Concrete Association 1954; Bull 48.

Boegh J, Gaudry D. personal communication. November 2008

Bouzoubaa N, Foo S. Use of fly-ash and slag in concrete: A best practice guide. Canmet Materials Testing Laboratory Canmet, Ottawa, Canada. 2004;

British adopted European Standard EN450-2. Fly ash for concrete, conformity evaluation. 2005.

Bruere GM. Air-entraining actions of anionic surfactants in Portland cement pastes. Journal of Applied Chemistry and Biotechnoly 1971; 21:61–4.

Burden D, MSc thesis, University of New Brunswick, Fredericton, NB, Canada. 2003.

Burton P, Kreeger A, Shefchick B. The use of fly ash in mine stabilization – a cost-effective method of domeout repair. Available online at http://www.burnsmcd.com/portal/page/portal/Internet/Content_Admin/Publications%20Repository/TechBriefs%20Link%20Repository/article-theuseofflyashinminestabilization-022.pdf (Accessed July 2009).

Campbell L. Aggregate and fly-ash concrete for Barkley Lock. Proceedings American Society of Civil Engineers 1961; 87:1-16.

Canadian Encyclopedia: available online at http://www.thecanadianencyclopedia.com/index.cfm?PgNm=TCE&Params=A1ARTA0001476 (Accessed July 2009).

Canadian Industry Program for Energy Conservation (CIPEC). Energy consumption benchmark guide: cement clinker production. Natural Resources Canada, Office of Energy Efficiency 2001; M27-01-1464E.

Canadian Industries Recycling Coal Ash (CIRCA). Fly-ash: its origin, applications and the environment 2002; Available online at http://www.circainfo.ca/pdf/CIRCA%20Fact%20Sheet%201%20-%20CTFinal.pdf (Accessed July 2009).

Canadian Standards Association (CSA). CSA-A3001-03: Cementitious materials for use in concrete. CSA: Cementious Materials Compendium. 2003.

Cardoso RJ, Shukla A, Bose AJ. Effect of particle size and surface treatment on constitutive properties of polyester-cenosphere composites. Journal of Materials Science 2002; 37:603-613.

Cement Association of Canada (CAS), Journal of commerce 2006; Available online at http://www.journalofcommerce.com/article/20060710500 (Accessed July 2009).

Cement Association of Canada (CAS) website Available online at http://www.cement.ca/index.php/en/Continual_Improvements_in_Energy_Efficiency.html (Accessed July 2009).

Cereda E, Marcazzan GMB, Pedretti M, Grime GW, Baldacci A. The microscopic nature of coal fly ash particles investigated by means of nuclear microscopy. Atmospheric Environment 1995; 29.17:2323-2329.

Chang JE, Lin TT, Ko MS, Liaw DS. Stabilization/solidification of sludges containing heavy metals by using cement and waste pozzolans. Journal of Environmental Science Health 1999; A34-5:1143-1160.

Chao CYH, Kwong PCW, Wang JH, Cheung CW, Kendall G. Co-firing with rice husk and bamboo and th impact of particulate matters and associated polycyclic aromatic hydrocarbon emissions. Bioresource Techonology 2008; 99:83-93.

Chindaprasirt P, Buapa N, Cao HT.Mixed cement containing fly ash for masonry and plastering work, Construction and Building Matierals 2005; 19:8:612-618.

Chindaprasirt P, Rukzon S, Sirivivatnanon V. Resistance to chloride penetration of blended Portland cement mortar containing palm fuel ash, rice husk ash and fly ash. Construction and Building Materials 2008; 22:932-938.

Chusilp N, Jaturapitakkul C, Kaittikamol K. Effects of LOI and ground bagasse ash on the compressive strength and sulphate resistance of mortars. Constructions and Building Materials 2009; *Article in press, Correct Proof.*

Clendenning TG, Durie ND. Properties and use of fly-ash from a steam plant operating under variable load. Proceedings ASTM62, 1962; 1019-1037.

Cohen H, Pelly I. Fly ash as a chemical scrubber for acidic wastes. The 25th Annual International Pittsburgh Coal Conference, Pittsburgh, PA, USA, Sept. 2008.

Conner JR. Chemical fixation and solidification of hazardous wastes. Van Nostrand Reinhold NY, USA. 1990.

Conner JR, Hoeffner SL. Critical review of stabilization/solidification technology. Critical Review Environmental Science Technology 1998; 28:397-462.

Costa U, Massazza F. Some properties of pozzolanic cements containing fly-ashes. Fly-ash, silica fume, slag and other mineral by-products in concrete vol I 1983; SP 79: 235-254.

Davis RE, Carlson RW, Kelly JW, Davis HE. Properties of cements and concretes containing fly-ash. Proceedings American Concrete Institute 1937; 33: 577-612.

Del Monte M, Sabbioni C. Morphology and mineralogy of fly ash from a coal-fueled power plant. Archives for Meteorology, Geophysics, and Bioclimatology 1984; B35:93-104.

Demirbas A. Heavy metal contents of fly ashes from selected biomass samples. Energy Sources 2005; 27:1269-1276.

Diamond S. The microstructure of cement paste and concrete – a visual primer. Cement and Concrete Composites 26 2004; 919-933.

Dodson VH. Concrete admixtures. 1st ed. New York: Van Nostrand Reinhold; 1990; 129–64.

Dube SK. A methodology for environmental impact assessment study for back filling of coal ash generated from a thermal power station in a mine filled with acid mine drainage. The 25th Annual International Pittsburgh Coal Conference, Pittsburgh, PA, USA, Sept. 2008.

Duxon P, Provis JL, Lukey GC, van Deventer JSJ. The role of inorganic polymer technology in the development of 'green concrete'. Cement and Concrete Research 2007; 37:1590-1597.

Epstein E. Silicon. Ann. Rev. Plant Physiol. Plant Mol. Biol. 1999; 50;641-664.

Euclid Chemical Company. Airextra technical data sheet. Available online at http://www.euclidchemical.com/fileshare/ProductFiles/techdata/airextra.pdf (Accessed July 2009)

Friis K. Use of admixtures and pozzolanic materials in concrete for dams and the influence of the finer sand particles. Sixth Congress on Large Dams, Question 23, General Report H New York, NY, USA. 1958.

Gajda J, Botha F, Bryant MM, Bhatty JI. Utilization of discarded fly ash as a raw material in the production of Portland cement. Journal of ASTM International 2006; 3-10: 1546-962X.

Gao YM, Shim HS, Hurt RH, Suuberg EM, Yang NYC. Effects of carbon on air entrainment in fly ash concrete: the role of soot and carbon black. Energy Fuels 1997; 11(2):457–62.

Gaudry D. personal communication. December 2008

Ghosal S, Ebert JL, Self SA. Chemical composition and size distribution for fly ashes. Fuel Processing Technology 1995; 44:81-94.

Ghose A, Pratt PL. Studies of the hydration reactions and microstructure of cement-fly-ash paste in: The conference "Effects of Fly-ash Incorporation in Cement and Concrete." Ed, Sydney Diamond, 1981; 82-91.

Goni S, Gurrero A. EX/EDX characterization of the hydration of products of belite cements from class c coal fly ash. Journal of American Ceramics Society 2007; 90-12:3915-3922.

Gougar MLD, Scheetz BE Roy DM. Ettringite and C-S-H Portland cement phases for waste ion immobilization: A review. Waste Management 1996; 16:295-303.

Green Brick Company Available online at http://www.greenestbrick.com (Accessed July 2009).

Grieb WE, Woolf DO. Concrete containing fly-ash as a replacement for portland blast-furnace slag cement. Proceedings ASTM 1961; 61: 1143-1153

Hasset DJ, Pflughoeft-Hasset DF. Use of coal combustion by-products for solidification/stabilization of hazardous wastes. Annual meeting of the North Dakota Academy of Science, Grand Forks, Department of Energy, Washington DC, USA. 1997; 24-25.

Helmuth R. Fly ash in cement and concrete. Portland Cement Association, 1st Ed, 1987; 58-64, 80-2.

Henry J, Towler MR, Stanton KT, Querol X, Moreno N. Characterization of the glass fraction of a selection of European coal fly ashes. Society of Chemical Industry 2004; doi.10.1002/jctb.1023

Hewlett, P. Lea's chemistry of cement and concrete. 4th Ed. Jordan Hill, Oxford, OX2 8DP: Butterworth-Heinemann Linacre House; 1997.

Independent Electricity System Operator (IESO). The Ontario Reliability Outlook. Toronto Ontario, December 2008.

Ipatti, A. Peat fly-ash as a supplementary cementing material in concrete. Nordic Concrete Research 1998; 7: 152-166.

Johnson AS, Morgan ME, Afonso RF, Dyas B, Carter HR. Optimizing Sootblower Operation in Response to Changing Coal Quality and Boiler Operation, in *The Impact of Ash Deposition in Coal-Fired Power Plants,* Eds J Williamson and F Wigley, Taylor and Francis, Washington DC, USA. 1994; 41-52

Karayigit AI, Gayer RA. Characterization of fly ash from the Kangal power plant, Eastern Turkey. International Ash Utilization Symposium, Center for Applied Energy Research, Lexington KY, USA. 2001.

Kalra N, Jain MC, Joshi HC, Choudhary R, Harit RC, Vasta SK, Sharma SK, Kumar V. Fly ash a soil conditioner and fertiliser. Bioresource Technology 1998; 64:163-167

Kosmatka SH, Kerkhoff B, Panarese WC, MacLoed NF, McGrath RJ. Design and Control of Concrete Mixtures. 7th Ed. Cement Association of Canada 2002.

Kovacs R. Effect of hydration products on the properties of fly ash cements. Cement and Concrete Research 1975; 5:73-82.

Kukier U, Summer ME. Boron release from fly ash and its uptake by corn. Journal of Environmental Quality 1994; 23:596-603

Lamond JF. Twenty-five years' experience using fly-ash in concrete. Fly-ash, silica fume, slag and other mineral by-products in concrete vol I 1983; SP 79: 47-70.

Larson TD. Air entrainment and durability aspects of fly ash concrete. Proceedings ASTM 1964; 64:866-866.

Lea FM. Chemistry of cement and concrete. New York Chemical Publishing Co, 1973

Lee H, Ha HS, Lee CH, Lee YB, Kim PJ. Fly ash effect on improving soil properties and rice production in Korean paddy soils. Bioresource Technology. 2006; 97:1490-1497. Lehigh cement Available online at http://www.lehighinland.com/inland/ (Accessed July 2009).

Lilkov V, Djarbarov N, Bechev G, Petrov O. Properties and hydration products of lightweight and expansive cements. Cement and Concrete Research 1999; 29:1641-1646.

Lorenzo MP, Goni S, Guerrero A. Role of alminous component of fly-ash on the durability of portland cement-fly-ash pastes in marine environment. Waste Management 2003; 23:785-792.

Lu G, Yan Y, Cornwell S, Whitehouse M, Riley G. Impact of co-firing of coal and biomass on flame characteristics and stability. Fuel 2008; 87:1133-1140.

Lu Z, Robl T, Marrs B. Utilization of ultra fine fraction of coal combustion fly ash as polymer composites. The 25th Annual International Pittsburgh Coal Conference, Pittsburgh, PA, USA, Sept. 2008.

Manz, OE. Coal fly-ash: A retrospective and future look. Fuel 1999; 78(2):133-136.

Mcarty GW, Siddaramappa R, Wright RJ, Cadling EE, Gao G. Evaluation of coal combustion by products as soil liming materials, their influence on soil pH and enzyme activity. Biology and Fertility of Soils 1994; 17:167-172.

McKinnon M. AGS aims to use 100% wood biomass. Atikokan Progress, April 2008, available online at http://www.atikokanprogress.ca/articles/1703/1/AGS-aims-to-test-use-of-100-wood-biomass/Page1.html (Accessed July 2009).

Mehta PK. Pozzolanic and cementious byproducts as mineral admixtures for concrete- a critical review. Fly-ash, silica fume, slag and other mineral by-products in concrete vol I 1983; SP 79: 1-46.

Meij R, van den Berg J. Coal fly ash management in Europe: trends, regulations and health and safety aspects. International Ash Utilization Symposium 2001 http://www.flyash.info/2001/keynote/108meij.pdf (Accessed July 2009).

Menetrier D, Jawed I, Sun TS, Skalny J, ESCA and SEM studies in early C3S hydration. Cement Concrete Res 1979; 473-82.

Menzies NW, Aitken RL. Evaluation of fly ash as a component of potting substrates. Scientia Horticulture 1996; 67: 87-89.

Mindness S, Young JF, Darwin D. Concrete, 2nd ed. Upper Saddle River, NJ: Pearson Education; 2003.

Minnick LJ. Reactions of hydrated lime with pulverized coal fly ash. USBM Information Circular 8348, Fly Ash Utilization 1967; 287-315National Asphalt Pavement Association (NAPA). Guidelines for materials, production and placement of stone matrix asphalt. NAPA Information Series 118. 1994.

Nantel JH. Recent Developments and Trends in Backfill Practices in Canada. Proceedings of the 6th International Symposium on Mining with Backfill, Brisbane, Australia, 14-16 April, Australasian Institute of Mining and Metallurgy. 1998: 11-14.

Nasvik J, Pistilli M. Are we placing too much air in our concrete? Concrete Construction World of Concrete 2004;49(2):51–5.

National Ready Mixed Concrete Association (NRMCA). Concrete in practice: what why and how? CIP 17 – flowable fill materials. 2000. Available online at http://www.nrmca.org/aboutconcrete /cips/17p.pdf (Accessed July 2009).

National Science Foundation. Follow the 'Green' Brick Road? Press Release 07-058, May 22, 2007. Available online at http://www.nsf.gov/news/news_summ.jsp?cntn_id=109594&org=ENG (Accessed July 2009)

Ngu L, Wu H, Zhang D. Characterization of ash cenospheres in fly ash from Australian power stations. Energy and Fuels 2007; 21:3437-3445.

Ontario Power Generation (OPG). Sustainable Development Report 2007. Available online at http://www.opg.com/pdf/sustainable%20development%20reports/sustainable%20development%20Report%202007.pdf (Accessed July 2009)

Paille´ re AM. Application of admixtures in concrete. 1st Ed. London: E & FN Spoon; 1995; 17–22.

Pan JR, Huang C, Kuo JJ, Lin SH. Recycling MSWI bottom and fly ash as raw materials for Portland cement. Waste Management 2008; 28:1113-1118.

Pasko TJ, Larson TD. Some statistical analysis of the strength and durability of fly-ash concrete. Proceedings, ASTM V. 62, 1962; 1054-1067.

Pedersen KH, Jensen AD, Skjoth-Rasmussen MS, Dam-Johansen K. A review of the interference of carbon containing fly ash with air entrainment in concrete. Progress in Energy and Combustion Science 2008; 34:135–154.

Pereira CF, Rodriguez-Pinero M, Vale J. Solidification/stailization of electric arc furnace dust using coal fly ash: analysis of stabilization process. Journal of Hazardous Materials 2001; B82:183-195.

Ramachandran VS, editor. Concrete admixtures handbook. Properties, science, and technology, 1st Ed. New Jersey: Noyes Publications; 1984; 1–2, 276.

Rautaray SK, Ghosh BC, Mittra BN. Effect of fly ash, organis wastes, and chemical fertilizers on yield, nutrient uptake, heavy metal content, and residual fertility in a rice-

mustard cropping sequence under acid lateric soils. Journal of Bioresource Technology 2003; 90:275-283.

Rixom R. The economic aspects of admixture use. Cement and Concrete Composites 1998; 20:141–7.

Saji K. The electron microscopy of hardening cement pastes. Zement-Kalk-Gips 1959; 12:418-423.

Sajwan KS. The effect of fly ash/sewage sludge mixtures and application rates on biomass production. Journal of Environmental Science Health 1995; 30(6):1327-1337.

Samarin A, Munn RL, Ashby JB. The use of fly-ash in concrete- Australian experience. Fly-ash, silica fume, slag and other mineral by-products in concrete vol I 1983; SP 79: 143-172.

Sarofim AF, Helble JJ. Mechanisms of Ash and Deposit Formation, in *The Impact of Ash Deposition in Coal-Fired Power Plants,* Eds J Williamson and F Wigley, Taylor and Francis, Washington DC, USA. 1994; 567-582.

Scheetz BE. Chemistry and mineralogy of coal fly ash: basis for beneficial use. Available online at http://www.mcrcc.osmre.gov/PDF/Forums/CCB5/1.4.pdf. (Accessed July 2009).

Schlorholtz S. Testing program for the evaluation of co-combustion fly-ash produced at Ottumwa Generating Station; Phase 2 (Second trial burn). 2005; Available online at http://www.iowaswitchgrass.com/__docs/pdf/Final% 20Fly%20Ash%20Test %20Report.pdf (Accessed July 2009).

Senneca O. Characterization of meat and bone mill for coal co-firing. Fuel 2008. 87: 3262-3270.

Shi HS, Kan LL. Leaching behaviour of heavy metals from municipal solid wastes incineration MSWI) fly ash used in concrete. Journal of Hazardous Materials 2008; doi.10.1016/jhazmat.08077.

Shikami G. On pozzolanic reactions of fly ash. Proceedings Japan Cement Engineering Association 1956; 221-227.

Steenari BM, Lindqvist O. Fly ash characteristics in co-combustion of wood with coal, oil, or peat. Fuel 1999; 78:479-488.

Taylor EM, Schuman GE. Fly ash and lime amendment of acidic coal spoil to acid revegetation. Journal of Environmental Quality 1988; 17:120-124.

Taylor HFW. Cement Chemistry. 2nd Ed. 1 Heron Quary London. E144 JD: Thomas Telford; 1997.

Thomas EG, Nantel JH, Notely KR. Fill Technology in Underground Metalliferous Mines. International Academic Services Limited, Kingston, Ontario. 1979.

Tishmack JK, Burns PE. The chemistry and mineralogy of coal and coal combustion products in: "Energy, waste and the environment: a geochemical perspective." Eds, R. Giere and Peter Stille, 2005; 223-246.

Todd J. Biomass Testing at Ontario Power Generation. Public Presentation at Lakehead University's Research and Innovation Week. February 2009.

US Department of Transportation (USDOT). Use of coal ash in embankments and bases. Technical Advisory T5080.9, US DOT, Federal Highway Administration, Washington DC, USA. 1988.

Vadapalli VRK, Ellendt A, Petrik LF, Hendricks N, Gitari W, Balfour G. Toxic element removal from acidic mine drainage using zeolites synthesized from fly ash derivatives. The 25th Annual International Pittsburgh Coal Conference, Pittsburgh, PA, USA, Sept. 2008.

Vassilev SV, Vassileva CG, Karayigit AI, Bulut Y, Alastuey A, Querol X. Phase-mineral and chemical compostion of fractions separated from composite fly ashes at the Soma power station, Turkey. International Journal of Coal Geology 2005; 61:65-85.

Vilches LF, Leiva C, Vale J, Fernandez-Pereira C. Isulating capacity of fly ash pastes used for passive protection against fire. Cement and Concrete Composites 2005; 27:776-781.

Vom Berg W, Feuerborn HJ. Present situation and perspective of CCP management in Europe. European Coal Combustion Products Association 2003.

Wang S, Baxter L. Comprehensive study of biomass fly-ash in concrete: strength, microscopy, kinetics and durability. Fuel Processing Technology 2007; 88(11-12):1165-1170.

Wang S, Miller A, Llamazos E, Fonseca F, Baxter L. Biomass fly-ash in concrete: mixture proportioning and mechanical properties. Fuel 2008a; 87(3): 365-371

Wang S, Miller A, Llamazos E, Fonseca F, Baxter L. Durability of biomass fly-ash concrete: freezing and thawing and rapid chloride permeability tests. Fuel 2008b; 87: 359-364.

Wang S, Miller A, Fonseca F, Baxter L. Biomass fly-ash in concrete: SEM, EDX and ESEM analysis. Fuel 2008c; 87: 372-379.

Washa GW, Withey NH. Strength and durability of concrete containing Chicago fly-ash. Proceedings American Concrete Institute 1953; 49: 701-712.

Watt JD, Thorne DJ. Composition and pozzolanic properties of pulverized fuel ashes. Journal of Applied Chemistry 1965; 15:585-594.

Wesche K. Fly ash in concrete: properties and performance. 1st Ed. London: E&FN Spoon 1991; 3-24, 42-62, 117-143.

Wigley F, and Williamson J. The Characterization of fly ash samples and their relationship to the coals and deposits from UK boiler trials, in *The Impact of Ash Deposition in Coal-Fired Power Plants,* Eds J Williamson and F Wigley, Taylor and Francis, Washington DC, USA. 1994; 385-398.

Wigley F, Williamson J. Modelling fly ash generation for pulverized coal combustion. Progress in Energy and Combustion Science. 1998; 24: 337-343.

Wilemski G, Srinivasachar S. Prediction of ash formation in pulverized coal combustion with mineral distribution and char fragmentation models, in *The Impact of Ash Deposition in Coal-Fired Power Plants,* Eds J Williamson and F Wigley, Taylor and Francis, Washington. 1994; 151-164.

Wilson HS, Burns JS. Beneficated products from fly ash: market research. Canmet Report, Minerals Research Program (Ottawa, Canada) 1982; 82-17E

Yeheyis MB, Shang JQ, Yanfyl EK. Characterization and environmental evaluation of Atikokan coal fly ash for environmental applications. Journal of Environmental Engineering Science 2008; 7:481-498.

Yu Q, Sawayana K, Sugita S, Shova S, Shova M, Isojima Y. The reaction between rice husk ash and $Ca(OH)_2$ solution: nature of its products. Cement and Concrete Research 1999; 29:37-43.

Zhang D. Air entrainment in fresh concrete with pfa. Cem and Conc Composites 1996; 18(6) 409-16.